Generation of the Higgs Boson with the HZHA Event Generator

Thomas Frågåt

Thesis submitted in partial fulfillment
of the requirements for the degree Cand. Scient.
at the Department of Physics, University of Oslo

August 2000

Abstract

In this thesis a description of some of the event generation techniques used in particle physics is given. One of these techniques is then applied to the inclusion of the interference term between Higgs-strahlung and WW fusion. The interference term arises from the two production amplitudes when the Z boson of the Higgs-strahlung decays into electron neutrinos. A comparison between two different implementations of the interference term, is also made.

Acknowledgement

It had not been possible to write this thesis without the support and help I have recieved from several persons. In particular I would like to thank my supervisors Lars Bugge and Alex Read for their help, ideas, comments and motivation. I am also grateful to Trond Myklebust for always helping me whenever I had a computer problem. I would also like to thank my fellow graduate students, the Ph.D. students and the staff at The Experimental Particle Physics Group, for always supporting and helping me when necessary. Especially I would like to mention the good professional and social environment at the group.

Contents

List of Figures

List of Tables

Chapter 1

Introduction

Particle physics is a child of 20th century physics, although already the ancient Greeks had some thoughts about what it was that made up the world. The tiniest pieces in our universe that we know today are the quarks together with the leptons and the force carriers. These particles are called elementary particles and are the fundamental pieces in everything around us. In this context fundamental means what we at present state are able to observe in experiments. This is to all times dependent on the total energy reached in experiments.

In the last century a lot of particle physic experiments were built, and a stream of new knowledge broke through the surface. Although the field of particle physics is fundamental science, it has a lot of spin-offs with a wide range of applications and it has had a great influence on our history as we will see in the next sections.

Still big experiments are continued and new ones are under construction. One of the main fields in particle physics today, is the search for the Higgs boson which is predicted by the Standard Model but is still not found. The main topic for this thesis is one of the tools used in the Higgs boson searches: The event generator. More precise, we will see how the inclusion of the interference term, arising from the production amplitudes of the WW fusion and Higgs-strahlung with electron neutrinos in the final state, is included into the HZHA generator.

In the next sections a presentation of some of the activities at CERN is made. A closer look at one of the four LEP expreiments, *DELPHI*, is also taken.

In Chapter 2 a presentation of the theoretical framework of the *Standard Model* (SM) and the *Minimal Supersymmetric extension of the Standard Model* (MSSM) is done. A description of the three main Higgs production channels (Higgs-strahlung, WW fusion and ZZ fusion with interference) has also been made.

Chapter 3 contains the techniques used to generate events by computers and how the interference term between Higgs-strahlung and WW fusion was implemented in HZHA02. A description of the tests performed to validate the new algorithms in HZHA02 is also given.

Chapter 4 presents the results of including interference between Higgs-strahlung and WW fusion, both for the Standard Model and the MSSM. A comparison of the two versions HZHA02 and HZHA03, both including the interference term, is also made.

Finally Chapter 5 contains the conclusion.

In addition there are two Appendices with two Delphi notes [1, 2] describing the inclusion of interference in HZHA02. The Delphi note in Appendix A, also contains the

Fortran code used to include interference.

1.1 The History of Particle Physics

In this section a short summary of the history of particle physics is given together with a short introduction on what *CERN* is. A description of the DELPHI experiment is given. A discussion on what benefits ordinary people can get from such experiments is also made.

1.1.1 The First Particle Physicists

What are the building blocks of the universe? and how did it all start? have been and still are among the biggest and most mysterious questions in the history of mankind. The ancient believed that the world consisted of four fundamental elements; earth, water, fire and air, and that every substance was a mixture of these. Around 400 BC Leucippus proposed that matter is discrete. Some years later his student Democritus considered the matter to be made of small, indivisible pieces of various size, colour, and mass, and he called them *atoms*. Although another Greek philosopher, Epicurus, supported and continued the idea, Aristotle and Socrates opposed it. Instead they argued that matter is continuous, there is no smallest piece. Until 1803 this was the leading idea, but this year John Dalton proposed the first modern atomic theory:

- Atoms are small, indivisible spheres.
- Atoms of a given element are identical.
- Atoms are elementary and cannot be created, destroyed or transformed.
- Compounds are the results of small whole number ratios of atoms.
- Relative numbers of different kinds of atoms in a compound are constant.

Dalton published a series of papers where he introduced his atomic hypothesis and even introduced the concept of interatomic forces, but since he never indicated the nature of the forces, the theory was not a great success.

In 1897 Joseph John Thomson produced cathode rays and deflected them in magnetic fields. He identified the rays as negatively charged particles that have mass. But J. J. Thomson is probably best known for his "plumpudding" modell of the atom. Later, in 1911, Millikan found the mass of the electron. Two years earlier, in 1909, Rutherford (a student of Thomson) discovered the nucleus of an atom by bombarding a gold foil with α particles. He found that the nucleus was positively charged.

1.1.2 History of 20th Century Particle Physics

In 1900 the German physicist, Max Planck, found that the energy of light and radiation[1] is quantizised. This was the foundation of *Quantum Mechanics*, the theory describing the particle nature. Thirteen years later, in 1913, the Danish physicist Niels Bohr proposed his atomic model. He suggested that the atom was made up of a nucleus in the center

[1] Strictly speaking, light is also radiation

surrounded by electrons orbiting in certain energy levels, Fig. 1.1. This theory was supported by experiments on the hydrogen atom. The theories of Max Planck and Niels Bohr

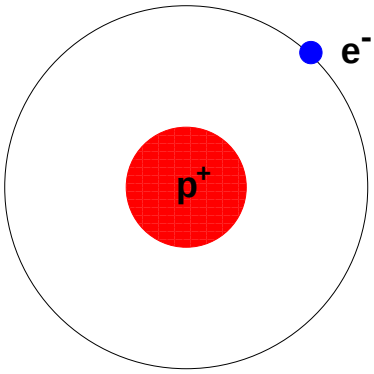

Figure 1.1: *The Bohr model of the hydrogen atom.*

were further developed by famous physicists like Schrödinger, Dirac, Pauli, Heisenberg, Feynman and others. See [3] for further reading.

In 1932 the positron (the anti-particle of the electron) was detected in an experiment by Anderson using a cloud chamber. This was a big success for the relativistic wave theory of Dirac which had predicted the existence of an anti-particle of the electron. In the same year the neutron was also discovered and in 1937 the second lepton, the *muon*, was observed in cosmic rays. In 1964 Gell-Mann and Zweig proposed, independent of each other, the existens of what they called quarks and aces, respectively. But it was not until 1967 that the discovery of the quark structure of the proton was made at *Stanford Linear Accelerator Center* (SLAC).

In the first years of modern experimental particle physics, the particles were observed in devices like cloud chambers, bubble chambers and with photographic emulsions, and their origin was cosmic ray. The first operational *Linac* (Linear accelerator) was designed and built by Rolf Wideröe in 1927 in Aachen, Germany [4]. In Fig. 1.2 Wideröe's diagram describing a method for accelerating ions is shown. This diagram inspired Ernest Lawrence to construct the cyclotron, shown in Fig. 1.3. This was the first successful cyclotron and was first operated in 1930. The development of accelerators went fast, and within 60 years there were linacs, like *SLAC* in California, and cyclic accelerators like *LEP* at *CERN* (The European Laboratory for Particle Physics) near Geneva on the Swiss-French border. In the 1950's the first real powerful accelerators were built and this led to discoveries of a lot of "new" hadrons. The detectors also became better with time and in 1968 Charpak introduced the first *multiwire proportional chamber* (MWPC) for which he, among other things, got the Nobel prize in 1992 [5]. This was a big break through within modern experimental particle physics. The MWPC allowed recording of up to one million tracks per second unlike the bubble chamber which can only record with a rate of one or two tracks per second. The spatial precision of the charged particle trajectory is less than 1mm. Placing the MWPC in a magnetic field one is able to compute the particle's momentum, and it is easier to study short lived exotic particles and rare interactions because of the high spatial resolution and high repetition rate. A lot of discoveries have been made since then thanks to Charpak's work, e.g. the discovery of the J/Ψ particle at Brookhaven and SLAC (made independently) in 1974 and the W and Z bosons in 1983

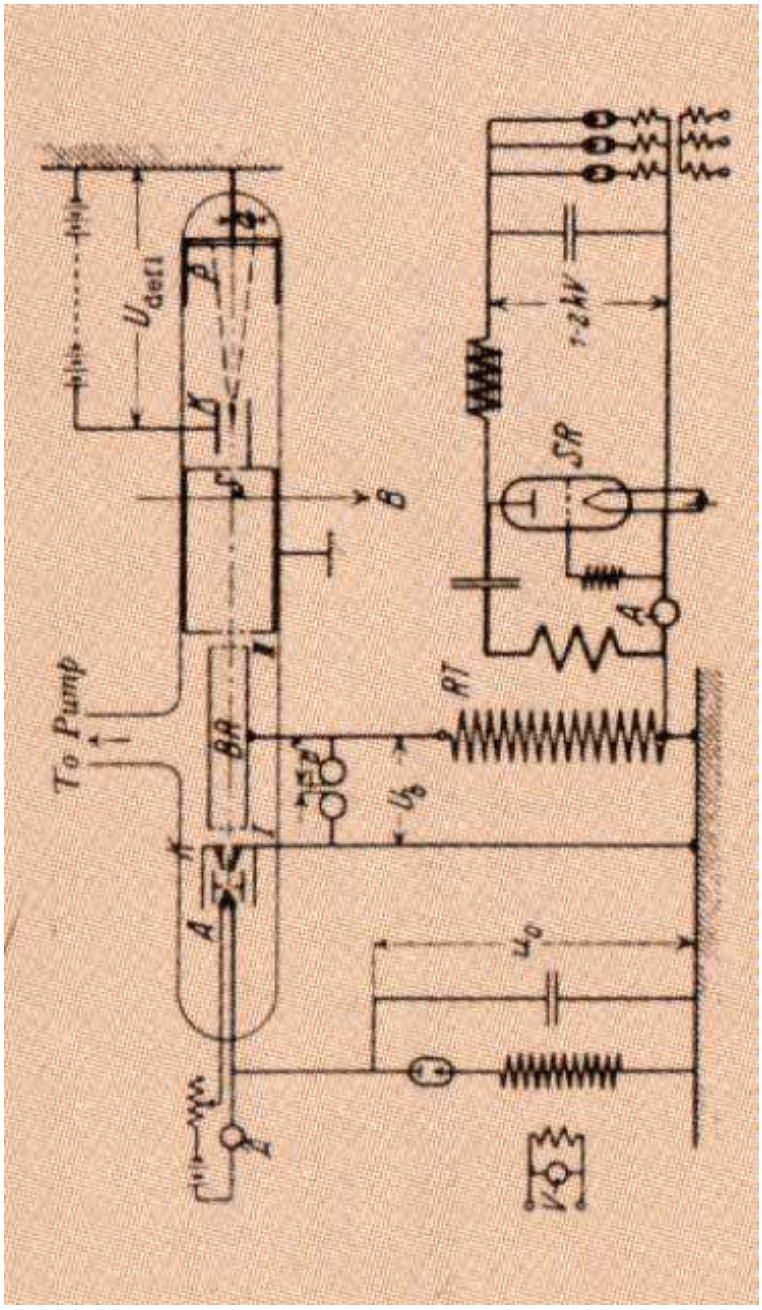

Figure 1.2: *R. Wideröe's diagram describing a method for accelerating ions, (Photo: Ernest Orlando Lawrence Berkeley National Laboratory).*

which were discovered at CERN. Both discoveries led to Nobel prizes in 1976 and 1984, respectively.

In the past 40 years a lot of discoveries have been made, and today we know there are seventeen elementary particles called fermions and bosons. There are twelve fermions (plus their anti-particles), which are spin–1/2 particles. They can be divided into two groups, *quarks* and *leptons*. These can so be divided into three generations, Table 1.1. The last elementary particle discovered, was the top-quark, t, which was first observed at the Tevatron proton-antiproton collider at Fermilab in 1995 (18 years after the bottom

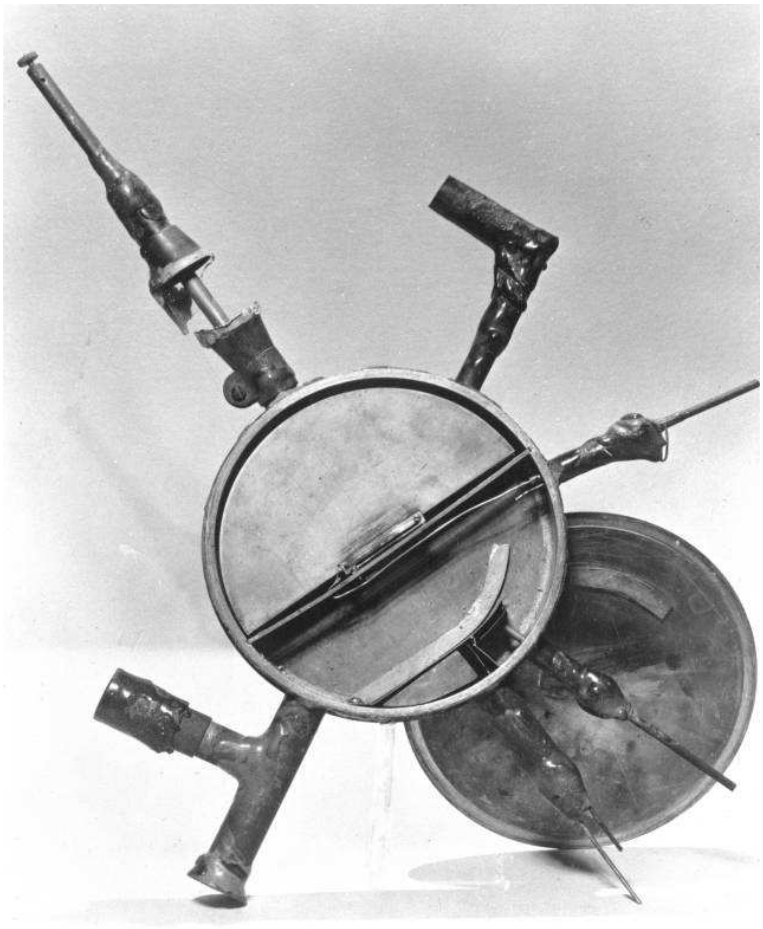

Figure 1.3: *The first cyclotron built by Lawrence and his graduate student M. Stanley Livingston in 1930, (Photo: Ernest Orlando Lawrence Berkeley National Laboratory).*

quark, b, was discovered, also at Fermilab). Besides the fermions there are five force carrying bosons. The bosons are identified by their integer spin.

Everything around us can be described by the interactions of the four fundamental forces of nature. One of them is the *electromagnetic interaction* which is the interaction between charged particles, the force carrier is the *photon*, γ. Another force is the *weak interaction*. This force is among other things responsible for the β-decay of the nuclei. The force carriers of the weak interaction are the $W^{\pm}$ and Z bosons. The neutrinos interact only through the weak interaction. The weak force only acts over short disances, less than about 10^{-15} centimeters while the influence of electromagnetism extends to infinite distances. The range of the two forces can be explained by the force carriers. The photon is massless whereas the $W^{\pm}$ and Z particles are about hundred times the mass of the proton. The third force of nature is the *strong interaction* which binds the quarks together. The force carrier is the gluon, g. The fourth force is *gravity*. This force is however so small between elementary particles compared to the three other forces that it, in practice, can be neglected when working within the field of particle physics.

Although there are four fundamental forces of nature, the interactions can be described by only three theories: the *electroweak theory* which is a "unification" of the electromagnetic and weak interactions, the strong theory often called *quantum chromodynamics*

$P_{article}^{Charge}$ $_{Mass}$			
u $^{+2/3}$ $_{0.003}$	c $^{+2/3}$ $_{1.3}$	t $^{+2/3}$ $_{175}$	γ ^{0} $_{0}$
d $^{-1/3}$ $_{0.006}$	s $^{-1/3}$ $_{0.1}$	b $^{-1/3}$ $_{4.3}$	g ^{0} $_{0}$
ν_e ^{0} $_{<1\times10^{-8}}$	ν_μ ^{0} $_{<0.0002}$	ν_τ ^{0} $_{<0.02}$	$W^{\pm}$ $^{+1,-1}$ $_{80.4}$
e $^{-1}$ $_{511\times10^{-6}}$	μ $^{-1}$ $_{0.106}$	τ $^{-1}$ $_{1.7771}$	Z^0 ^{0} $_{91.187}$

Table 1.1: *The elementary particles. The three columns to the left are the fermions (spin-1/2) particles, where the two upper rows are the quarks, while the two lower rows are the leptons. The 4th column contains the force carriers, bosons (spin = 0, 1, 2,...). To each fermion there is also an anti-particle. All the masses are given in GeV.*

(QCD) and the theory of general relativity which describes the gravity.

Today the main fields in experimental particle physics is the Higgs boson search, searches for neutrino oscillations, searches for CP-violation in $b\bar{b}$ (bottom-quark) production and searches for supersymmetric particles. Some new accelerators and experiments are also under construction, like the *Large Hadron Collider* (LHC) at CERN. This accelerator with all its detectors is going to, among other things, search for the Higgs boson and supersymmetric particles.

But what is the gain of all this research? Is it only the scientists that will have some outcome of all this? It is fundamental science, and the practical applications can seem to be far away, but that is not the truth. Some spin-offs from the field of particle physics research to be mentioned are the *WorldWideWeb*, which was created by scientists at CERN, cancer therapy, radiation processing, medical and industrial imaging, electronics and a lot of other things. An example is the MWPC which is now used in medicine, biology and industry. In [6] a more detailed description of spinoffs is given.

1.2 LEP

LEP is a storage ring which collides electrons and positrons at center of mass energies about $\sqrt{s} \sim 200$ GeV. The maximum center of mass energy reached so far (April 2000) is 208 GeV. The closing date of LEP is in October year 2000. Then LEP is taken apart to give place for a new and more powerful accelerator, namely the LHC, which will be operated from around year 2005. The high energies of LEP and LHC (which will reach a center of mass energy around $\sim$ 14 TeV), can only be obtained with instruments of

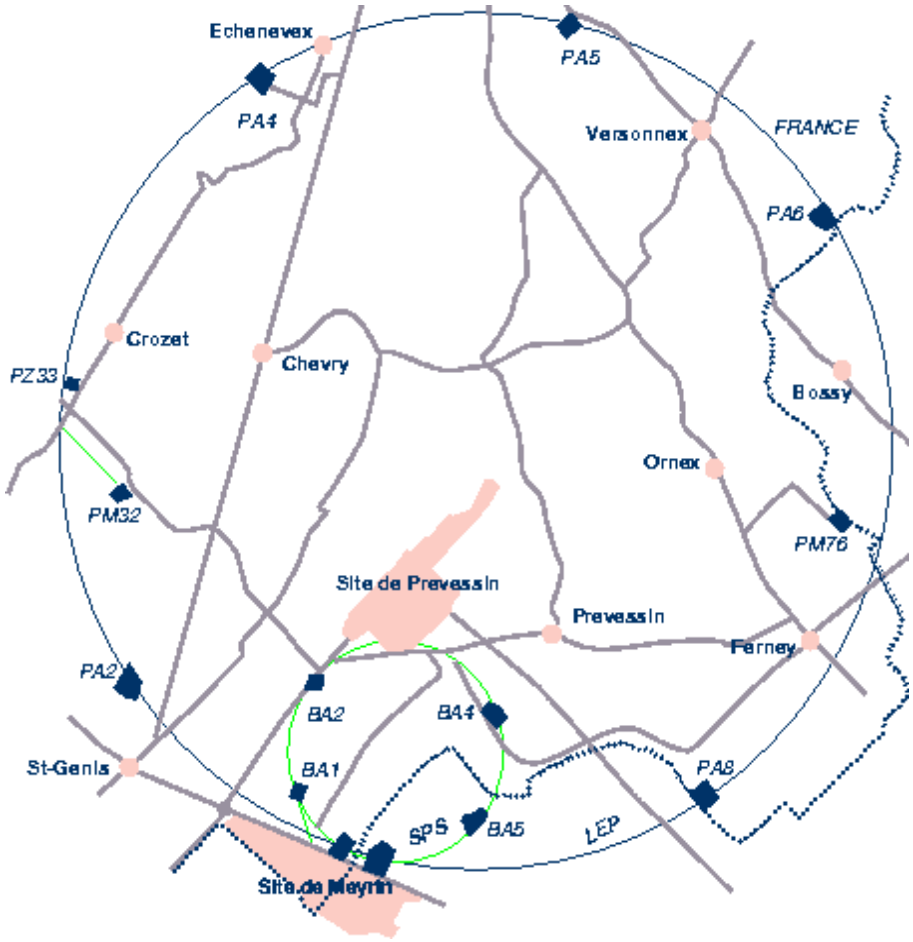

Figure 1.4: *LEP and SPS (Super Proton Synchrotron) at CERN. L3 is located at PA2, Aleph at PA4, Opal at PA6 and Delphi at PA8.*

high precision. The ring of these two accelerators is about 27 kilometres long. The LEP ring has eight location points for *Radio frequency* (RF) cavities which are accelerating the electrons and positrons. There are four experiments located along the storage ring: Aleph, Opal, L3 and Delphi. LEP is shown in Fig. 1.4. As can be seen, all the detectors and most of LEP is located in France.

1.3 The Delphi experiment

The Delphi experiment [7] is one of the four experiments at LEP. Delphi is an abbreviation for DEtector with Lepton, Photon and Hadron Identification. The countries involved in this specific experiment are: Austria, Belgium, Brazil, Czech Republic, Denmark, England, Finland, France, Germany, Greece, Italy, Netherlands, Norway, Poland, Portugal, Russian Federation, Slovakia, Slovenjia, Spain, Sweden, Switzerland, and USA. But only 20 of 22 countries listed here are member states of CERN (USA and the Russian Federation are only observer states).

In this section a short presentation of the DELPHI detector and the DELPHI organisation is made.

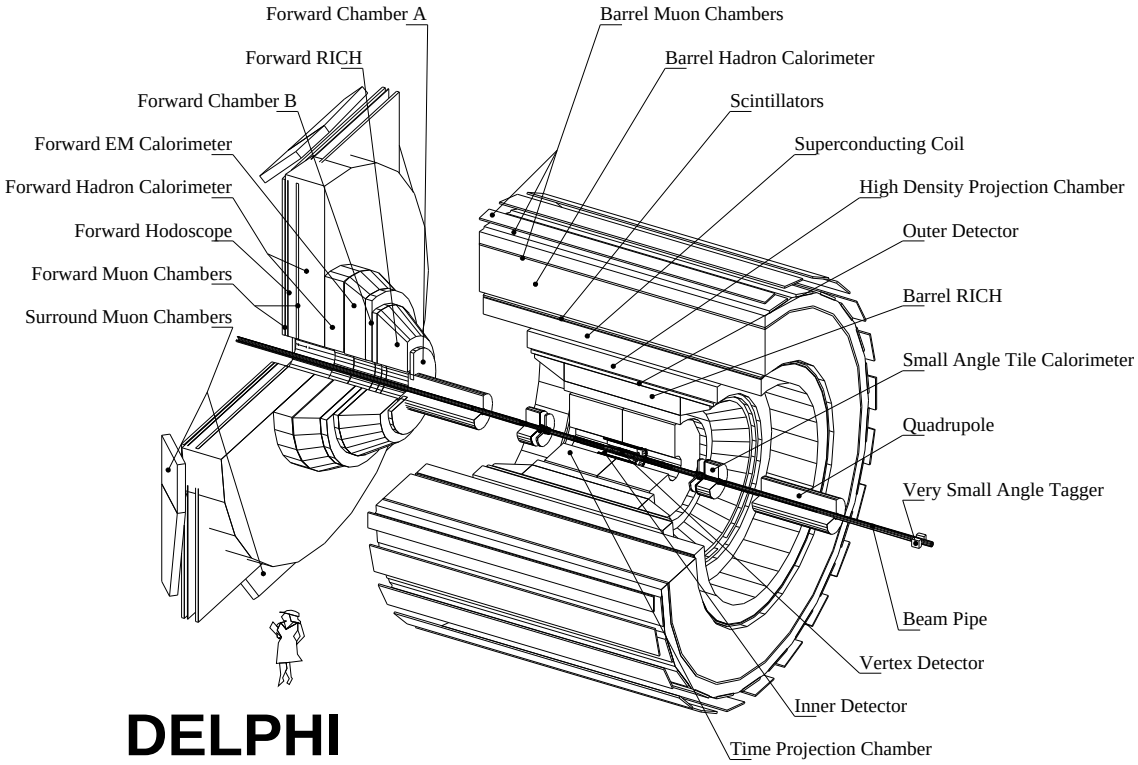

Figure 1.5: *The DELPHI detector.*

1.3.1 The Delphi detector

The Delphi detector took its first data in 1989. In Fig. 1.5 the detector with all its subdetectors is shown. The advantages of Delphi are precise vertex determination, particle identification, high granularity and information in three dimensions. The main parts of the detector are (beginning with the barrel detector going from the center and outwards) [8]:

- The **Vertex Detector** which is a silicon detector located nearest the collision point. It is provided to track very precisely in order to detect very short lived particles.
- Outside the vertex detector is the **Inner detector**. It consists of a JET chamber and the Trigger Layers, which provide intermediate precision positions.
- The next detector is the **Time Projection Chamber** (TPC) which tracks the particles and also helps in charged particle identification. This is the main tracking device of DELPHI.
- The **Barrel RICH** detector is placed outside the TPC. This is a Ring Imaging Cherenkov detector which is together with the TPC used for particle identification.
- The **Outer Detector**, which is placed outside the Barrel RICH, consists of several drift tubes. It makes a final precise measurement of the direction.

The **electromagnetic calorimeters** and **scintillation counters** are located outside the tracking detectors and the Barrel RICH. These detectors are primarily constructed for photon and electron identification:

- The first calorimeter is the **High-density Projection Chamber** (HPC). This is the barrel electromagnetic calorimeter.
- The **lead-scintillators** detect high energy photons, thus providing complete hermeticity for high energy photon detection.
- **Scintillators** are also used as fast triggers for beam events and cosmic radiation.
- The **Barrel Hadron calorimeter** (HCAL) surrounds the scintillators. It is a sampling gas detector and consists mainly of iron and it is incorporated in the magnetic yoke. The hadron calorimeter measures the energy of neutral and charged hadrons.
- The outer layer of the Delphi detector consists of the **Barrel muon chambers**. These are tracking detectors, which are, since the muons interact hardly and are very penetrating (in fact, the muons are the only charged particles that are able to traverse the lead and iron of the calorimeters nearly unaffected), located outside all the other detectors[2]. It is expected that most muons with momenta greater than 2 GeV/c will reach the muon chambers.

The superconducting coil is located between the HPC and scintillators, it produces a magnetic field of 1.23 Tesla. The high magnetic field curves the particle trajectories, thus, the particle momenta can be found.

The luminosity measurements are done with the **Small angle TIle Calorimeter** (STIC) which is a sampling lead-scintillator calorimeter and the **Very Small Angle Tagger** (VSAT) which detects electrons and positrons coming from the Bhabha scattering.

The endcaps of the DELPHI detector are built after nearly the same principles as the barrel detector. The endcaps consist of:

- The **Very Forward Tracker**, which is located on each side of the vertex detector, is the forward part of the (vertex) silicon tracker.
- The **Forward Chamber A** and **Forward Chamber B** are both drift chambers. The Forward Chamber A is located nearest the collision point, while the Forward Chamber B is located outside the Forward RICH:
- The **Forward RICH** is, like the Barrel RICH, used for particle identification.
- The **Forward ElectroMagnetic Calorimeter** (FEMC) consists of two 5 m diameter disks made of Cherenkov lead-glass.
- The **Forward Hadron Calorimeter**, **Forward Muon Chambers** and **Surround Muon Chambers** are all constructed after the same principles as for their barrel partners.
- The **Forward Hodoscope** is practically a scintillation trigger on muon events in the endcap regions.

[2]Note that this is a simplified description. The structure is more complicated than this. Partly the muon chambers are embedded in the HCAL, and partly the muon chambers are outside all the other detectors. See [9] for more information.

The *quadrupoles* shown in the figure, are focusing magnets that provide the correct beam trajectories into the DELPHI detector.

1.3.2 DELPHI searches

The Delphi searches teams, working mainly on data analysis, are divided into three main fields which are:

- The Higgs searches,
- the SUSY searches,
- and the searches for exotica.

Each of these are so divided into subcategories.

Chapter 2

Theory

In this chapter a brief presentation of the underlying theories of the Standard Model and the MSSM will be given. A presentation of the Higgs mechanism and an explanation of why the Higgs is required is also given. Finally the formulae used to generate the $e^+e^- \to H\nu_e\bar{\nu}_e$ with interference are presented. This chapter is inspired by [10, 11]. In this and all later chapters we will use the *natural units* (NU), that is $\hbar = c = 1$.

2.1 The Standard Model

The Standard Model is one of the great successes of quantum field theory and it is based on the $SU(3) \otimes SU(2) \otimes U(1)$ gauge group. It can describe all known fundamental forces in nature except gravity, and has been confirmed by a lot of experiments. The Standard Model can be split into two: The Weinberg-Salam Model and *quantum chromodynamics* (QCD). In this section a presentation of the two models is made before they are put together to form the Standard Model.

2.1.1 The Weinberg-Salam Model

The Weinberg-Salam Model unifies electromagnetic interaction of *quantum electrodynamics* (QED) and the weak interaction. Strictly speaking, it is not a "unified theory" of QED and weak interactions, since it is neccesary to introduce two distinct coupling constants g and g' for the $SU(2)$ and $U(1)$ interactions.

QED

By coupling the covariant form of the Dirac equation,

$$(i\gamma^\mu \partial_\mu - m)\psi = 0 \,, \tag{2.1}$$

with the Maxwell's equations we will obtain QED. In Equation 2.1 we have defined

$$\gamma^\mu = (\gamma^0, \boldsymbol{\gamma}), \tag{2.2}$$

where $\gamma^0 = \beta$ and $\gamma^i = \beta\alpha^i$. We demand that the α and β matrices satisfy

$$\begin{aligned} \{\alpha_i, \alpha_k\} &= 2\delta_{ik} \\ \{\alpha_i, \beta\} &= 0 \\ \alpha_i^2 &= \beta^2 = 1 \,. \end{aligned} \tag{2.3}$$

The Maxwell's equations should be well known:

$$\begin{aligned} \boldsymbol{\nabla}\cdot\mathbf{E} &= \rho\,, \qquad \boldsymbol{\nabla}\times\mathbf{E} = -\frac{\partial\mathbf{B}}{\partial t}\,, \\ \boldsymbol{\nabla}\cdot\mathbf{B} &= 0\,, \qquad \boldsymbol{\nabla}\times\mathbf{B} = \mathbf{j}+\frac{\partial\mathbf{E}}{\partial t}\,. \end{aligned} \tag{2.4}$$

These equations are equivalent to the covariant equation for the four-vector potential A^μ:

$$\Box^2 A^\mu - \partial^\mu(\partial_\nu A^\nu) = j^\mu\,, \tag{2.5}$$

where $A^\mu = (\phi, \mathbf{A})$ and $j^\mu = (\rho, \mathbf{j})$. The D'Alembertian operator is defined as

$$\Box^2 \equiv \partial_\mu\partial^\mu\,. \tag{2.6}$$

We have replaced the electric and magnetic field with

$$\mathbf{E} = -\frac{\partial\mathbf{A}}{\partial t} - \boldsymbol{\nabla}\phi\,, \qquad \mathbf{B} = \boldsymbol{\nabla}\times\mathbf{A}\,. \tag{2.7}$$

We can now derive Maxwell's equations for a massless, spin-1 field by writing down the following action:

$$\mathcal{L} = -\frac{1}{4}F_{\mu\nu}F^{\mu\nu}\,, \tag{2.8}$$

where

$$F_{\mu\nu} \equiv \partial_\mu A_\nu - \partial_\nu A_\mu\,. \tag{2.9}$$

The Maxwell theory is invariant under a local symmetry, i.e. the parameters are dependent on space-time. Further, since the Maxwell's equations are locally invariant under a $U(1)$ transformation we will find that the Maxwell tensor $F_{\mu\nu}$ is an invariant, and so the Lagrangian[1] is also invariant.

Now we can couple Maxwell's theory to Dirac's theory to form QED. We use the electron current given as $-e\bar{\psi}\gamma^\mu\psi$ as the source for the Maxwell field and propose the following coupling:

$$eA_\mu\bar{\psi}\gamma^\mu\psi\,. \tag{2.10}$$

This coupling emerges because of the invariance of the Dirac equation under the symmetry transformation

$$\psi \to e^{i\alpha(x)}\psi\,.$$

Since $\alpha(x)$ is a function of space-time we get an extra term $\partial_\mu\alpha(x)$ under the transformation

$$\begin{aligned} \psi(x) &\to \psi'(x) = e^{i\alpha(x)}\psi(x) \\ A_\mu &\to A'_\mu = A_\mu + \frac{1}{e}\partial_\mu\alpha(x)\,, \end{aligned} \tag{2.11}$$

which is eliminated if we introduce the *covariant derivative*:

$$\partial_\mu \to D_\mu \equiv \partial_\mu - ieA_\mu\,. \tag{2.12}$$

Now we obtain a gauge invariant Lagrange function

$$\mathcal{L}_{QED} = \bar{\psi}(i\gamma^\mu D_\mu - m)\psi - \frac{1}{4}F_{\mu\nu}F^{\mu\nu}\,, \tag{2.13}$$

which couples the Maxwell theory with the Dirac theory.

[1] Strictly speaking, $\mathcal{L}$ is the Lagrangian density, but for convenience we will only call it the Lagrangian.

Weak interactions

The weak interaction only acts over small distances, $\sim 10^{-15}$ centimeters, and is recognized by the parity, P, and charge conjugation, C, violation. But the weak interaction is (almost always) invariant under the combined CP operation because of the $\gamma^\mu(1-\gamma^5)$ form, where γ^5 is defined as

$$\gamma^5 \equiv i\gamma^0\gamma^1\gamma^2\gamma^3 \ . \tag{2.14}$$

This is called the $V-A$ (vector-axial vector) structure of the weak current. The consequence is that there are only ν_L and $\bar{\nu}_R$ (the index L stands for left and R stands for right) states in the nature, this is also confirmed in many experiments. In this approach of weak interactions we will study the Fermi theory which couples the currents of decaying processes like β-decay, μ-decay, τ-decay and quark decay. The interaction amplitudes are of the form

$$\mathcal{M} = \frac{4G_F}{\sqrt{2}} J^\mu J^\dagger_\mu \ , \tag{2.15}$$

where G_F is the weak coupling constant (also called the Fermi constant) which is determined by experiments and J^μ is the *charge-raising* weak current

$$J^\mu = \bar{u}_\nu \gamma^\mu \frac{1}{2}(1-\gamma^5) u_e \ , \tag{2.16}$$

and $J^\dagger_\mu$ is the *charge-lowering* weak current

$$J^\dagger_\mu = \bar{u}_e \gamma_\mu \frac{1}{2}(1-\gamma^5) u_\nu \ . \tag{2.17}$$

The index e is either the electron, muon or tau particle and ν is the corresponding neutrino; u is the particle spinor. For processes involving the neutral current, the invariant amplitude is given by

$$\mathcal{M} = \frac{4G_F}{\sqrt{2}} 2\rho J^{NC}_\mu J^{NC,\mu} \ . \tag{2.18}$$

The neutral currents, unlike the charged currents, are not pure $V-A$ currents since they also have right-handed components. In the Standard Model $\rho = 1$ and this is confirmed by experiments within small errors. The definition of the neutral currents is

$$J^{NC}_\mu(\nu) = \frac{1}{2}\left(\bar{u}_\nu \gamma_\mu \frac{1}{2}(1-\gamma^5) u_\nu\right) \ , \tag{2.19}$$

$$J^{NC}_\mu(q) = \left(\bar{u}_q \gamma_\mu \frac{1}{2}(c^q_V - c^q_A \gamma^5) u_q\right) \ . \tag{2.20}$$

In the Standard Model all the $c^i_V, c^i_A, (i = \nu, e, u...)$, are given in terms of one parameter. Fig.2.1 and 2.2 in Section 2.3 are examples of processes involving weak interactions.

Coupling of QED and Weak Interactions

Unfortunately, we are not able to form a symmetry group of weak interactions. But we will be able to form a symmetry group of both electromagnetic- and weak interactions. First we introduce the left-handed isodoublet consisting of a Weyl neutrino and a Dirac electron:

$$\chi_L \equiv \begin{pmatrix} \nu_e \\ e \end{pmatrix}_L \tag{2.21}$$

and a right-handed isosinglet consisting of the right-handed electron:

$$e_R\,. \tag{2.22}$$

This form is a consequence of the fact that the weak interactions violate parity and are mediated by $V-A$ interactions.

Let us define the step-up and step-down operators:

$$\tau_\pm = (\tau_1 \pm i\tau_2)\,, \tag{2.23}$$

where the τ's are the Pauli spin matrices:

$$\sigma_1 = \tau_1 = \begin{pmatrix} 0 & 1 \\ 1 & 0 \end{pmatrix}, \quad \sigma_2 = \tau_2 = \begin{pmatrix} 0 & -i \\ i & 0 \end{pmatrix}, \quad \sigma_3 = \tau_3 = \begin{pmatrix} 1 & 0 \\ 0 & -1 \end{pmatrix}. \tag{2.24}$$

With the defenitions of Equation 2.21–2.24 we are now able to construct a isospin triplet of weak currents:

$$J^i_\mu(x) = \bar{\chi}_L \gamma_\mu \frac{1}{2}\tau_i \chi_L, \qquad \text{with } i = 1,2,3. \tag{2.25}$$

By replacing τ_i with $\tau_\pm$ in Equation 2.25, we will get the charge-raising, $J^+_\mu \equiv J_\mu$, and charge-lowering, $J^-_\mu \equiv J^\dagger_\mu$, currents in Equation 2.16 and 2.17, respectively. The corresponding charges are

$$T^i = \int d^3x\, J^i_0(x) \tag{2.26}$$

which generate an $SU(2)_L$ algebra

$$[T^i, T^j] = i\epsilon_{ijk} T^k. \tag{2.27}$$

T^i is called the *weak isospin* and the subscript L on $SU(2)$ reminds us that the weak isospin current couples only left-handed fermions. Since $J^3_\mu(x)$ only couples left-handed fermions, it can not be identified with the neutral current in Equation 2.19 and 2.20. In order to save the $SU(2)_L$ symmetry, we include the electromagnetic current

$$j^{em}_\mu = \bar{\psi}\gamma_\mu Q \psi\,, \tag{2.28}$$

where Q is the charge operator, and introduce the *weak hypercharge current*

$$j^Y_\mu = \bar{\psi}\gamma_\mu Y \psi\,, \tag{2.29}$$

where the *weak hypercharge* Y is defined by

$$Q = T^3 + \frac{Y}{2}\,, \tag{2.30}$$

where $T^3 = \pm 1/2$ and $Y = -1$ for the left-handed electron and neutrino and $T^3 = 0$ and $Y = -2$ for the right singlet. Like Q is a generator of the $U(1)_{em}$ symmetry group, the hypercharge operator Y generates a symmetry group $U(1)_Y$. We can now write

$$j^{em}_\mu = J^3_\mu + \frac{1}{2} j^Y_\mu\,. \tag{2.31}$$

Thus, by combining the $SU(2)$ and $U(1)$ sectors we have got the charge correct. The result is that we have "unified" the electromagnetic and weak interaction. The relation between the coupling constants is

$$g \sin\theta_W = g' \cos\theta_W = e \ , \tag{2.32}$$

where θ_W is the weak mixing angle. In the Standard Model an isotriplet of vector fields W_μ^i is coupled to the weak isospin current J_μ^i with strength g and a single neutral vector field B_μ is coupled to the weak hypercharge current with strength $g'/2$. The fields given by

$$W_\mu^\pm = \sqrt{\frac{1}{2}} \left(W_\mu^1 \mp i W_\mu^2 \right) \tag{2.33}$$

describe the massive charged bosons $W^\pm$. When generating the masses of the bosons by symmetry breaking (see the Higgs Mechanism below), the two neutral fields will mix and form physical states

$$A_\mu = B_\mu \cos\theta_W + W_\mu^3 \sin\theta_W \ , \tag{2.34}$$

$$Z_\mu = -B_\mu \sin\theta_W + W_\mu^3 \cos\theta_W \ . \tag{2.35}$$

where W_μ^3 is a neutral vector field like B_μ. Equation 2.34 describes a massless physical state, whereas Equation 2.35 describe a massive physical state. By expressing the basic electroweak interaction,

$$-i\, g (J^i)^\mu W_\mu^i - i \frac{g'}{2} (j^Y)^\mu B_\mu \ , \tag{2.36}$$

in terms of A_μ and Z_μ for $W_\mu^i = W_\mu^3$ and using Equation 2.31 (which has to be multiplied by e on both sides) and Equation 2.32 we obtain the observed neutral current

$$J_\mu^{NC} \equiv J_\mu^3 - \sin^2\theta_W j_\mu^{em} \ , \tag{2.37}$$

which is equivalent to Equations 2.19 and 2.20

The Higgs Mechanism

In quantum field theory the electromagnetic and the weak interactions arise from a common symmetry as already shown (this is what is called electroweak theory). But still the electromagnetic and the weak interactions have different range because of the lacking of mass of the photon and the large mass of the $W^\pm$ and Z bosons. What is it that makes the $W^\pm$ and Z bosons massive? In the 1960s Peter Higgs proposed that there should be a neutral particle of spin–0 that gives rise to the mass, not only to the $W^\pm$ and Z bosons, but also to all the constituents-quarks and leptons by interacting with them. This particle is called the Higgs boson. Unfortunately the theory does not predict the mass of the Higgs boson, but experimental searches show that it must weigh more than 107.9 GeV [12] and consistency arguments (when loop-corrections etc. are taken into account) require that it weigh less than 1 TeV.

To see where the masses come from we have to introduce the mechanism of *spontaneous symmetry breaking*, i.e. the Hamiltonian is invariant under some symmetry, but the symmetry is broken because the vacuum state of the Hamiltonian is not invariant.

The gauge invariant Lagrangian for a theory of complex scalar particles coupled to Maxwell's theory is

$$\mathcal{L} = D_\mu \phi^* D^\mu \phi - V(\phi) - \frac{1}{4} F_{\mu\nu} F^{\mu\nu} \,, \tag{2.38}$$

where

$$V(\phi) = \mu^2 \phi^* \phi + \lambda (\phi^* \phi)^2 \,, \tag{2.39}$$

and μ is the mass of a charged scalar particle. D_μ is the same as in Equation 2.12. The coupled system is invariant under a local $U(1)$ gauge transformation:

$$\phi \rightarrow e^{+i\alpha(x)} \phi \tag{2.40}$$

$$\phi^* \rightarrow e^{-i\alpha(x)} \phi^* \tag{2.41}$$

$$A_\mu \rightarrow A_\mu + \frac{1}{e} \partial \alpha(x) \tag{2.42}$$

We take $\mu^2 < 0$ (and $\lambda > 0$) since we want to generate masses by spontaneous symmetry breaking. The vacuum expectation value is given by:

$$\langle \phi \rangle_0 \equiv \langle \phi \rangle_{vacuum} \equiv \langle 0 | \phi | 0 \rangle = v/\sqrt{2} \,, \tag{2.43}$$

where

$$v^2 = -\frac{\mu^2}{\lambda} \,. \tag{2.44}$$

We expand the Lagrangian $\mathcal{L}$ about the vacuum in terms of fields η and ξ by substituting

$$\phi(x) = \sqrt{\frac{1}{2}} [v + \eta(x) + i\xi(x)] \tag{2.45}$$

into Equation 2.38 and obtain

$$\begin{aligned} \mathcal{L}' &= \frac{1}{2}(\partial_\mu \xi)^2 + \frac{1}{2}(\partial_\mu \eta)^2 - v^2 \lambda \eta^2 + \frac{1}{2} e^2 v^2 A_\mu A^\mu \\ &\quad - ev A_\mu \partial^\mu \xi - \frac{1}{4} F_{\mu\nu} F^{\mu\nu} + \text{interaction terms.} \end{aligned} \tag{2.46}$$

Unfortunately the particle spectrum now consists of a massless Goldstone boson ξ, a massive scalar η and a massive vector A_μ. The Goldstone boson is unwanted, so we note that

$$\phi = \sqrt{\frac{1}{2}} (v + \eta + i\xi) \simeq \sqrt{\frac{1}{2}} (v + \eta) e^{i\xi/v} \tag{2.47}$$

to lowest order in ξ. From this we see that if we substitute a set of real fields h, θ and A_μ, where

$$\begin{aligned} \phi &\rightarrow \sqrt{\frac{1}{2}} (v + h(x)) e^{i\theta(x)/v} \\ A_\mu &\rightarrow A_\mu + \frac{1}{ev} \partial_\mu \theta \end{aligned} \tag{2.48}$$

into Equation 2.38 we obatin

$$\begin{aligned} \mathcal{L}'' &= \frac{1}{2}(\partial_\mu h)^2 - \lambda v^2 h^2 + \frac{1}{2} e^2 v^2 A_\mu^2 - \lambda v h^3 - \frac{1}{4} \lambda h^4 \\ &\quad + \frac{1}{2} e^2 A_\mu^2 h^2 + v e^2 A_\mu^2 h - \frac{1}{4} F_{\mu\nu} F^{\mu\nu} \,. \end{aligned} \tag{2.49}$$

In this very special choice of gauge, $\theta(x)$ is chosen so that h is real and we saw in Equation 2.49 that the theory is independent of θ. Fortunately the Goldstone boson has disappeared completely. That is to say it has been "eaten up" by the vector field. This is what is called the Higgs mechanism. The Lagrangian describes two independent interacting massive particles, the massive scalar h, called a Higgs particle, and a vector gauge boson A_μ.

Above we studied the spontaneous breaking of a $U(1)$ gauge symmetry. Now we want to repeat the above procedure for an $SU(2)$ gauge symmetry. This is slightly more difficult than for the $U(1)$ case.

First we define the covariant derivative

$$D_\mu = \partial_\mu + ig\frac{\tau_a}{2}W_\mu^a \tag{2.50}$$

where $W_\mu^a(x)$ with $a = 1, 2, 3$ are three gauge fields. $W_\mu^a(x)$ transforms as

$$\mathbf{W}_\mu \to \mathbf{W}_\mu - \frac{1}{g}\partial_\mu \boldsymbol{\alpha} - \boldsymbol{\alpha} \times \mathbf{W}_\mu \,, \tag{2.51}$$

where $\alpha_a(x)$ are the group parameters, under an infinitesimal gauge transformation

$$\phi(x) \to \phi'(x) = (1 + i\boldsymbol{\alpha}(x) \cdot \boldsymbol{\tau}/2)\phi(x) \,, \tag{2.52}$$

ϕ is a $SU(2)$ doublet consisting of complex scalar fields:

$$\phi = \begin{pmatrix} \phi_1 + i\phi_2 \\ \phi_3 + i\phi_4 \end{pmatrix} . \tag{2.53}$$

From this we can write the local $SU(2)$ invariance of the Lagrangian

$$\mathcal{L} = \left(\partial_\mu\phi + ig\frac{1}{2}\boldsymbol{\tau} \cdot \mathbf{W}_\mu\phi\right)^\dagger \left(\partial^\mu\phi + ig\frac{1}{2}\boldsymbol{\tau} \cdot \mathbf{W}^\mu\phi\right) - V(\phi) - \frac{1}{4}\mathbf{W}_{\mu\nu} \cdot \mathbf{W}^{\mu\nu} \,, \tag{2.54}$$

where

$$V(\phi) = \mu^2\phi^\dagger\phi + \lambda(\phi^\dagger\phi)^2 \tag{2.55}$$

and

$$\mathbf{W}_{\mu\nu} = \partial_\mu\mathbf{W}_\nu - \partial_\nu\mathbf{W}_\mu - g\mathbf{W}_\mu \times \mathbf{W}_\nu \,, \tag{2.56}$$

has been added with the kinetic energy term of the gauge field. The last term in Equations 2.51 and 2.56 arises because of the non-Abelian character of the group.

We are still interested in the case where $\mu^2 < 0$ and $\lambda > 0$. Under these requirements the minimum of the potential is

$$2|\phi|^2 \equiv 2\phi^\dagger\phi = -\frac{\mu^2}{\lambda} \equiv v^2 \,. \tag{2.57}$$

We choose

$$\phi_1 = \phi_2 = \phi_4 = 0 \quad \text{and} \quad \phi_3 = v^2 \,. \tag{2.58}$$

Expanding $\phi(x)$ about this particular vacuum,

$$\phi_0 \equiv \sqrt{\frac{1}{2}}\begin{pmatrix} 0 \\ v \end{pmatrix} , \tag{2.59}$$

we can substitute the expansion

$$\phi \equiv \sqrt{\frac{1}{2}} \begin{pmatrix} 0 \\ v + h(x) \end{pmatrix} , \tag{2.60}$$

into the Lagrangian in Equation 2.54. Since the Lagrangian is locally $SU(2)$ invariant, only one of the four scalar fields remains, namely the Higgs field $h(x)$. The masses of the generated gauge bosons W_μ^a are found by substituting ϕ_0 of Equation 2.59 into the Lagrangian 2.54. The relevant term is

$$\left| ig\frac{1}{2}\boldsymbol{\tau} \cdot \mathbf{W}_\mu \phi \right|^2 = \frac{g^2 v^2}{8} \left[\left(W_\mu^1\right)^2 + \left(W_\mu^2\right)^2 + \left(W_\mu^3\right)^2 \right] . \tag{2.61}$$

In the electroweak model we expand the left side of Equation 2.61 [11] to

$$\left| \left(-ig\frac{1}{2}\boldsymbol{\tau} \cdot \mathbf{W}_\mu - i\frac{g'}{2}B_\mu \right) \phi \right|^2 , \tag{2.62}$$

and calculating this we find

$$M_W = \frac{1}{2} v g \tag{2.63}$$

and

$$M_Z = \frac{1}{2} v \sqrt{g^2 + g'^2}. \tag{2.64}$$

Using Equation 2.32 together with Equations 2.63 and 2.64 we find the relation between the W and Z boson masses:

$$\frac{M_W}{M_Z} = \cos\theta_W . \tag{2.65}$$

The experimental value of $\cos\theta_W$ can be found from

$$\sin^2\theta_W = 0.23124 . \tag{2.66}$$

The boson masses are found to be

$$M_W = 80.41 \text{ GeV}/c^2 \qquad \text{and} \qquad M_Z = 91.187 \text{ GeV}/c^2 . \tag{2.67}$$

The difference between M_W and M_Z is due to the mixing between the W_μ^3 and B_μ fields.

Because of the $V - A$ structure of the weak currents, it is not possible to use mass terms of the form

$$m^2 \bar{\psi}\psi \tag{2.68}$$

for the fermions since this will break the invariance of the Lagrangian. Fortunately the same Higgs doublet which generates the $W^\pm$ and Z masses apply also to the fermions. As an example we will study the generation of the electron mass.

First we include the following $SU(2)\otimes U(1)$ gauge invariant terms into the Lagrangian:

$$\mathcal{L} = -G_e \left[\bar{\chi}_L \phi e_R + \bar{e}_R \bar{\phi} \chi_L \right] , \tag{2.69}$$

where ϕ is given in Equation 2.53. We now spontaneously break the symmetry and substitutes Equation 2.60 into Equation 2.69. The only field left behind after the spontaneously

symmetry breaking is the neutral Higgs field $h(x)$. The other three fields can all been gauged away. After substituting ϕ into Equation 2.69 the Lagrangian becomes:

$$\begin{aligned}\mathcal{L} &= \frac{-G_e}{\sqrt{2}}\left[v(\bar{e}_L e_R + \bar{e}_R e_L) + (\bar{e}_L e_R + \bar{e}_R e_L)h\right] \\ &= -m_e\bar{e}e - \frac{m_e}{v}\bar{e}eh\,, \end{aligned} \tag{2.70}$$

where the last term is an interaction term which couples the Higgs scalar to the electron, and

$$m_e = \frac{G_e}{\sqrt{2}}\,. \tag{2.71}$$

Unfortunately the theory does not predict the value of G_e, so the electron mass has to be found by experiments. The quark masses are generated in the same way as described above. The only difference is for the upper member of the quark doublet (i.e. u, c and t). In this case we have to replace ϕ by

$$\tilde{\phi} = \begin{pmatrix} -\phi_3 + i\phi_4 \\ \phi_1 - i\phi_2 \end{pmatrix}\,, \tag{2.72}$$

which after spontaneously symmetry breaking becomes:

$$\tilde{\phi} = \sqrt{\frac{1}{2}}\begin{pmatrix} v + h(x) \\ 0 \end{pmatrix}\,. \tag{2.73}$$

2.1.2 QCD

Quantum chromodynamics (QCD) is the theory describing the strong interactions. The approach to QCD is more difficult than for the Weinberg-Salam model, only the main results are given here.

The Lagrangian for the QCD is given by

$$\mathcal{L}_{QCD} = -\frac{1}{4}F^a_{\mu\nu}F^{a,\mu\nu} + \sum_{i=1}^{6}\bar{\psi}_i(i\not{D} - m_i)\psi_i\,, \tag{2.74}$$

where the Yang-Mills fields are massless and carries the $SU(3)$ "colour" force (which there are three of). The force carriers are called gluons. The index i of Equation 2.74 is taken over the quark flavours listed in Table 1.1, and the flavour index a represents a global symmetry. In summary the quarks come in six flavours and three colours, but it is only the colour index that participates in the local symmetry.

2.1.3 Weinberg-Salam model + QCD = Standard Model

Now that we have developed the Weinberg-Salam model and the QCD theory, we are ready to marry the two theories. The Standard Model is based on the gauge group $SU(3)\otimes SU(2)\otimes U(1)$. As already mentioned, it can describe all the known fundamental forces of nature except for the gravity.

The Lagrangian of the Standard Model can be written as

$$\mathcal{L}_{SM} = \mathcal{L}_{WS,1} + \mathcal{L}_{WS,2} + \mathcal{L}_{WS,3} + \mathcal{L}_{WS,4} + \mathcal{L}_{QCD} \tag{2.75}$$

where the subscript WS stand for the Weinberg-Salam model. The ingredients of $\mathcal{L}_{WS,1}$[2] are the kinetic energies and self interactions of $W^{\pm}, Z$ and γ. $\mathcal{L}_{WS,2}$ contains the lepton and quark kinetic energies and their interactions with $W^{\pm}, Z$ and γ. The $W^{\pm}, Z, \gamma$ and Higgs masses and couplings are found in the $\mathcal{L}_{WS,3}$ term, while $\mathcal{L}_{WS,4}$ contains the lepton and quark masses and couplings to the Higgs boson.

2.2 The Minimal Supersymmetric extension of the Standard Model

Many scientists do not believe that the Standard Model is the final theory. It can not predict the exact values of the fermion masses and various coupling constants. One of the main goals is to create a theory that unifies all the forces at a sufficiently high energy. Such a theory is called a *Grand Unified theory* (GUT) and the GUT energy scale (where all the forces unify, i.e. there exists only one coupling constant) is $M_x \sim 10^{16}$ GeV. So what we want is a theory where all the gauge interactions belong to a single group

$$G \supset SU(3) \otimes SU(2) \otimes U(1) \; . \tag{2.76}$$

Unfortunately, the Standard Model is not a GUT theory. There are too many unsolved problems like the hierarchy problem[3], the origin of the values of the weak mixing angle and the Cabibbo-Kobayashi-Maskawa(CKM) angles etc.

One approach to solve the hierarchy problem is to introduce *supersymmetric theories* (SUSY) [14] which is the maximum possible extension of the Lorentz group. One consequence of supersymmetry is that it mixes fermionic and bosonic fields:

$$Q|\text{boson}\rangle = |\text{fermion}\rangle \qquad Q|\text{fermion}\rangle = |\text{boson}\rangle \, . \tag{2.77}$$

That is, every fermion get a supersymmetric bosonic partner and the bosons gets supersymmetric fermionic partners. Q is the fermionic generator which satisfy

$$\begin{aligned} \{Q, \bar{Q}\} &= -2\gamma_\mu P^\mu \\ [Q, P^\mu] = \{Q, Q\} &= \{\bar{Q}, \bar{Q}\} = 0 \end{aligned} \tag{2.78}$$

where P^μ is the momentum operator and γ_μ is as usual the Dirac matrices.

To distinguish the names of the supersymmetric and Standard Model particles, it is usual to put an "s" in front of the Standard Model fermion name to create the supersymmetric boson name, f.ex. the supersymmetric partner to the electron becomes selectron in SUSY. In Table 2.1 a list of the chiral multiplets in the MSSM are given, and in Table 2.2 the vector supermultiplets in the MSSM are given.

The B and W^0 mix as in the Standard Model after symmetry breaking, and the Higgsinos mix with the winos and bino to give two charginos $\tilde{\chi}_i^{\pm}$ and four neutralinos $\tilde{\chi}_i^0$.

[2] See [11] pp. 341 for the complete $\mathcal{L}_{WS}$'s.

[3] The hierarchy problem raises the question why there is such a large mass range from the lightest lepton to the heaviest quark, and why the $W^{\pm}$ and Z boson masses are much so smaller than the Planck mass ($\sim 10^{19}$ GeV). The hierarchy problem also arises when calculating the Higgs mass to higher order, when loop-corrections will add up to give an infinite Higgs mass. See [13] for further information.

NAME	spin 0	spin 1/2
squarks, quarks	$\tilde{Q} = (\tilde{u}_L, \tilde{d}_L)$ $\tilde{u}^*_R$ $\tilde{d}^*_R$	$Q = (u_L, d_L)$ $\bar{u}_R$ $\bar{d}_R$
sleptons, leptons	$\tilde{L} = (\tilde{\nu}, \tilde{e}_L)$ $\tilde{e}^*_R$	$L = (\nu, e_L)$ $\bar{e}_R$
Higgs, Higgsinos	$H_u = (H^+_u, H^0_u)$ $H_d = (H^0_d, H^-_d)$	$\tilde{H}_u = (\tilde{H}^+_u, \tilde{H}^0_u)$ $\tilde{H}_d = (\tilde{H}^0_d, \tilde{H}^-_d)$

Table 2.1: *The chiral multiplets in MSSM.*

NAME	spin 1/2	spin 1
gluino, gluon	$\tilde{g}$	g
winos, W's	$\tilde{W}^{\pm}, \tilde{W}^0$	$W^{\pm}, W^0$
bino, B	$\tilde{B}$	B

Table 2.2: *The vector supermultiplets in MSSM.*

SUSY solves the hierarchy problem because it has an equal number of bosons and fermions; thus, the opposite signs in loops cancel the quadratic divergences that appear in the Standard Model.

We are not going to explore the full Minimal Supersymmetric extension of the Standard Model here, but note that in this model we get five physical Higgs bosons after symmetry breaking, h, H, A and $H^{\pm}$. For further reading about MSSM and other SUSY theories see [10, 15].

2.3 Higgs boson production processes in the Standard Model

The leading Higgs production channel at LEP200 is the Higgs-strahlung, Fig. 2.1, but at center of mass energies above $\sqrt{s} \sim 190$ GeV, the WW fusion becomes more important. This is because the energy needed to create a W pair is reached above a center of mass energy of 160 GeV ($m_W = 80.41$ GeV/c^2) and for Higgs masses above ~ 100 GeV/c^2 the Higgs-strahlung becomes less important since $m_Z = 91.187$ GeV/c^2. Another production channel is the ZZ fusion, but as will be shown later, it does not contribute significantly.

2.3.1 Higgs-strahlung, WW fusion and interference

The production amplitude for the Higgs-strahlung (hs) process interfere with the production amplitude for the WW fusion (WW) when the Z boson of the Higgs-strahlung decays into electron neutrinos, i.e.:

$$|\mathcal{M}_{Tot}| \;=\; |\mathcal{M}_{hs} + \mathcal{M}_{WW}|^2$$

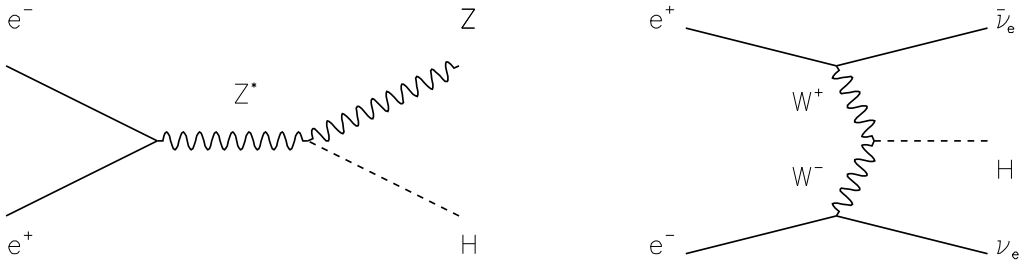

Figure 2.1: *The Higgs-strahlung and WW fusion diagrams.*

$$\begin{aligned} &= |\mathcal{M}_{hs}|^2 + |\mathcal{M}_{WW}|^2 + \mathcal{M}_{hs}^* \mathcal{M}_{WW} + \mathcal{M}_{WW}^* \mathcal{M}_{hs} \\ &= |\mathcal{M}_{hs}|^2 + |\mathcal{M}_{WW}|^2 + 2\mathrm{Re}\{\mathcal{M}_{hs}^* \mathcal{M}_{WW}\} \,, \end{aligned} \tag{2.79}$$

where $2\mathrm{Re}\{\mathcal{M}_{hs}^* \mathcal{M}_{WW}\}$ is the interference term. In [16, 17] the production amplitudes for the Higgs-strahlung and WW fusion are found, respectively.

The differentiated cross section formulae for these processes are found in [18, 19]:

$$\frac{d\sigma(H\nu_e\bar{\nu}_e)}{dE_H\, d\cos\,\theta} = \frac{G_F^3 m_Z^8 p}{\sqrt{2}\pi^3 s}\,(\mathcal{G}_S + \mathcal{G}_I + \mathcal{G}_W) \tag{2.80}$$

with

$$\mathcal{G}_S = \frac{v_e^2 + a_e^2}{96} \frac{s s_\nu + s_1 s_2}{(s - m_Z^2)^2\,[(s_\nu - m_Z^2)^2 + m_Z^2\Gamma_Z^2]} \tag{2.81}$$

$$\mathcal{G}_I = \frac{(v_e + a_e)\,\cos^4\theta_W}{8} \frac{s_\nu - m_Z^2}{(s - m_Z^2)\,[(s_\nu - m_Z^2)^2 + m_Z^2\Gamma_Z^2]} \tag{2.82}$$

$$\times \left[2 - (h_1+1)\,\log\frac{h_1+1}{h_1-1} - (h_2+1)\,\log\frac{h_2+1}{h_2-1} + (h_1+1)(h_2+1)\frac{\mathcal{L}}{\sqrt{r}}\right] \tag{2.83}$$

$$\mathcal{G}_W = \frac{\cos^8\theta_W}{s_1 s_2 r}\left\{(h_1+1)(h_2+1)\left[\frac{2}{h_1^2-1} + \frac{2}{h_2^2-1} - \frac{6s_\chi^2}{r} + \left(\frac{3t_1t_2}{r} - c_\chi\right)\frac{\mathcal{L}}{\sqrt{r}}\right]\right.$$

$$\left. - \left[\frac{2t_1}{h_2-1} + \frac{2t_2}{h_1-1} + (t_1 + t_2 + s_\chi^2)\frac{\mathcal{L}}{\sqrt{r}}\right]\right\} \tag{2.84}$$

These formulae are written explicitly in terms of the polar angle θ of the Higgs, the Higgs momentum $p = \sqrt{E_H^2 - m_H^2}$ and the energy $\epsilon_\nu = \sqrt{s} - E_H$ and invariant mass squared $s_\nu = \epsilon_\nu^2 - p^2$ of the electron neutrino pair. E_H is the Higgs energy. In addition the following abbreviations are adopted from [17]:

$$\begin{aligned} s_{1,2} &= \sqrt{s}(\epsilon_\nu \pm p\,\cos\theta) & t_{1,2} &= h_{1,2} + c_\chi h_{2,1} \\ h_{1,2} &= 1 + 2m_W^2/s_{1,2} & r &= h_1^2 + h_2^2 + 2c_\chi h_1 h_2 - s_\chi^2 \\ c_\chi &= 1 - s s_\nu/(s_1 s_2) & \mathcal{L} &= \log\frac{h_1 h_2 + c_\chi + \sqrt{r}}{h_1 h_2 + c_\chi - \sqrt{r}} \\ s_\chi^2 &= 1 - c_\chi^2\,. \end{aligned} \tag{2.85}$$

The total cross section is obtained by integrating the differential cross section over

$$-1 < \cos\theta < 1 \quad \text{and} \quad m_H < E_H < \frac{\sqrt{s}}{2}\left(1 + \frac{m_H^2}{s}\right) . \tag{2.86}$$

As pointed out in [20], the differential cross section suffers from numerical instability when $p \to 0$ or $\cos\theta \to 0$. To remove the instability the following changes are made. First define

$$\alpha \equiv 1 + c_\chi = \frac{2p^2(1-\cos^2\theta)}{(\epsilon_\nu^2 - p^2\cos^2\theta)} \tag{2.87}$$

$$\Delta_h \equiv h_2 - h_1 = \frac{2m_W^2}{\sqrt{s}}\frac{2p\cos\theta}{(\epsilon_\nu^2 - p^2\cos^2\theta)} . \tag{2.88}$$

We use the following definitions

$$c_\chi = \alpha - 1 \quad \text{and} \quad s_\chi^2 = 2\alpha - \alpha^2 . \tag{2.89}$$

The next step is to break up $\mathcal{G}_W$ into terms of nearly the same order to avoid numerical overflow,

$$\mathcal{G}_W = \frac{\cos^8\theta_W}{s_1 s_2 r}(\mathcal{A} + \mathcal{B} - \mathcal{C} - \mathcal{D}) \tag{2.90}$$

$$\mathcal{A} = (h_1+1)(h_2+1)\left[\frac{2}{h_1^2-1} + \frac{2}{h_2^2-1} - \frac{2\mathcal{L}}{\sqrt{r}}\right] \tag{2.91}$$

$$\mathcal{B} = (h_1+1)(h_2+1)\left[\left(2 + \frac{3t_1t_2}{r} - c_\chi\right)\frac{\mathcal{L}}{\sqrt{r}}\right] \tag{2.92}$$

$$\mathcal{C} = (h_1+1)(h_2+1)\left[\frac{6s_\chi^2}{r}\right] \tag{2.93}$$

$$\mathcal{D} = \left[\frac{2t_1}{h_2-1} + \frac{2t_2}{h_1-1} + (t_1+t_2+s_\chi^2)\frac{\mathcal{L}}{\sqrt{r}}\right] . \tag{2.94}$$

Now $\mathcal{B}$ should be replaced by

$$\mathcal{B} = (h_1+1)(h_2+1) \times \left[(2\alpha\Delta_h^2 + 3\alpha^2(h_1h_2+1) - 2\alpha^2(h_1h_2-1) + 6\alpha(h_1h_2-1) - \alpha^3)\frac{\mathcal{L}}{r\sqrt{r}}\right] , \tag{2.95}$$

to avoid the numerical problem. Although these changes have been made in HZHA02 (see Section 3.5, the energy and angular distributions of the Higgs boson are not significantly changed. But these changes allow us to generate Higgs bosons almost at rest and should therefore not be omitted.

2.3.2 ZZ fusion

The differentiated cross section for the Higgs-strahlung (with Z decaying to e^+e^-), ZZ fusion and interference [19] is given by

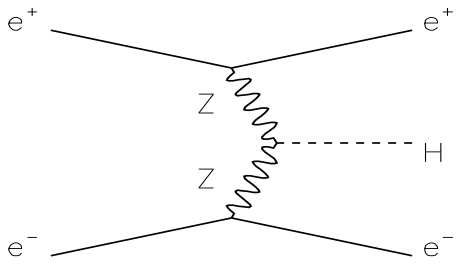

Figure 2.2: *The ZZ fusion diagram.*

$$\frac{d\sigma(He^+e^-)}{dE_H\, d\,\cos\,\theta} = \frac{G_F^3 m_Z^8 p}{\sqrt{2}\pi^3 s}\,(\mathcal{G}_S + \mathcal{G}_I + \mathcal{G}_{Z1} + \mathcal{G}_{Z2})\ , \tag{2.96}$$

with

$$\mathcal{G}_S = \frac{(v_e^2+a_e^2)^2}{192}\,\frac{s s_e + s_1 s_2}{(s-m_Z^2)^2\,[(s_e-m_Z^2)^2+m_Z^2\Gamma_Z^2]} \tag{2.97}$$

$$\mathcal{G}_I = \frac{(v_e^2+a_e^2)^2+4v_e^2a_e^2}{64}\,\frac{s_e-m_Z^2}{(s-m_Z^2)\,[(s_e-m_Z^2)^2+m_Z^2\Gamma_Z^2]} \tag{2.98}$$

$$\times\ \left[2-(h_1+1)\,\log\frac{h_1+1}{h_1-1}-(h_2+1)\,\log\frac{h_2+1}{h_2-1}+(h_1+1)(h_2+1)\frac{\mathcal{L}}{\sqrt{r}}\right] \tag{2.99}$$

$$\mathcal{G}_{Z1} = \frac{(v_e^2+a_e^2)^2+4v_e^2a_e^2}{32 s_1 s_2 r}\left\{(h_1+1)(h_2+1)\left[\frac{2}{h_1^2-1}+\frac{2}{h_2^2-1}-\frac{6s_\chi^2}{r}+\left(\frac{3t_1t_2}{r}-c_\chi\right)\frac{\mathcal{L}}{\sqrt{r}}\right]\right.$$

$$\left.-\ \left[\frac{2t_1}{h_2-1}+\frac{2t_2}{h_1-1}+(t_1+t_2+s_\chi^2)\frac{\mathcal{L}}{\sqrt{r}}\right]\right\} \tag{2.100}$$

$$\mathcal{G}_{Z2} = \frac{(v_e^2-a_e^2)^2}{16 s_1 s_2 r}\,(1-c_\chi)\,\left[\frac{2}{h_1^2-1}+\frac{2}{h_2^2-1}-\frac{6s_\chi^2}{r}+\left(\frac{3t_1t_2}{r}-c_\chi\right)\frac{\mathcal{L}}{\sqrt{r}}\right]\ . \tag{2.101}$$

The abbreviations are the same as in Equation 2.85 with the replacements $\nu \to e$ and $W \to Z$. The ZZ fusion diagram is shown in Fig. 2.2. In this case the interference term arises when the Z boson in the Higgs-strahlung channel decays into a electron-positron pair. Unfortunately, in Equation 2.96 one has already integrated over the electron-positron distributions so it is not possible to generate energy and angular distributions of this pair from this formula.

However, the cross section for the $e^+e^- \to He^+e^-$ is too low, as seen in Fig. 2.3 (the total cross section for all the Higgs production channels is $\sigma_{tot} \sim 295$ fb for $\sqrt{s} = 204$ GeV and $m_H = 105$ GeV), to have any significant contribution to the Higgs searches at LEP, so the interference term between Higgs-strahlung and ZZ fusion is not included in HZHA02. In fact the interference term is negative and will decrease the total cross section for the $e^+e^- \to He^+e^-$ process.

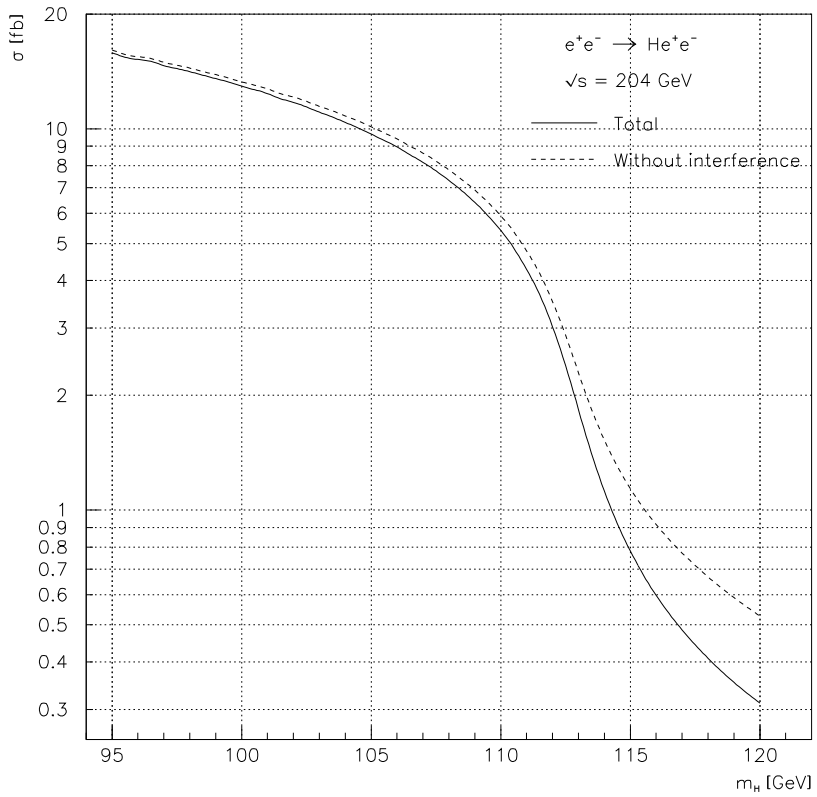

Figure 2.3: *The $e^+e^- \to He^+e^-$ cross section for $\sqrt{s} = 204$ GeV as a function of the Higgs mass. The solid line is with interference while the dashed line is without.*

Chapter 3

Methods

To understand the physics and to know what to look for in particle physics experiments one has to simulate the processes that are known and expected to occur. Simulations are done with computers, and high precision and efficiency are needed. But how are the events generated, and what is needed to make the simulations fast and precise? These questions are the topics of this chapter.

The official LEP physics generator used in Higgs searches is the HZHA [21, 22]. This generator includes all the important Higgs production channels like the Higgs-strahlung, WW fusion and ZZ fusion. A description of how the HZHA generator is built up and how it works will also be given, together with a presentation of the methods used to include the interference term between the Higgs-strahlung and WW fusion (this term was not previously included in HZHA). There are also other possible methods to generate events, see for example [16, 23].

3.1 Event generation

Event generation is done with computer programs simulating physical processes, taking into account every known details. In this section we will study the methods used to generate a process.

First one process has to be chosen. This is done after the theoretical cross sections for each process are computed by the generator. The total cross section,

$$\sigma_{tot} = \sum_{i=1}^{N} \sigma_i \ , \tag{3.1}$$

where the index i is the process number, is then calculated. It is only the processes requested that are included in σ_{tot}, all the other cross sections are set to zero.

The next step takes the cross section from the first process, σ_1, and divides this with σ_{tot}. The resulting number, x_1, is then compared with a random number r between 0 and 1 (this number is generated just once for each generation). If x_1 is less than r, one adds the next process' cross section, σ_2, divided by σ_{tot} to x_1, i.e. x_i will expand as

$$x_i = \frac{\sigma_1 + \sigma_2 + ... + \sigma_i}{\sigma_{tot}} \ , \qquad \text{where} \quad i = 1, 2, ..., N \ , \tag{3.2}$$

until

$$x_i > r \ . \tag{3.3}$$

Process i is then chosen. A schematic diagram of this algorithm is sketched in Fig. 3.1. As can be seen, process number 4 is in this case not requested and σ_4 is therefore set to zero. The first process that gives $x_i > r$ in this example is process number 9, and so this process is generated further.

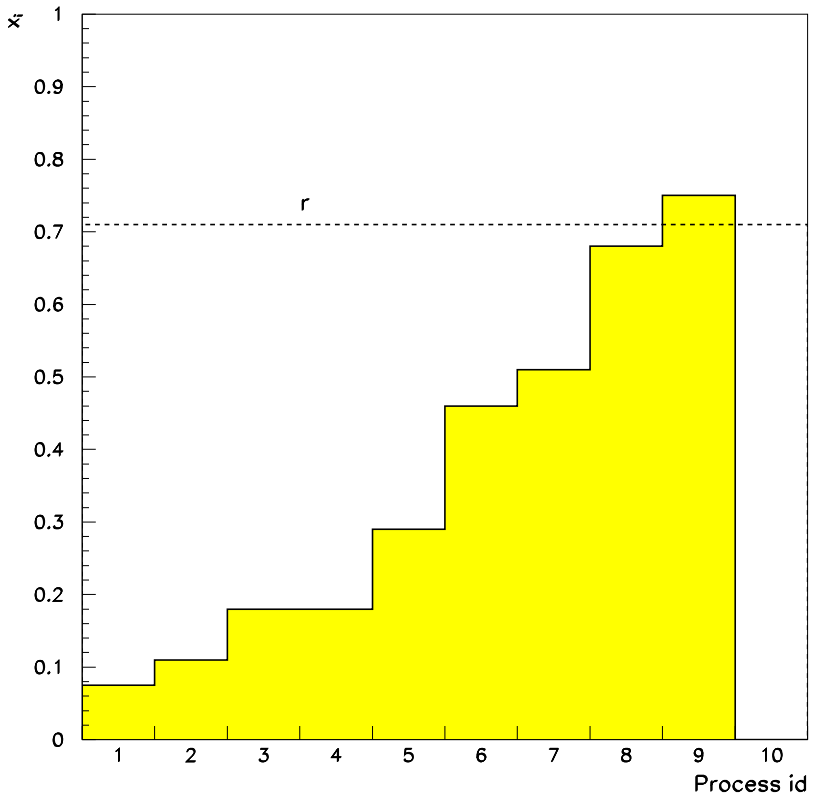

Figure 3.1: *Choosing the process that is to be generated (see the text).*

Once the process to be generated is chosen, the energy and angles for the final particles of the process chosen have to be generated. One approach is to first compute a maximum weight, W_{max}, and then generate the 4-momentum vectors. W_{max} is easiest found by using the differential cross section formulae for the process. As an example we will generate the Higgs boson energy, E_H, and the Higgs angle, $\cos\theta$. First take the value of the lower integration limit of the Higgs energy, $E_{H,low}$, and keep this fixed while the value of $\cos\theta$ is changed from the lower, $\cos\theta_{low}$, to the upper integration limit, $\cos\theta_{high}$, with steps of Δy. The differential cross section is calculated for each value of $\cos\theta$ and E_H. The highest value achieved,

$$z \equiv \frac{d^2\sigma}{dE_H\, d\cos\theta}(E_H, \cos\theta)\,, \tag{3.4}$$

is then stored and a new value for the Higgs energy, E_H, is chosen, i.e. $E_H = E_{H,low} + n\Delta x$, where Δx is the steplength and n is the number of steps performed. $\cos\theta$ will again be varied from the lower to the upper integration limit. If there is calculated a value greater than z, the old value will be replaced by the new one. This process is repeated until the

Higgs energy reaches the upper intgration limit, $E_{H,high}$. The highest z value found is then multiplied with

$$\Delta E_H = E_{H,high} - E_{H,low} \qquad \text{and} \qquad \Delta \cos\theta = \cos\theta_{high} - \cos\theta_{low} \; . \tag{3.5}$$

An example of an algorithm finding W_{max} is shown here:

DO $E_H = E_{H,low}$ **TO** $E_{H,high}$ **STEP** Δx
  DO $\cos\theta = \cos\theta_{low}$ **TO** $\cos\theta_{high}$ **STEP** Δy
    $\mathcal{F} = \frac{d^2\sigma(E_H, \cos\theta)}{dE_H \, d\cos\theta} * \Delta E_H * \Delta\cos\theta$
    IF $\mathcal{F} > z$ **THEN**
      $z = \mathcal{F}$
    ENDIF
  ENDDO
ENDDO
$W_{max} = z$

Now the W_{max} is found, and the event can be generated. We use the differential cross section formula also this time.

The first step is to generate the variables, E_H and $\cos\theta$. These are found by generating a random number that lies between the integration limits. The values are then put into the differential cross section formula and after multiplying it with $\Delta E_H \Delta\cos\theta$ a weight is created. If the weight W_i is greater than W_{max}, a new maximum weight is created by setting $W_{max} = W_i$, then a new weight is generated with new values for E_H and $\cos\theta$ as described above. If W_i is less than W_{max}, the weight is divided by W_{max} and a random number r between 0 and 1 is generated. If now the random number is less than W_i/W_{max}, the weight is "accepted". The 4-momentum vectors are then created for every particle involved in the process. Otherwise, if r is greater than W_i/W_{max}, a new weight has to be generated, this is repeated until, finally, a weight is accepted. An algorithm describing the generation of weights is given below:

start
$E_H = E_{H,low} + random(0,1) * (E_{H,low} - E_{H,high})$
$\cos\theta = -1 + 2 * random(0,1)$
$W_i = \frac{d^2\sigma(E_H, \cos\theta)}{dE_H \, d\cos\theta} * \Delta E_H * \Delta\cos\theta$
IF $W_i > W_{max}$ **THEN**
  $W_{max} = W_i$
ENDIF
IF $W_i/W_{max} < random(0,1)$ **THEN**
  GOTO *start*
ELSE
  $\phi = 2 * \pi * random(0,1)$
  create all the $4-$*momentum vectors*
ENDIF

In the above algorithm, ϕ is the azimuthal angle.

It is important to generate the 4-momentum vectors of all the final state particles, for example for the ZZ fusion the electron and positron also have to be generated. For the WW fusion case it is not necessary because the ν_e's are invisible, and their 4-momentum vectors can be created by using the generated 4-momentum vector of the Higgs boson and conservation of energy and momentum.

It is very important that W_{max} is not too high or low. This will clearly change the outcome of the generation. If W_{max} is too high the efficiency of HZHA will decrease. And if the W_{max} is too low the Higgs energy and angular spectrum will be shifted, an example of this is shown in Fig 3.2. As can be seen the peak of the X (where X can be any variable) distribution has been cut off, instead the distribution has got a bigger tail. In this example the W_{max} is only 1% of the ideal value. To understand this behaviour we

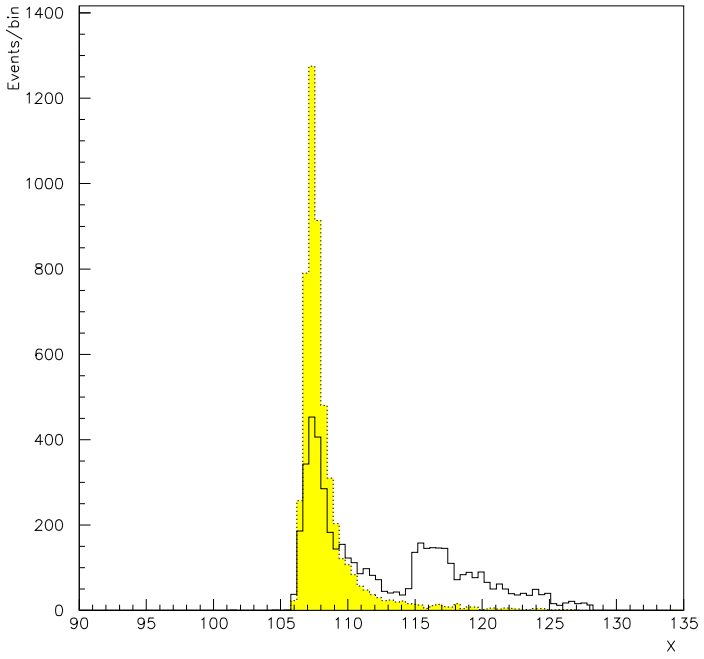

Figure 3.2: *Example on how W_{max} influences the X distribution. The shaded histogram is generated with the correct W_{max} while in the other histogram W_{max} is only 1% of its correct value.*

have to remember the rejection algorithm:

$$\frac{W_i}{W_{max}} > r \ , \tag{3.6}$$

where r is a random number between 0 and 1. When the condition in Equation 3.6 is fulfilled, the event is accepted. But if W_{max} is less than the weight that is generated, a new W_{max} is constructed and a new weight is generated. But this time the weight generated will easier be accepted, even if it is very low. If this happens too often, the distribtuion will clearly be affected.

It is not difficult to construct a generated cross section, σ_{gen}, from the above algorithm. First the sum of all the weights less than W_{max} is obtained:

$$W_{tot} = \sum_{i=1}^{n_{try}} W_i \ , \tag{3.7}$$

where n_{try} is the total number of all the weights *generated* (note that this number is not the same as the number of events that is accepted). σ_{gen} then becomes

$$\sigma_{gen} = \frac{W_{tot}}{n_{try}} \ . \tag{3.8}$$

Also the uncertainty can be computed in a simular way, $\Delta\sigma_{gen}$ then becomes

$$\Delta\sigma_{gen} = \sqrt{\frac{W_{tot}^2}{n_{try}} - \sigma_{gen}^2} \ , \tag{3.9}$$

where

$$W_{tot}^2 = \sum_{i=1}^{n_{try}} W_i^2 \ .$$

3.2 Generating with ISR

Generation of events with *Initial State Radiation* (ISR) is a lot more complicated than without.

In every possible e^+e^- process, ISR will occur and it will therefore contribute to the correction to the process. Correction of the order of 50% may occur for processes where the cross section vary abruptly with energy and the ISR correction should therefore not be neglected. In [16] a full description of the calculation of ISR is given. In this section only an outline of the procedure of generating ISR is given.

In Fig. 3.3 Feynman diagrams for hard, soft and virtual brehmsstrahlung are shown for the process $e^+e^- \to Z$. The decay products of the Z (which also could have been γ and H) is not important in this context and is therefore omitted in the figures.

The first step is to calculate the cross sections for each process without ISR. Then the bremsstrahlung photon's momentum is generated and a choice between the e^+ and e^- beam is made. The initializing of the photon spectrum is done by using iterated interval stretching[1] and the nonradiative cross section. The reduced center of mass energy squared, s', is now found and the event is generated with this value instead of the nonreduced s which is used when generating without ISR. The final step is to rotate and boost the momenta of the final particles by Lorentz-transforming them from the center of mass frame (in which they were generated) to the laboratory frame.

A typical bremsstrahlung photon spectrum is shown in Fig. 3.4. This spectrum was generated with HZHA at $\sqrt{s} = 200$ GeV.

[1]Iterated interval stretching is a technique to approximate a function by a histogram with the same area. This histogram also shows the detailed structure of the function itself. To do this all the bins are made such that the area of all the bins are approximately the same. See Appendix C in [16] for further information.

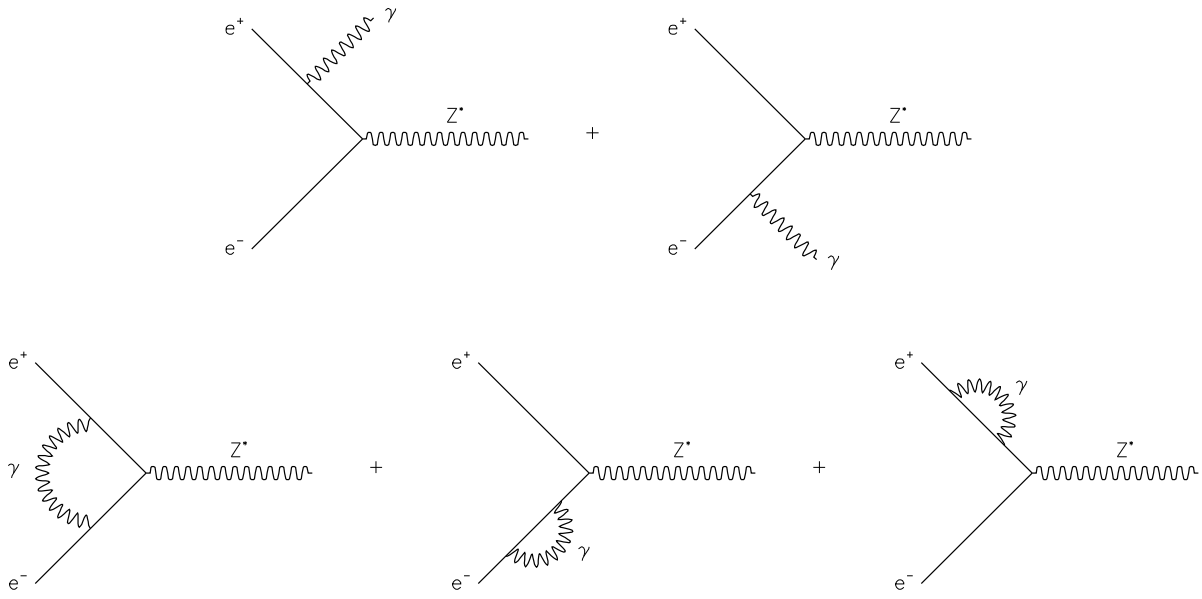

Figure 3.3: *Feynman diagrams for the process $e^+e^- \to Z$ with ISR. The upper diagrams are for soft and hard bremsstrahlung while the three lower diagrams are for virtual photon corrections.*

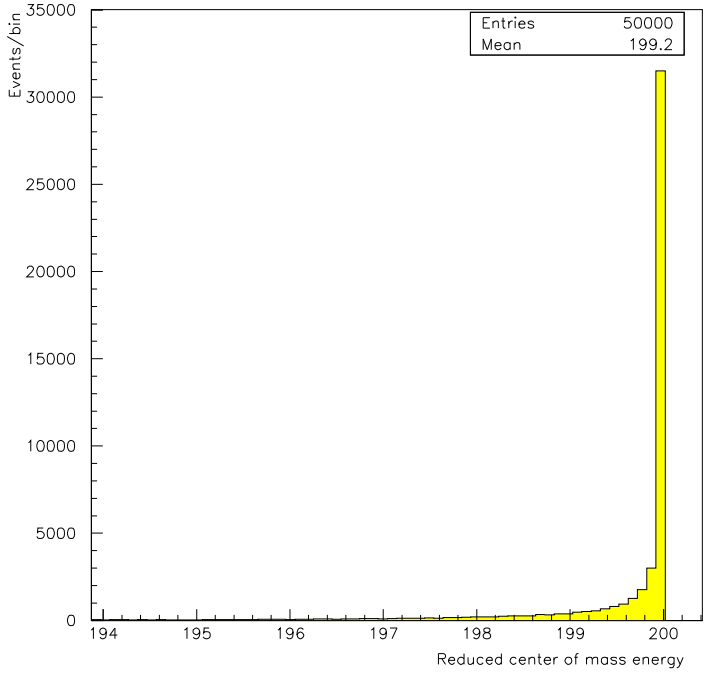

Figure 3.4: *The $\sqrt{s'}$ (see text) distribution for $\sqrt{s} = 200$ GeV.*

3.3 How the HZHA generator works

HZHA is an event generator containing all important neutral Higgs boson production and decay channels in the Standard Model (Higgs-strahlung, WW fusion and ZZ fusion), and neutral and charged Higgs boson production and decay channels in the MSSM (both pair production and single H production) and any type II two-doublet model. In MSSM the masses of H^+H^- are fixed (i.e. $m^2_{H^\pm} = m^2_A + m^2_{W^\pm}$) and generally high, while in the two-doublet model the user can define its own masses and mixing angles.

There are three official versions of HZHA at present (HZHA01, HZHA02 and HZHA03). In addition a modified version of HZHA02 [1, 2] including the interference term between Higgs-strahlung and WW fusion has been released. In Section 3.4 a detailed describtion of how this term was included is given.

The Higgs boson decay modes in HZHA are: $\gamma\gamma$, gg, $\tau^+\tau^-$, $c\bar{c}$, $b\bar{b}$, $t\bar{t}$, W^+W^-, ZZ, $h, H \to AA, A \to Zh$, $H \to hh$, γZ, e^+e^-, $\mu^+\mu^-$, $s\bar{s}$, $\tilde{\chi}\tilde{\chi}$ and $\tilde{\chi}^+\tilde{\chi}^-$.

The initial state radiation (ISR) is generated with the method suggested in [16], but is modified for the possibility of radiation of two photons.

HZHA is linked to `JETSET 7.4` which hadronizes the final state quarks and it is linked to `TAUPOLEP2` which decays the tau leptons.

3.3.1 HZHA step by step

When HZHA is run, it first determines the relevant masses, coupling constants and mixing and then all the branching ratios and decay widths for the Higgs boson are computed. The final initializing step is to calculate the cross sections with and without ISR.

Now the process that is to be generated is found as described in Section 3.1. Then W_{max} is found and the Higgs boson is generated. The Higgs mass and momentum is then stored in an array which is transported to the part of the HZHA which decays the Z boson originating from the Higgs-strahlung channel and then decays the Higgs boson. The decay products of the Z boson and the Higgs boson are hadronized and decayed by `JETSET 7.4` and `TAUPOLEP2`. Then a new process is generated. This is repeated until the number of events requested by the user is reached.

HZHA is finally closed with a summary statistics of the total number of events generated in each of the processses requested and the number of Higgs decays into different channels. During the run of HZHA the Higgs boson production cross sections and decay branching ratios are printed.

3.3.2 The data cards

The data cards enable the user to switch on and off processes, decay modes, ISR etc. The data cards are found in `runhzha.csh`. There are thirteen cards.

The first card is the `GENE` (generator parameters) card. Here the center of mass energy, the ISR flag, SM and MSSM flag and so on is set. This is also the data card where the interference term between Higgs-strahlung and WW fusion is turned on and off in HZHA02 with the `INCL` switch. If interference is requested by the user, the Z boson decay into electron neutrinos in the Higgs-strahlung channel is disabled, since Higgs-strahlung, WW fusion and interference have to be generated as one single process (as will be discussed in the next section), so that this channel is not counted twice. If the user

has asked for both interference and $Z \to \bar{\nu}_e\nu_e$, a warning appears on the screen telling the user that this channel is already included.

The next card is the `GSMO` (Standard Model parameters) where the Z mass and width, top mass, Higgs mass, $\Lambda^{(5)}_{QCD}$ are set. The $\Lambda^{(5)}_{QCD}$ value is used to compute the running strong coupling constant.

In `GSUS`, the SUSY parameters are set. These are the A mass, $\tan\beta$, soft breaking gaugino mass, the mixing terms μ, A_t, A_b and the soft breaking mass terms m_Q, m_U, m_D, m_L, m_E.

The next card is the `PRYN` card where the processes to be generated are chosen for the Standard Model, MSSM and the two-doublet model.

The `GCH1`, `GCH2` and `GCH3` cards enable the H, h and A decays, respectively.

`GHCC` sets the charged Higgs parameters like the decay channels for the two Higgses, m_H, m_h, m_A, m_{H^+}, vacuum expectation values' ratio ($\tan\beta$) and the mixing angle in the neutral scalar sector (α) for the two-doublet model.

The `GCHC` card switches ON and OFF the decay channels for the charged Higgses.

There are also two other data cards, `TRIG` and `DEBU` which decide the first and the last events to be generated and the first and last events to be printed out, respectively.

3.4 Including the interference term into the HZHA02 generator

The inclusion of interference between Higgs-strahlung (with the Z boson decaying into electron neutrinos) and WW fusion into HZHA02 was done by considering all the three terms as *one* single process. Otherwise negative weights could be generated since the differential cross section of the interference term can be negative. The interference term is neither a physical process creating a new particle, and this is also one reason that it has to be included as a separate channel with WW fusion and Higgs-strahlung. The new production channel was given process number 10.

The Z boson decay to electron neutrinos for process number 1, the Higgs-strahlung, is disabled when interference is requested so that this channel is not counted twice. So when interference is requested the $e^+e^- \to HZ \to H\bar{\nu}_e\nu_e$ process is found in process number 10 together with WW fusion and intereference.

3.4.1 Tests to confirm the validity of the inclusion of the interference term into HZHA02

Since (at the time) there were no other accepted physics generators which included the interference term, a lot of tests had to be performed. First the original cross sections of HZHA02 for various combinations of center of mass energies and Higgs masses were compared to the new ones[2] for Higgs-strahlung and WW fusion without interference. In Table 3.1 some cross sections for different Higgs masses are shown for $\sqrt{s}$ =200 GeV. The comparison was also done for cross sections with ISR, and also here there was a good agreement.

[2]See Section 2.3.1.

	Original			New		
m_H [GeV]	σ_{hs} [fb]	σ_{WW} [fb]	σ_{hs+WW} [fb]	σ_{hs} [fb]	σ_{WW} [fb]	σ_{hs+WW} [fb]
95.	29.2	6.25	35.5	29.3	6.12	35.4
100.	22.7	5.21	27.9	22.7	5.10	27.8
105.	14.3	4.30	18.6	14.4	4.21	18.6
110.	2.65	3.51	6.16	2.68	3.44	6.12
115.	0.733	2.83	3.56	0.739	2.77	3.51
120.	0.352	2.24	2.59	0.355	2.19	2.55

Table 3.1: *The theoretical cross sections computed by HZHA for the process* $e^+e^- \to H\nu_e\bar{\nu}_e$ *at* $\sqrt{s} = 200$ *GeV (*σ_{hs} *= Higgs-strahlung cross section,* σ_{WW} *= WW fusion cross section and* σ_{hs+WW} *= the total cross section for Higgs-strahlung and WW fusion without interference).*

Later it was discovered some unstabilities in the cross sections for low Higgs masses. But these unstabilities were corrected in the second version of the modified HZHA02. This will be discussed in Section 3.5.

Now the interference term was disabled in the new formulae and algorithms and the energy and angular distributions for the Higgs-strahlung and WW fusion were compared to the original distributions of HZHA02 as shown in Fig. 3.5. The agreement is, as seen, very good. This is also true for Higgs masses above the Higgs-strahlung threshold, i.e. $m_H > \sqrt{s} - m_Z$ as shown in Fig 3.6. The complete process, including Higgs-strahlung, WW fusion and interference, was compared to the theoretical energy and angular distribution as shown in Fig. 3.7.

The new formulae and algorithms also had to be verified with ISR for the energy and angular distributions. The interference term was once again disabled. The distributions were also this time in very good agreement with the original distributions as shown in Fig 3.8. But now the interference term could not be compared to any theoretical distributions since the ISR photons are *generated* in HZHA, however since the cross sections and distributions of the Higgs-strahlung and WW fusion with ISR and the distributions with interference and without ISR were in very good agreement with the theoretical formulae and the original cross sections and distributions of HZHA, we conclude that the interference term is correctly implemented.

3.5 An update of HZHA02

In March 2000 a new version of the modified HZHA02 was released. In this version several changes were done. One of the changes was the correction suggested in [20] as mentioned in Section 2.3.1. The formula for $\mathcal{G}_W$ in the Higgs generation part of process number 10 was replaced by Equation 2.90. Now a Higgs boson with $p \to 0$ or $\cos\theta \to 0$ can be generated. But the change does not have any significant effect on the energy and angular distributions.

The fluctuations in the cross sections for low Higgs masses were also removed. These unstabilities were caused by the precision chosen for the integration of the differential cross section formula. This is integrated with the `CERNLIB` routine [24] `DGMLT2`, which performs

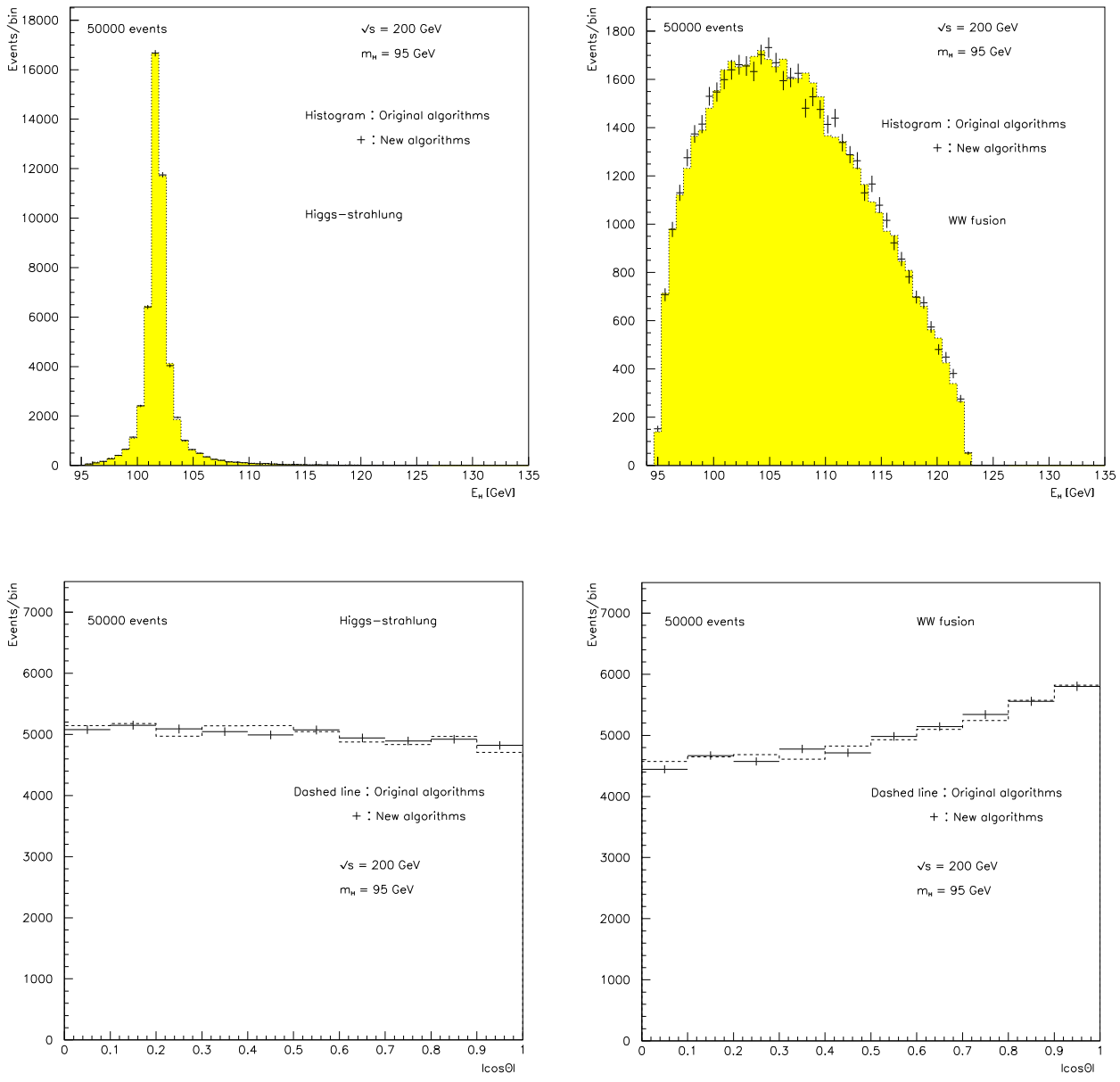

Figure 3.5: *Comparison of the Higgs energy and angular distribution between the original and new formulae and algorithms of HZHA02 at* $\sqrt{s} = 200$ *GeV for* $m_H = 95$ *GeV. Interference is not included.*

a Gaussian quadrature integration for double integrals. Since the energy distributions of the Higgs-strahlung and the interference term have very sharp peaks, the integration over the Higgs energy becomes difficult with a small number of integration intervals as was the case here. The energy distribution for $\sqrt{s} = 200$ GeV and $m_H = 60$ GeV is shown in Fig. 3.9. This was taken care of by increasing the number of integration intervals for the Higgs-strahlung and interference term. But to avoid HZHA02 from getting slower, the WW fusion part of the formula was separated and the number of integration intervals

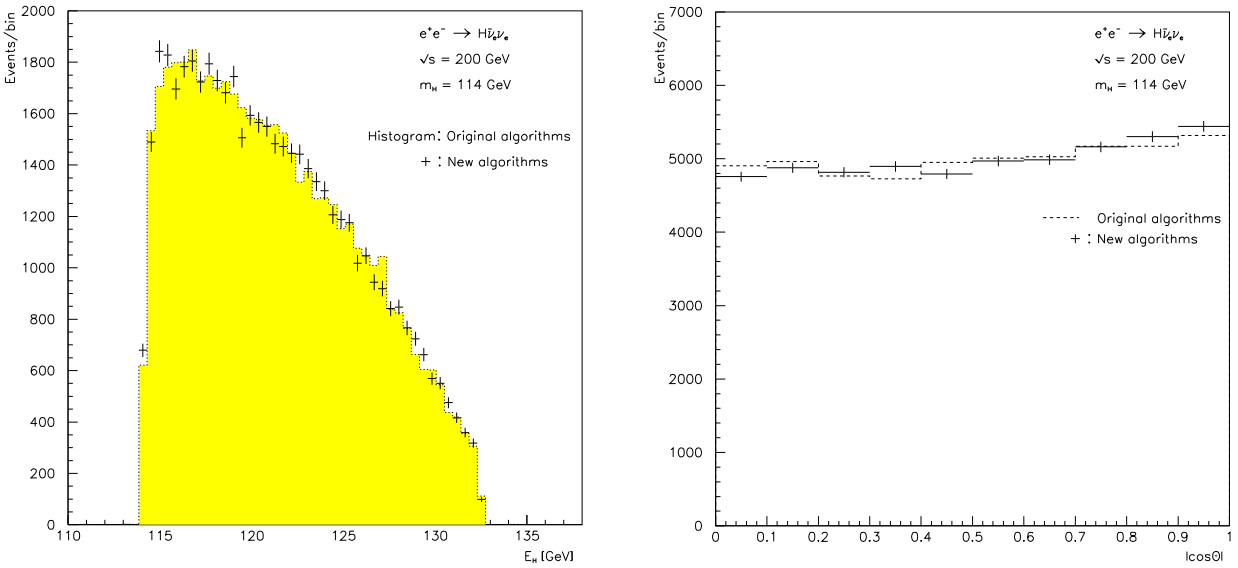

Figure 3.6: *Comparison of the Higgs energy and angular distributions for the Higgs-strahlung + WW fusion between the original and new formulae and algorithms of HZHA02 at $\sqrt{s} = 200$ GeV for $m_H = 114$ GeV. Interference is not included.*

was set lower for this process, this could be done since the energy distributon of the WW fusion is almost flat. For the same reason the integration over $\cos\theta$ could also be done with a smaller number of integration intervals for both the Higgs-strahlung and interference part and WW fusion part. Still the cross sections become unstable at Higgs masses below $\sim \sqrt{s} - 135$ GeV, but at this scale the interference term is no longer important and should be omitted to increase the efficiency of HZHA02. If the user by accident still requests generation with interference below this limit, a warning will appear on the output. The old and new cross sections can be seen in Fig. 3.10.

In the new version *Improved Born approximation* (IBA), ZZH- and WWH-vertex corrections [25] were included for process number 10. In the first modified version of HZHA02 which included interference, there was a difference in the cross sections between HZHA03[3] and HZHA02 of about 2% for Higgs masses between 115 GeV and 120 GeV for $\sqrt{s} = 200$ GeV. After IBA and ZZH- and WWH-vertex corrections were included the difference is now below 1% which is the claimed accuracy of HZHA [26]. In Fig. 3.10 the new cross section as a function of the Higgs mass together with

$$\frac{\delta\sigma}{\sigma} = \frac{\sigma_{HZHA03} - \sigma_{HZHA02}}{\sigma_{HZHA03}} \tag{3.10}$$

where σ_{HZHA02} and σ_{HZHA03} are the cross sections of HZHA02 and HZHA03, respectively, are shown.

It is also possible to generate the MSSM CP-even light scalar Higgs boson in the new modified version of HZHA02. Since the couplings to W and Z gauge bosons in MSSM

[3]HZHA03 is the new public release of HZHA, this version also includes interference between the Higgs-strahlung and WW fusion.

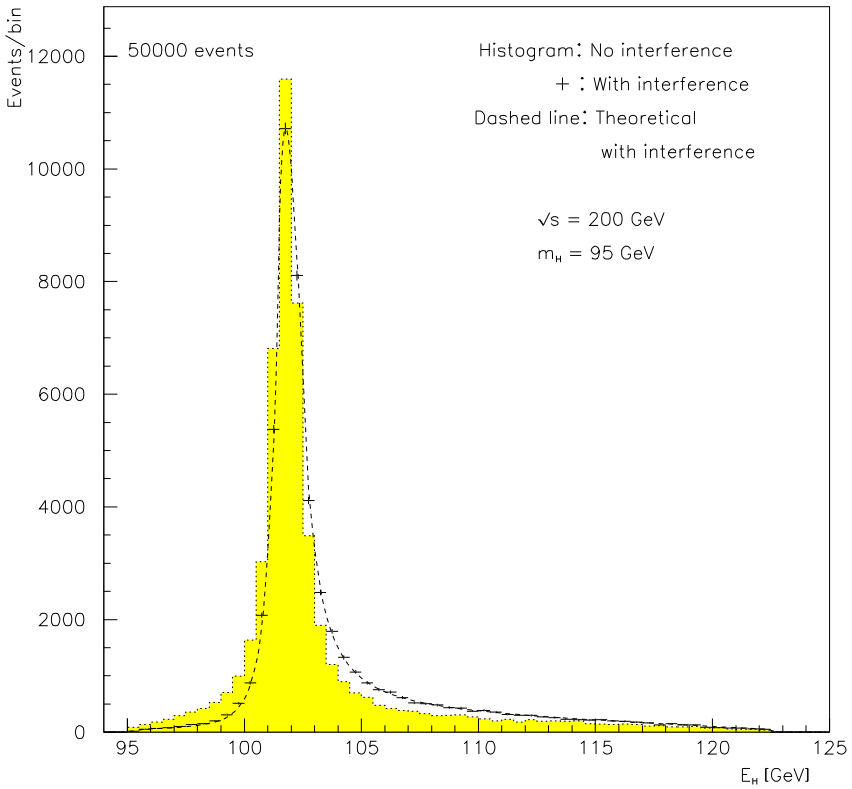

Figure 3.7: *Comparison of the generated energy spectrum (crosses) for the process* $e^+e^- \to H\nu_e\bar{\nu}_e$ *with interference with the theoretical distribution (dashed line) for* $\sqrt{s} = 200$ *GeV and* $m_H = 95$ *GeV. The histogram is the generated energy distribution without interference. The total cross section is 37.9 fb.*

are shared by the CP-even light scalar Higgs bosons [27], only the overall normalization of the cross section with respect to the Standard Model is changed. The cross section formula becomes

$$\sigma(h)_{MSSM} = \sin^2(\beta - \alpha) \times \sigma(H)_{SM} \tag{3.11}$$

in MSSM, where β is the mixing angle determined by the ratio of the vacuum expectation values of the two neutral Higgs fields in MSSM, while α is the mixing angle in the CP-even Higgs sector. It is not difficult to include the heavy scalar Higgs boson, H, in MSSM too, but this is not done in the modified version of HZHA02. The cross section formula in this case is:

$$\sigma(H)_{MSSM} = \cos^2(\beta - \alpha) \times \sigma(H)_{SM} \, . \tag{3.12}$$

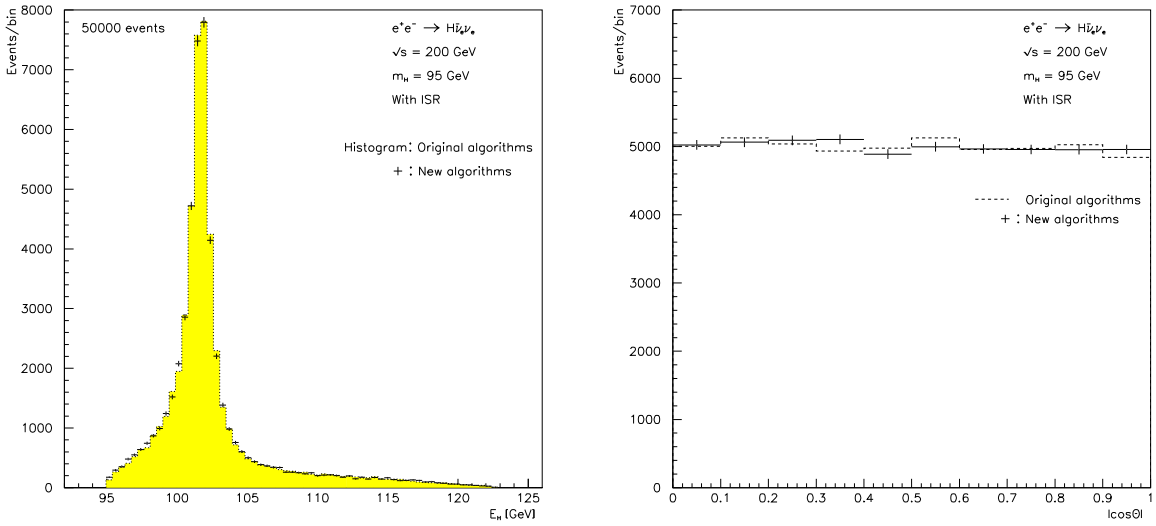

Figure 3.8: *Comparison of the original version of HZHA02 and the new version for the energy (left) and angular (right) distributions with ISR for the Higgs-strahlung + WW fusion, $\sqrt{s} = 200$ GeV and $m_H = 95$ GeV. Interference is not included.*

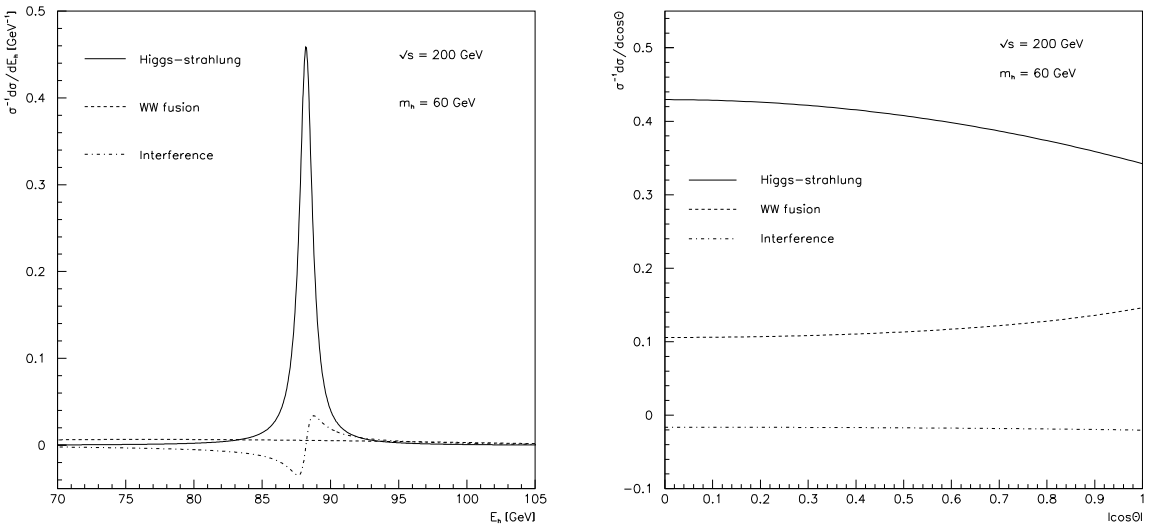

Figure 3.9: *The individual differential cross sections versus Higgs energy (left) and $|cos\theta|$ (right) of the Higgs boson for the process $e^+e^- \to h\nu_e\bar{\nu}_e$ at $\sqrt{s} = 200$ GeV and $m_H = 60$ GeV. The individual curves are normalized to the total cross section of 74.1 fb.*

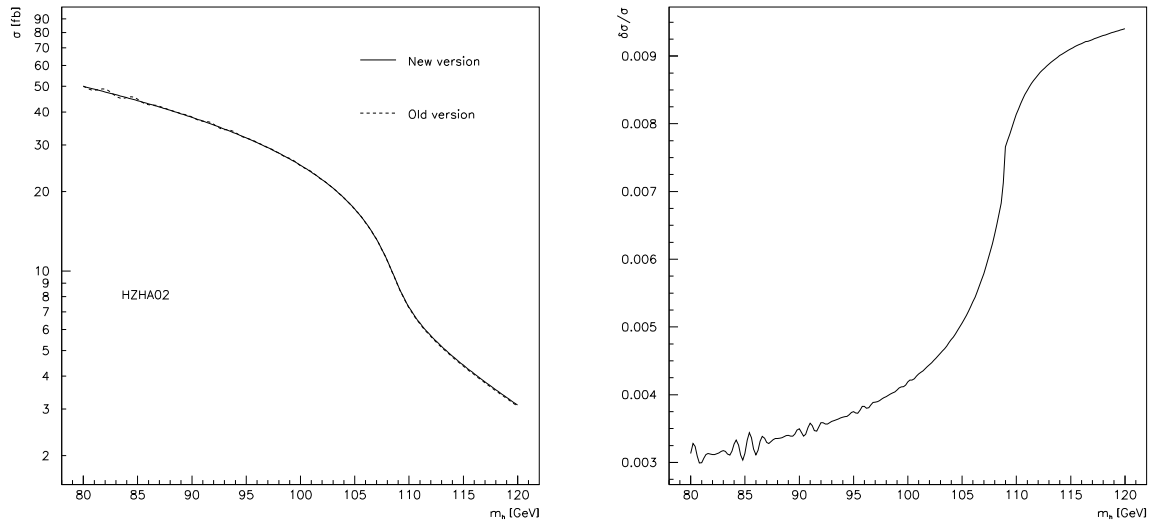

Figure 3.10: *The cross section with ISR for the process $e^+e^- \to h\nu_e\bar{\nu}_e$ with interference at $\sqrt{s}$ = 200 GeV (left). The dashed line shows the cross section for the old modified version of HZHA02, while the solid line shows for the new modified version with IBA and ZZH- and WWH- vertex corrections. The plot to the right shows $\delta\sigma/\sigma$ as a function of the Higgs mass, where $\delta\sigma$ is the difference between HZHA03 and the modified version of HZHA02 (see the text).*

Chapter 4

Results

12th of November 1999 a new public version of HZHA was released, namely the HZHA03. This version also includes the interference term between Higgs-strahlung and WW fusion, but the work with including the interference term into HZHA02 has not been wasted since there are different sets of formulae and algorithms in the two versions. Further, HZHA02 and HZHA03 have been tested and compared to each other.

In this chapter the results of including the interference term is presented. First for the Standard Model and then for MSSM. Also comparisons between the modified version of HZHA02 and HZHA03 are made.

Before presenting the results, a summary of the changes from the first modified version of HZHA02 (in this chapter refered to as HZHA02TF$_1$) and the updated modified version (in this chapter refered to as HZHA02TF$_2$) and the changes from HZHA02TF to HZHA03 [21] will be given. All the changes from HZHA02TF$_1$ to HZHA02TF$_2$ concern the Higgs-strahlung with $H\nu_e\bar{\nu}_e$ in the final state, WW fusion and interference channel:

- Instabilities occuring in the cross section for low Higgs masses were corrected.
- Improved Born approximation and ZZH- and WWH-vertex corrections were included.
- Corrections to the original formulae were made, allowing generation of Higgs bosons almost at rest.
- Possibility to generate the CP even light scalar Higgs boson of the MSSM.

The most important changes from HZHA02TF to HZHA03 are:

- All routines were rewritten with double precision.
- A bug in the Higgs-strahlung production was corrected.
- A numerical singularity in the $H \to Z\gamma$ decay was corrected.
- Interference between the Higgs-strahlung and ZZ fusion with He^+e^- in the final state was included.
- Radiative corrections to Higgs boson masses in the MSSM were included.

- Top threshold two loop corrections to the Higgs boson masses and couplings were also implemented.
- Possibility to compute SUSY spectrum in the SUGRA framework.
- The linear combination of the gaugino mass terms M_1 and M_2 was replaced by M_2.
- Anomalous Higgs couplings were modified.

4.1 The Standard Model

At higher energies, i.e. energies above $\sim$ 190 GeV, the WW fusion becomes important, specially when the interference term in the $e^+e^- \to H\nu_e\bar{\nu}_e$ process is included. In Fig. 4.1 the cross section for the Higgs-strahlung, WW fusion and interference is shown as a function of the Higgs mass for $\sqrt{s}$ = 204 GeV. In Table 4.1, the effect of interference is shown for some Higgs masses. Note that the cross sections shown in Fig. 4.1 and

m_H [GeV]	σ [fb]	σ_{int} [fb]	**effect** [%]
95.	37.3	39.0	4.55
100.	31.0	33.4	7.74
105.	24.0	27.0	12.5
110.	14.9	18.5	24.2
115.	4.84	7.38	52.5
120.	3.11	4.65	49.5
125.	2.30	3.31	43.9

Table 4.1: *The effect of the interference for the process* $e^+e^- \to H\nu_e\bar{\nu}_e$ *at* $\sqrt{s} = 204$ *GeV* (σ *is the cross section without interference and* σ_{int} *is with the interference term).*

Table 4.1 are only the theoretical cross sections without ISR, IBA and ZZH- and WWH-vertex corrections. The effect of the corrections were shown in Fig. 3.10 for $\sqrt{s}$ = 200 GeV. The threshold for Higgs-strahlung production, i.e. maximum Higgs mass for on-shell ZH production, is given by

$$m_{H,thr} = \sqrt{s} - m_Z \ . \tag{4.1}$$

Above the threshold it is the WW fusion with interference that dominates as can be seen in Fig. 4.1. Below this value a typical differential cross section versus Higgs energy and Higgs angle can be like as already shown in Fig. 3.9 or as shown in Fig. 4.2 at $\sqrt{s} = 200$ GeV for m_H = 60 and m_H = 95 GeV, respectively. Notice the negative contribution from the interference in the Higgs energy spectrum. As can be seen the interference term makes the Higgs energy spectrum a little harder.

For Higgs masses above the Higgs-strahlung threshold, the differential cross section versus Higgs energy is different from that below threshold. This is shown in Fig. 4.3 for $\sqrt{s} = 200$ GeV and $m_H = 112$ GeV.

When ISR is included both the cross section and the energy distribution are affected. In Table 4.2 the effect of ISR on the total cross section for the process $e^+e^- \to H\nu_e\bar{\nu}_e$ at $\sqrt{s}$ = 204 GeV for various Higgs boson masses is shown (here we have included the

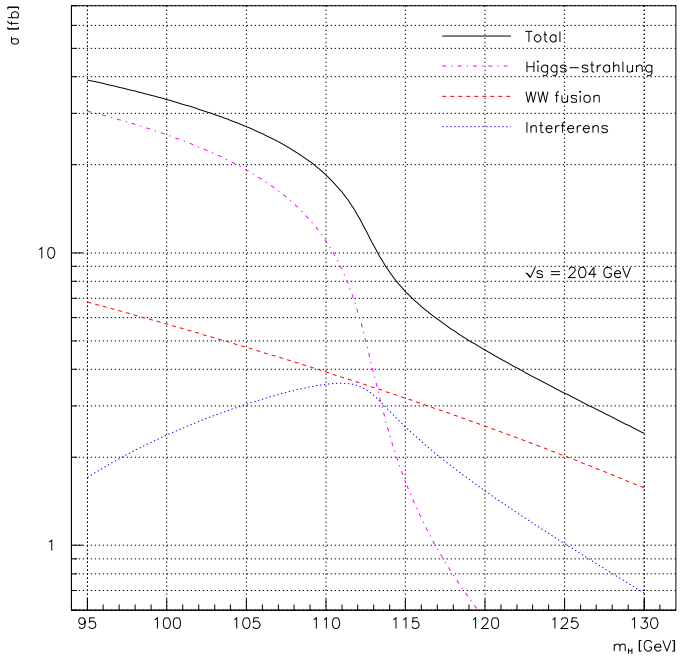

Figure 4.1: *The cross section for the process* $e^+e^- \to H\nu_e\bar{\nu}_e$ *as a function of the Higgs mass for* $\sqrt{s} = 204\ GeV$.

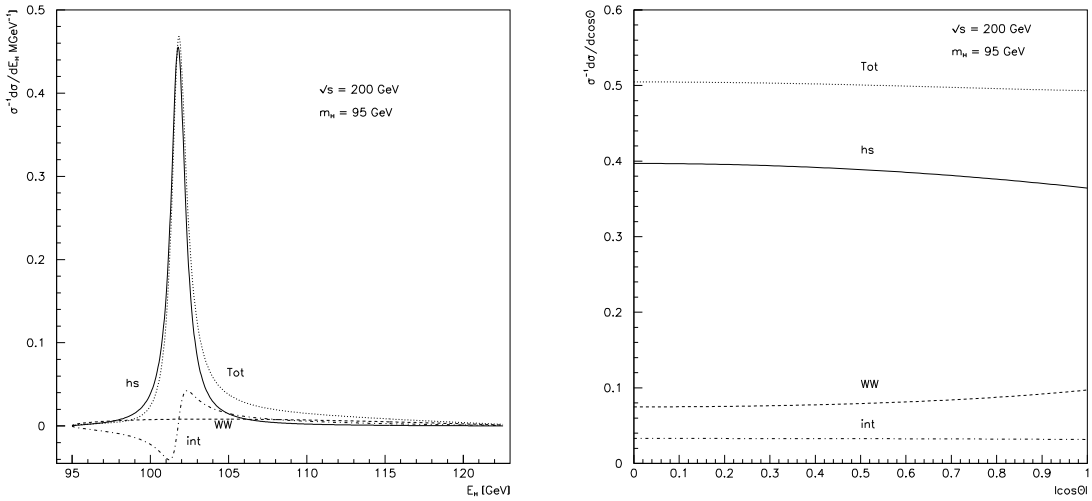

Figure 4.2: *Theoretical differential cross sections versus Higgs energy (left) and* $|cos\theta|$ *(right) of the Higgs boson for* $e^+e^- \to H\nu_e\bar{\nu}_e$ *at* $\sqrt{s} = 200\ GeV$ *and* $m_H = 95\ GeV$. *The individual curves are normalized to the total cross section of 37.9 fb (hs = Higgs-strahlung, WW = WW fusion, int = interference term and Tot = total distribution).*

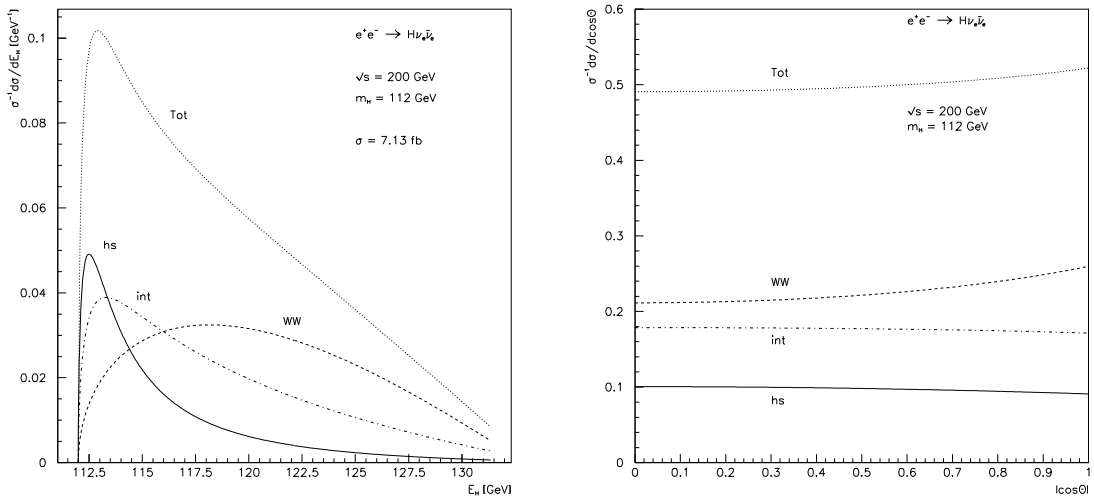

Figure 4.3: *Theoretical differential cross sections versus Higgs energy (left) and $|cos\theta|$ (right) of the Higgs boson for $e^+e^- \to H\nu_e\bar{\nu}_e$ at $\sqrt{s} = 200$ GeV and $m_H = 112$ GeV. The individual curves are normalized to the total cross section of 7.13 fb (hs = Higgs-strahlung, WW = WW fusion, int = interference term and Tot = total distribution).*

m_H [GeV]	σ [fb]	σ_{ISR} [fb]	**effect** [%]
95.	38.9	33.5	-13.9
100.	33.4	27.8	-16.8
105.	27.0	21.5	-20.4
110.	18.5	14.0	-24.3
115.	7.42	5.94	-19.9
120.	4.69	3.85	-17.9

Table 4.2: *The effect of the ISR for $e^+e^- \to H\nu_e\bar{\nu}_e$ including contributions from Higgs-strahlung, WW fusion and interference at $\sqrt{s} = 204$ GeV for some Higgs masses (σ is without and σ_{ISR} is with ISR).*

IBA, ZZH- and WWH-vertex corrections). The effect of ISR first increases for low Higgs masses and then decrease at higher masses. this behaviour can be related to the slope on the cross section curve shown in Fig. 4.1. In Fig. 4.4 the cross section without ISR and interference is shown for the process $e^+e^- \to H\nu_e\bar{\nu}_e$ together with the cross section with interference and no ISR and the cross section with both ISR and interference. Actually as can be seen, the cross section for high Higgs masses is greater with interference and ISR than without ISR and interference while for low Higgs masses the opposite is true. The effect of ISR on the Higgs energy and angular distributions is shown in Fig. 4.5. As can be seen the ISR part makes the energy peak a little lower and it is generated a lot more Higgses with energy between 95 GeV and $\sim$ 101 GeV than without ISR, while the tail is almost unchanged. The angular distribution is, as for the effect of interference, not significantly affected. The angular and energy distributions above the Higgs-strahlung

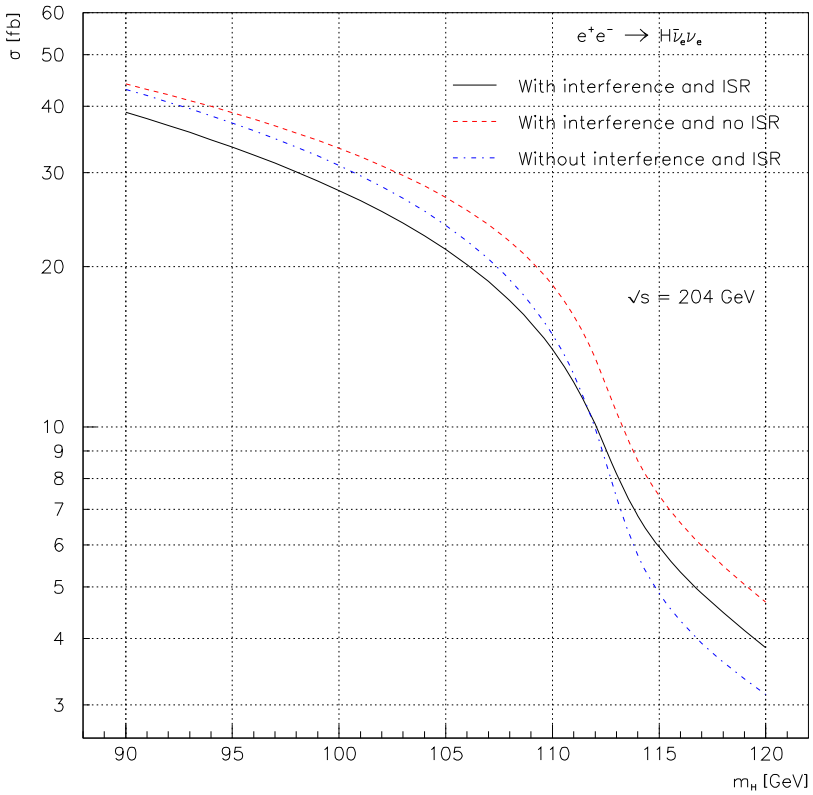

Figure 4.4: *Cross sections for $e^+e^- \to H\nu_e\bar{\nu}_e$ as functions of Higgs mass with and without interference and ISR at $\sqrt{s} = 204$ GeV.*

threshold are, as shown in Fig. 4.6, almost unchanged. So the only significant effect for Higgs masses above the threshold is on the production cross section.

4.2 MSSM

As already mentioned in Chapter 3.5 HZHA02TF$_2$ can generate the CP-even light scalar Higgs boson in the MSSM. Since the only change to the cross section is an overall normalization factor, $0 < \sin^2(\beta - \alpha) < 1$, the cross section will only be reduced with respect to $\sin^2(\beta - \alpha)$ term for each m_h. This factor has no influence on the Higgs energy and the Higgs angle, so the energy and angular distributions will not be changed. In Fig. 4.7 the cross section for $e^+e^- \to h\nu_e\bar{\nu}_e$ with interference as a function of m_h is shown. In this figure $\tan\beta = 20$ and $\sqrt{s} = 200$. Note that α depends on the H, h and Z mass. In fact the Standard Model cross section for the $e^+e^- \to h\nu_e\bar{\nu}_e$ decreases slower with m_h than $\sin^2(\beta - \alpha)$ is increasing. As can be seen the Higgs-strahlung cross section decreases at $m_h > 106$ GeV, and the WW fusion and interference cross sections at $m_h > 114$ GeV.

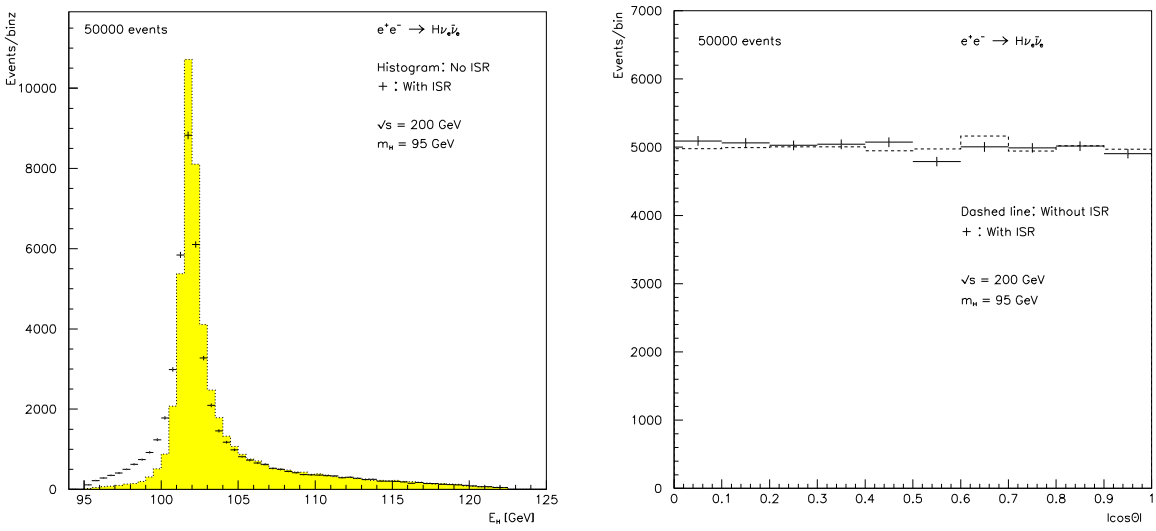

Figure 4.5: *The energy (left) and angular (right) distributions for* $e^+e^- \to H\nu_e\bar{\nu}_e$ *with and without ISR at* $\sqrt{s} = 200$ *GeV and* $m_H = 95$ *GeV. The total cross section without ISR is 37.9 fb and with ISR it is 31.9 fb.*

4.3 Comparing the modified version of HZHA02 with HZHA03

After the release of HZHA03 a serie of tests were performed to verify the inclusion of interference in this new version. HZHA03 uses other formulae and algorithms than HZHA02TF

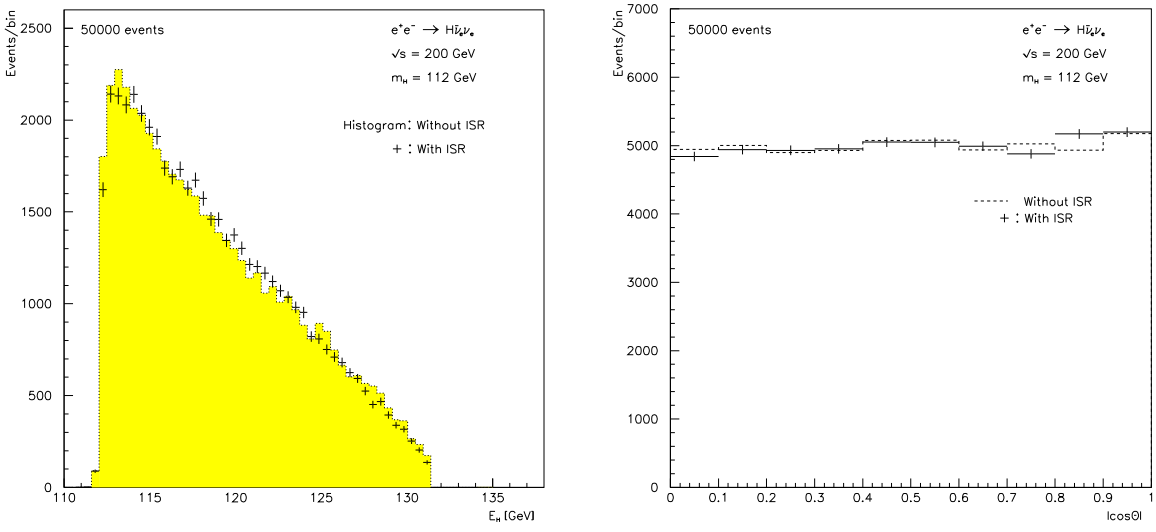

Figure 4.6: *The energy (left) and angular (right) distributions for* $e^+e^- \to H\nu_e\bar{\nu}_e$ *with and without ISR above the Higgs-strahlung threshold,* $\sqrt{s} = 200$ *GeV and* $m_H = 112$ *GeV. The total cross section without ISR is 7.03 fb and with ISR it is 5.69 fb.*

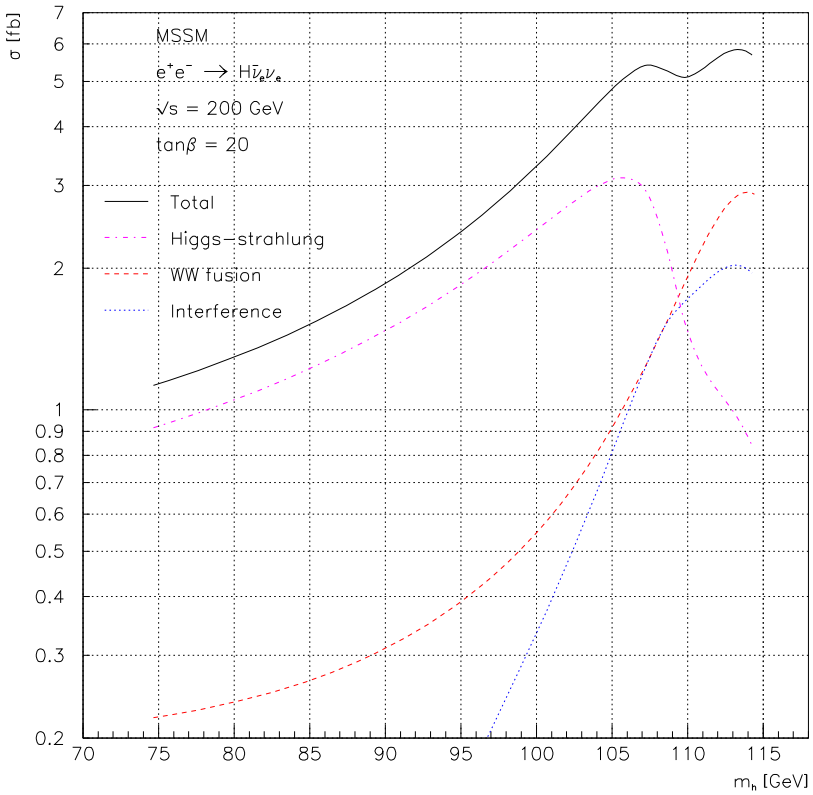

Figure 4.7: *The MSSM cross section at* $\sqrt{s} = 200$ *GeV for* $\tan\beta = 20$ *as a function of the* h *mass.*

and it is therefore perfect to compare the results of the two generators. When this was done there were found a couple of bugs in the energy spectrum of HZHA03 both for Higgs masses below and above the Higgs-strahlung threshold for the $e^+e^- \to H\nu_e\bar{\nu}_e$ process. After some correspondance with the author of HZHA, P. Janot, the bugs were corrected [21].

The Standard Model cross sections were compared and the difference, Equation 3.10, was shown in Fig. 3.10. As already mentioned the difference is now below 1% which is the claimed accuracy of HZHA [26]. The MSSM cross sections were also compared, Table 4.3. The differences in m_h for HZHA02TF$_2$ and HZHA03 for fixed values of m_A and $\tan\beta$ are due to the implementation of radiative corrections to the Higgs boson masses and top threshold loop corrections for MSSM in HZHA03 [21]. The differences in the Higgs masses also lead to the differences in the cross sections as shown in Table 4.3. To see this we have to cheat a little: First the cross sections of HZHA02TF$_2$ are computed in the Standard Model for the same Higgs masses as for the HZHA03 (which are computed in MSSM). Then the Standard Model cross sections of HZHA02TF$_2$ are multiplied by the same $\sin^2(\beta - \alpha)$ factor as for HZHA03. The results are shown in Table 4.4. As can be seen, the cross sections of both the versions are this time within 1% of each other, which is the claimed accuracy of HZHA [26].

		HZHA02TF$_2$			HZHA03		
m_A [GeV]	$tan\beta$	m_h [GeV]	σ [fb]	σ_{ISR} [fb]	m_h [GeV]	σ [fb]	σ_{ISR} [fb]
75	2	60.084	46.42	46.03	60.835	45.61	45.13
75	20	74.672	1.096	1.035	74.691	1.045	0.9866
90	2	66.177	48.28	46.92	67.068	47.32	45.87
90	20	89.354	1.805	1.602	89.396	1.654	1.470

Table 4.3: *Cross sections for Higgs-strahlung, WW fusion and interference in MSSM for production of the lightest neutral Higgs at* $\sqrt{s} = 204$ *GeV* (σ *is the cross section without ISR, while* σ_{ISR} *is with ISR).*

		HZHA02TF$_2$			HZHA03		
m_A [GeV]	$tan\beta$	m_h [GeV]	σ [fb]	σ_{ISR} [fb]	m_h [GeV]	σ [fb]	σ_{ISR} [fb]
75	2	60.84	45.19	44.70	60.84	45.61	45.13
75	20	74.69	1.036	0.9784	74.69	1.045	0.9866
90	2	67.07	46.92	45.47	67.07	47.32	45.87
90	20	89.40	1.647	1.461	89.40	1.654	1.470

Table 4.4: *Cross sections for the* $e^+e^- \to h\nu_e\bar{\nu}_e$ *process with interference in MSSM for production of the lightest neutral Higgs at* $\sqrt{s} = 204$ *GeV* (σ *is the cross section without ISR, while* σ_{ISR} *is with ISR). In this table the cross sections of HZHA03 are computed in the usual way, while the cross sections of HZHA02TF*$_2$ *are first computed in the SM with the same* m_h *as for the HZHA03 cross sections and then multipied by* $\sin^2(\beta - \alpha)$ *(which was calculated for each Higgs mass by HZHA03) to obtain the MSSM cross section (Eq. 3.11).*

Since the energy and angular distributions only differ by a normalization factor, only the MSSM energy and angular spectrums are shown for Higgs masses below the Higgs-strahlung threshold in Fig. 4.8. For Higgs masses above the threshold, the Standard Model distributions are shown in Fig. 4.9. As can be seen there is a very good agreement between the two generators. The small differences in the MSSM energy distribution can in fact be explained by the difference in m_h that occurs in the two different versions of HZHA.

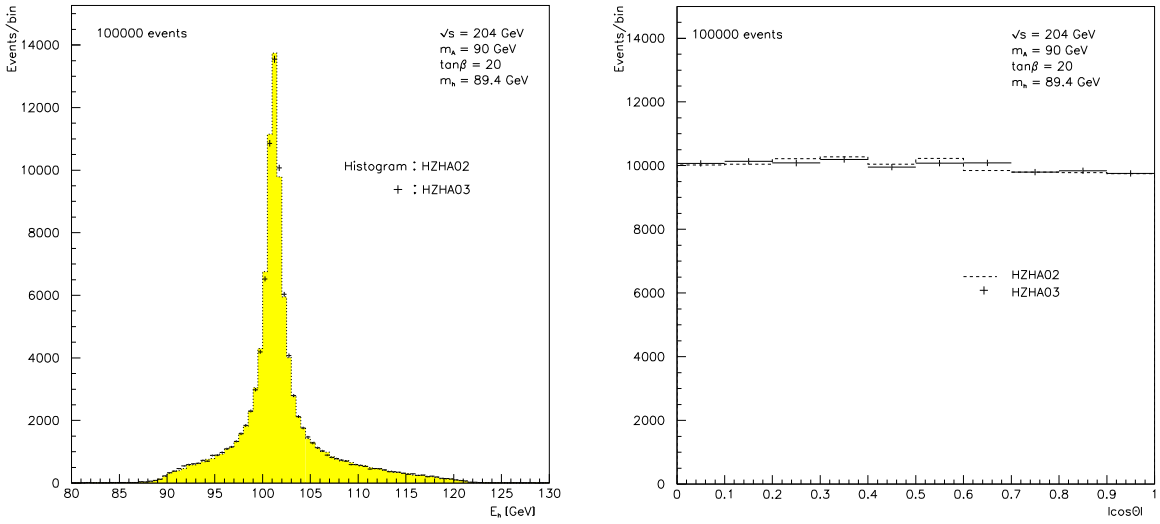

Figure 4.8: *The generated energy distribution (left) and angular distribution (right) of HZHA02TF$_2$ and HZHA03 for the process* $e^+e^- \to h\nu_e\bar{\nu}_e$ *with interference and ISR in MSSM at* $\sqrt{s} = 204$ *GeV,* $m_A = 90$ *GeV and* $\tan\beta = 20$.

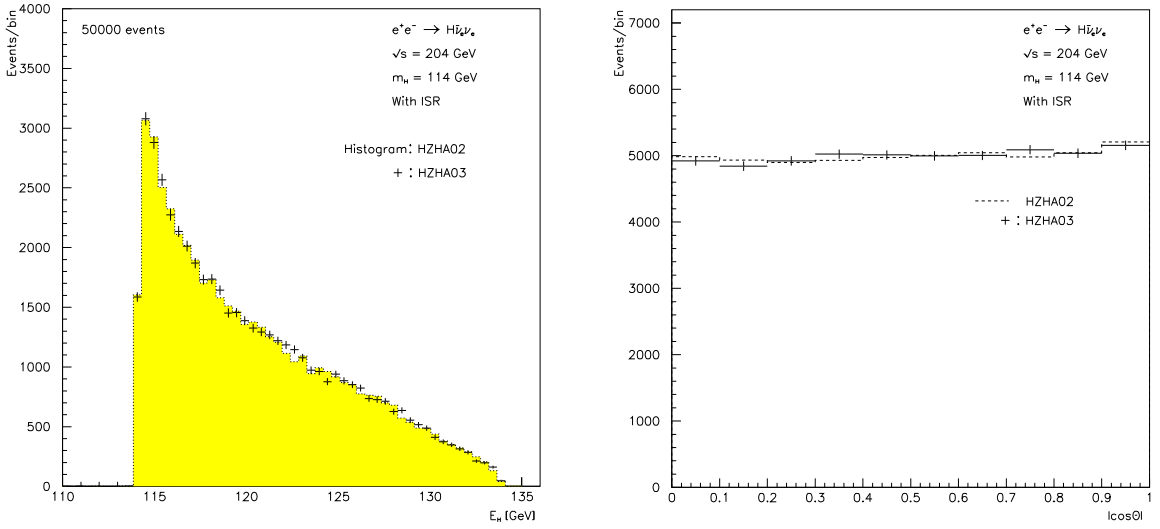

Figure 4.9: *The generated energy distribution (left) and angular distribution (right) of HZHA02TF$_2$ and HZHA03 for the process* $e^+e^- \to H\nu_e\bar{\nu}_e$ *with interference in the SM at* $\sqrt{s} = 204$ *GeV,* $m_H = 114$.

Chapter 5

Conclusion

In this thesis it has been shown that the WW fusion becomes important at high Higgs masses at center of mass energies above $\sqrt{s} \sim 190$ GeV. At these energies it is also important to take the interference term between Higgs-strahlung and WW fusion into account as has been shown. This term has been included in a modified version of HZHA02 which was released in September 1999 [1]. In November 1999 a new public version of HZHA, namely HZHA03 [21], also including interference between Higgs-strahlung (with $H\nu_e\bar{\nu}_e$ in the final state) and WW fusion was released. This version and an updated modified version of HZHA02 (released in March 2000) [2] has been put to detailed tests and comparison. They are found to be in very good agreement with each other and with theoretical expectations, although they use different formulae and algorithms. The modified version of HZHA02 can be used, though the official version HZHA03 is recommended.

Appendix A

First Delphi note

DELPHI Collaboration

DELPHI 99-161 PHYS 836
02 November, 1999

The interference term between Higgs-strahlung and WW fusion in the HZHA generator

T. Frågåt
Physics Department, University of Oslo, Blindern, 0316 Oslo, Norway

Abstract

Higgs-strahlung is the most important Higgs production mechanism at low energies, but at energies above $\sqrt{s} \sim 190$ GeV at LEP200 WW fusion becomes more important. The two production amplitudes interfere when the Z boson decays into electron neutrinos. The original HZHA generator did not include this interference term, so the task has been to implement it into HZHA. In this note I will describe what has been done to include the interference term and how to use the new generator. I will also show some results obtained by the new code.

1 Introduction

The Higgs-strahlung process, $e^+e^- \to HZ$, and WW fusion, $e^+e^- \to H\nu_e\bar{\nu}_e$, fig. 1, are the most important Higgs production processes at LEP200. When the Z boson decays into electron neutrinos, the two production amplitudes interfere. This interference term is of the same order of magnitude as the two production mechanisms. Since the HZHA event generator has not contained the calculation and generation of the Higgs-strahlung and WW fusion with the interference term, the task has been to include this into the generator.

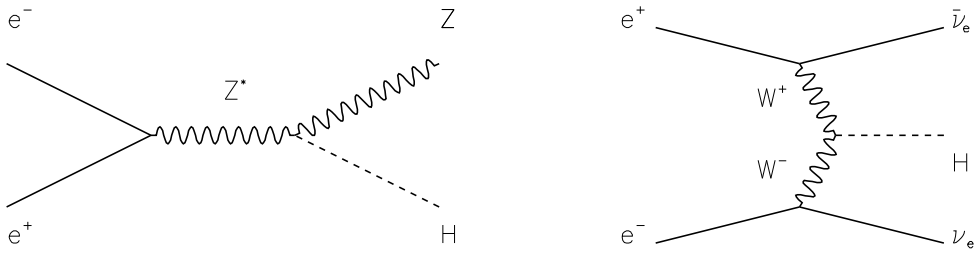

Figure 1: *Higgs-strahlung and WW fusion diagrams.*

2 Methods and how to run HZHA

The Higgs-strahlung with the Z boson decay into electron neutrinos, the WW fusion and the interference term, had to be included into HZHA as a separate channel, since the interference term is not a physical process creating a new particle, and since the interference is also able to contribute with negative cross sections. The formulae used to include the interference term can be found in ref. [1], it is important to note that these formulae do not give exactly the same cross sections for the Higgs-strahlung and the WW fusion as the original formulae in HZHA. This can be seen in table 1 for some Higgs masses for center of mass energy 200 GeV. The formulae in [1] do not take the Higgs width into account, and this may be part of the reason why the separate theoretical cross sections for the Higgs-strahlung and WW fusion slightly differ.

In `runhzha.csh` the new channel can be turned on and off with the *INCLU* switch in the *GENE* card. When this is done the WW fusion in the *PRYN* card and the Z decay to electron neutrinos in the *GZDC* card are switched off, otherwise these channels will be counted twice. (It should be noted that the interference term will not be included if *IKLEI = 0* (i.e. Z boson on shell approximation + width). In this case HZHA will run like the original generator.) In the program code the new channel has process number 10.

Even if the generation of the process including the interference is a little faster than the original generation of the Higgs-strahlung and WW fusion, it is slower when HZHA is running with ISR, *Initial state radiation*. The reason for this can be found in the subroutine `remt1` in HZHA which computes the ISR photon spectrum [2]. This subroutine is with the new formulae a factor about 20 slower than with the old formulae. The cross section for the process including the interference term is computed with the `CERNLIB`

	Original			New		
m_H [GeV]	σ_{hs} [fb]	σ_{WW} [fb]	σ_{hs+WW} [fb]	σ_{hs} [fb]	σ_{WW} [fb]	σ_{hs+WW} [fb]
95.	29.2	6.25	35.5	29.3	6.12	35.4
100.	22.7	5.21	27.9	22.7	5.10	27.8
105.	14.3	4.30	18.6	14.4	4.21	18.6
110.	2.65	3.51	6.16	2.68	3.44	6.12
115.	0.733	2.83	3.56	0.739	2.77	3.51
120.	0.352	2.24	2.59	0.355	2.19	2.55

Table 1: *The theoretical cross sections computed by HZHA for the process* $e^+e^- \to HZ$ *at* $\sqrt{s}$ *= 200 GeV.* σ_{hs} *= Higgs-strahlung cross section,* σ_{WW} *= WW fusion cross section and* σ_{hs+WW} *= the total cross section for Higgs-strahlung and WW fusion.*

routine `DGMLT2` [3]. This routine is performing a Gaussian quadrature integration for double integrals. The subroutine `remt1` is slower because the number of integration intervals had to be increased in order to maintain the required accuracy of the cross section.

Determining the generated cross section is technically complicated when running with ISR. In that case only the theoretical cross section is considered.

3 Results

The interference term is, as mentioned earlier, important at large energies. Fig. 2 shows the total cross section as a function of the Higgs mass for Higgs-strahlung (with Z decaying into electron neutrinos) and WW fusion, with and without interference for center of mass energy 200 GeV. In table 2 the effect of the interference is shown for some Higgs masses.

m_H [GeV]	σ [fb]	σ_{int} [fb]	**effect** [%]
95.	35.6	37.9	6.46
100.	28.0	31.1	11.1
105.	18.7	22.4	19.8
110.	6.11	9.22	50.9
115.	3.51	5.32	51.6
120.	2.55	3.73	46.3

Table 2: *The effect of the interference for the process* $e^+e^- \to H\nu_e\bar{\nu}_e$ *at* $\sqrt{s}$ *= 200 GeV.* σ *is the cross section without interference and* σ_{int} *is with the interference term.*

To make sure that the new program code, Appendix A, and the new formulae [1], were correct, some tests had to be made. The first step was to write the new formulae in FORTRAN code and reproduce the cross sections, Higgs energy- and angular distributions in [1]. Then the new formulae and code were implemented into HZHA, and the interference term was temporarily disabled, so what was left was only the Higgs-strahlung and WW fusion. Then the generated Higgs energy- and angular distributions from the original HZHA could be compared with the new ones, figs. 3, 4. The Higgs energy mean value for

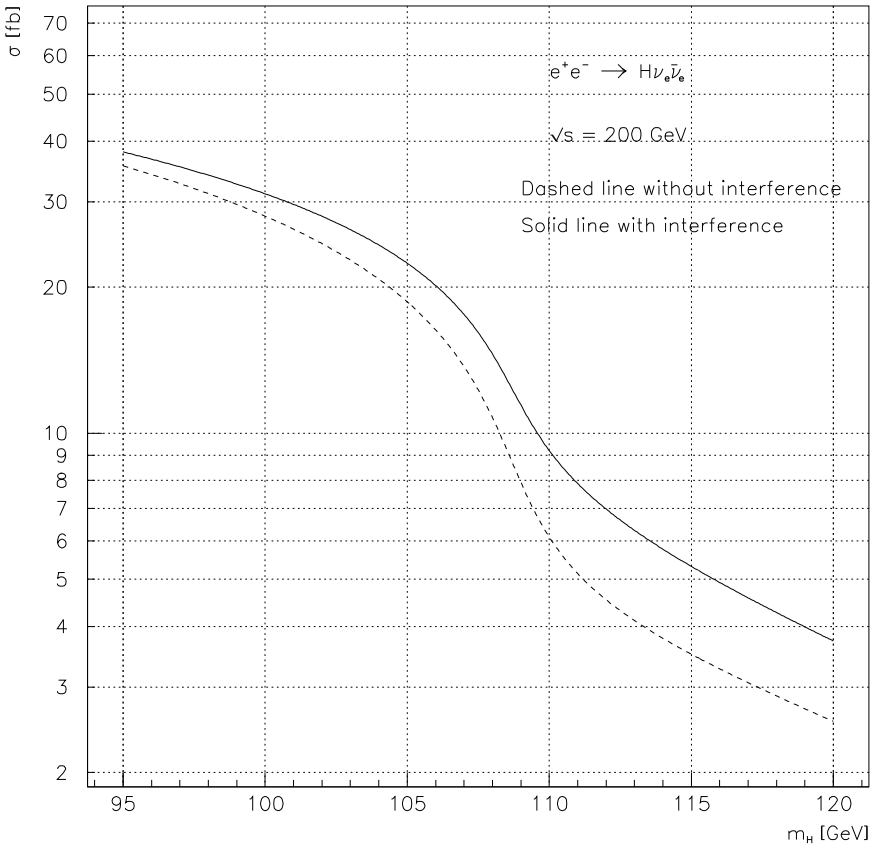

Figure 2: *The cross section for the process $e^+e^- \to H\nu_e\bar{\nu}_e$ as a function of the Higgs mass. The solid line is the cross section with the interference term and the dashed line is without the interference. The center of mass energy is 200 GeV.*

the old HZHA is 102.9 GeV and the RMS is 3.858 GeV, while for the new HZHA the mean value is 103.0 GeV and the RMS is 3.863 GeV. The center of mass energy is 200 GeV and the Higgs mass is 95 GeV. When studying the figures one should also remember that the generated distribution from the original HZHA has some uncertainty in each bin. In fig. 5 the theoretical Higgs energy- and angular distribution is shown for Higgs-strahlung, WW fusion and interference. Notice the energy distribution of the interference term. The interference does not have any big effect on the Higgs angular distribution.

Now one has some confidence in the new algorithms and formulae, so some investigation on the effect of the interference term can begin. In fig. 6 the energy distribution for the Higgs-strahlung and WW fusion with and without interference is shown for center of mass energy 200 GeV and a Higgs mass of 95 GeV. Also shown is the theoretical Higgs energy distribution. There is a good agreement between the theoretical and generated distribution. As can be seen in the figure, the interference term makes the energy spectrum a little harder. The theoretical angular distribution is almost unchanged when including the interference, fig. 5. This is also true for the generated angular distribution.

The effect of the ISR on the theoretical cross section for the process $e^+e^- \to H\nu_e\bar{\nu}_e$ with interference is shown in fig. 7 for center of mass energy 200 GeV. In table 3 the effect of the ISR is shown for some Higgs masses. It is interesting to notice that the effect

of the ISR first increases, then decreases as the Higgs mass grows. In fig. 8 and fig. 9 the energy- and angular distribution with and without ISR are shown respectively. The center of mass energy is 200 GeV and the Higgs mass is 95 GeV. As can be seen from fig. 8, the peak is now a little lower and there are more events with Higgs energy between 95 and 101 GeV with ISR than without ISR. But the high energy tail of the Higgs energy distribution is almost unchanged.

m_H [GeV]	σ [fb]	σ_{ISR} [fb]	**effect** [%]
95.	37.8	31.9	-15.7
100.	30.9	25.0	-19.1
105.	22.4	17.1	-23.4
110.	9.22	7.26	-21.3
115.	5.32	4.36	-17.9

Table 3: *The effect of the ISR for* $e^+e^- \to H\nu_e\bar{\nu}_e$ *including contributions from Higgs-strahlung, WW fusion and interference at* $\sqrt{s} = 200$ *GeV for some Higgs masses.* σ *is without and* σ_{ISR} *is with ISR.*

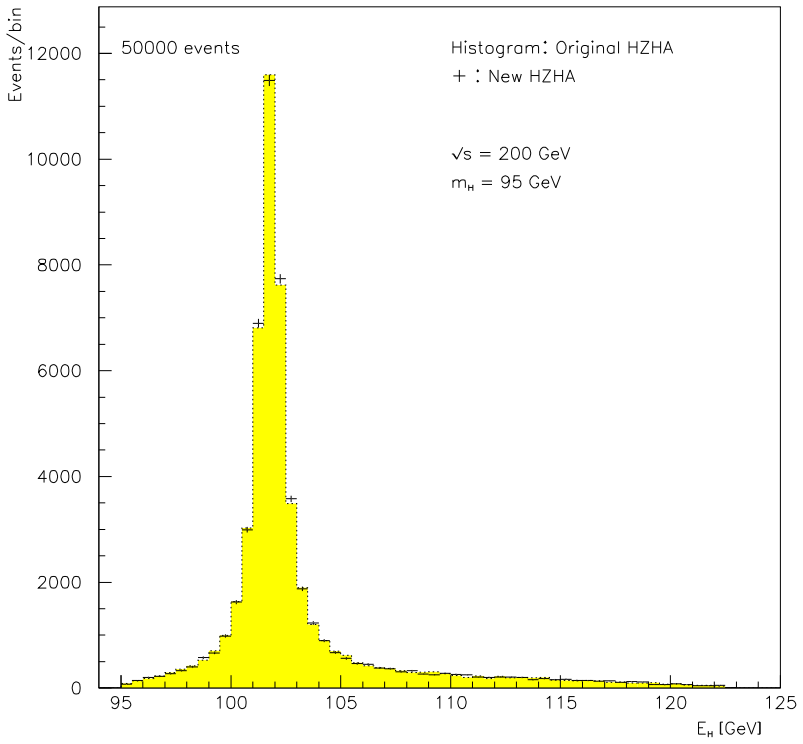

Figure 3: *Energy distribution of the Higgs boson for the process* $e^+e^- \to H\nu_e\bar{\nu}_e$ *without the interference at* $\sqrt{s} = 200$ *GeV and* $m_H = 95$ *GeV. The histogram shows the original HZHA distribution, while the crosses show the new energy distribution.*

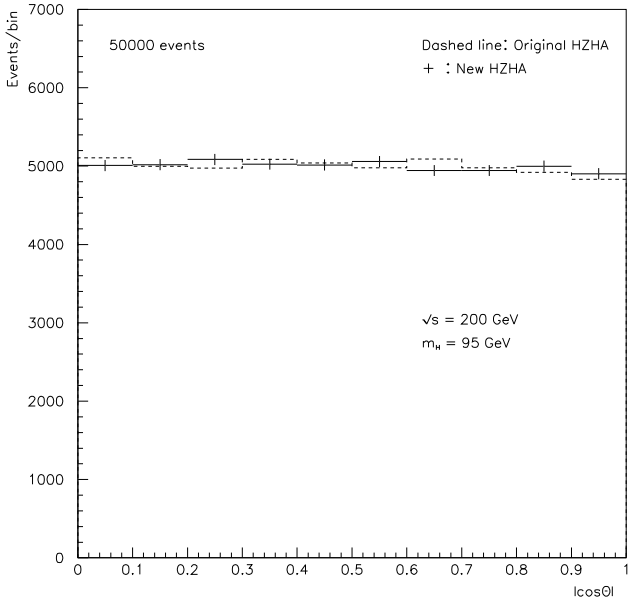

Figure 4: *Angular distribution of the Higgs boson at $\sqrt{s}$ = 200 GeV and m_H = 95 GeV for the process $e^+e^- \to H\nu_e\bar{\nu}_e$ without the interference. The dashed line shows the original HZHA angular distribution, while the crosses show the new.*

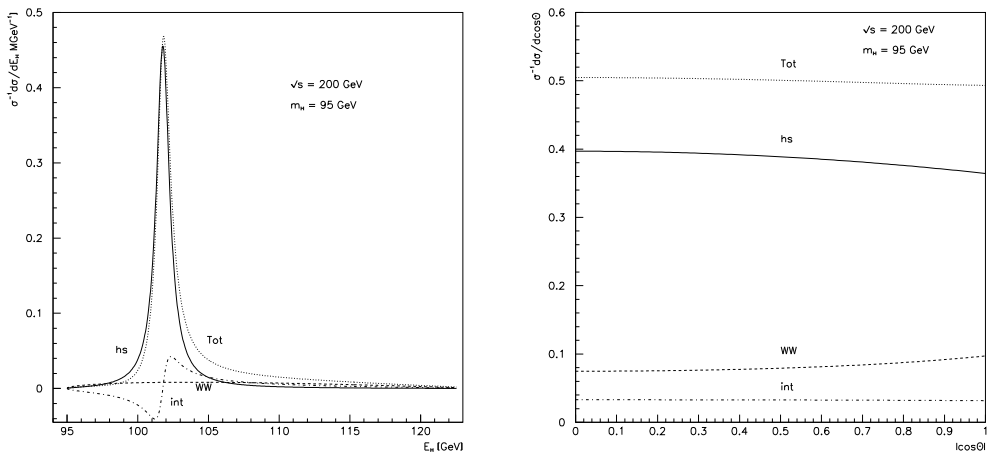

Figure 5: *Theoretical differential cross sections versus Higgs energy (left) and $|cos\theta|$ (right) of the Higgs boson for $e^+e^- \to H\nu_e\bar{\nu}_e$ at $\sqrt{s}$ = 200 GeV and m_H = 95 GeV. The individual curves are normalized to the total cross section of 37.9 fb. hs = Higgs-strahlung, WW = WW fusion, int = interference term and Tot = total distribution.*

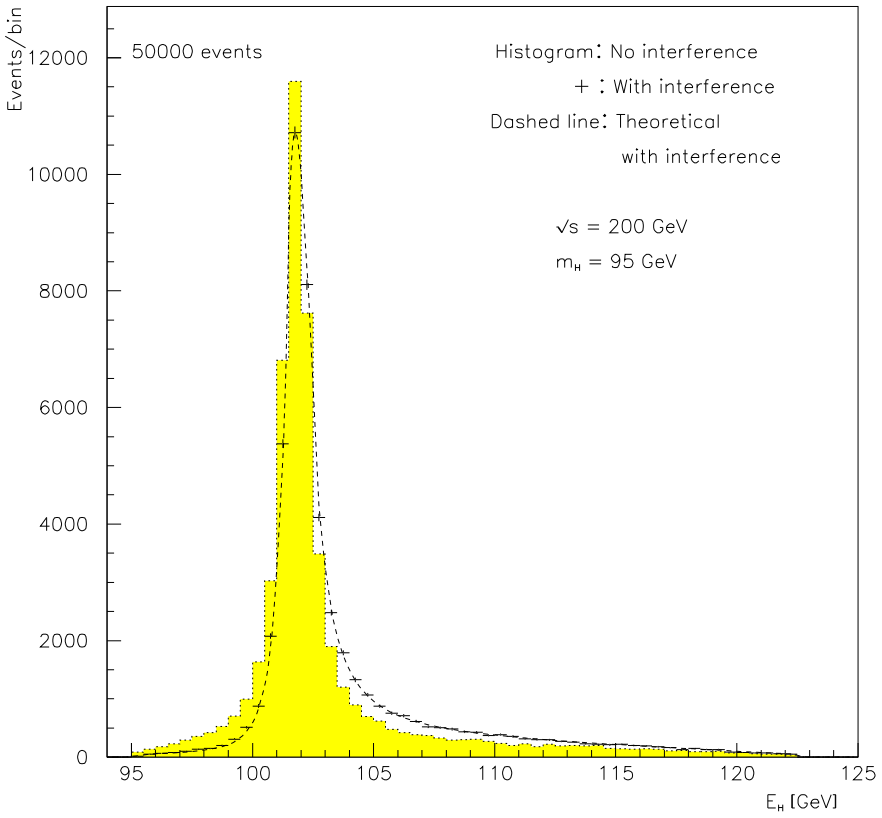

Figure 6: *Energy distribution of the Higgs boson with and without the interference term for* $e^+e^- \to H\nu_e\bar{\nu}_e$ *at* $\sqrt{s} = 200\ GeV$ *and* $m_H = 95\ GeV$*. The histogram is without and the crosses are with the interference term. The dashed line is the theoretical energy distribution with interference.*

4 Conclusion

There is, as shown, good agreement between the new and the old algorithms and formulae of the HZHA generator when only the Higgs-strahlung and WW fusion are considered. There is also good agreement between the new algorithms and the theoretical formulae for the Higgs-strahlung, WW fusion and interference for the cross sections, energy distributions and angular distributions.

5 Acknowledgement

I would like to thank my supervisors Lars Bugge and Alex Read for all the help and comments I have received during my work on including the interference term into HZHA. I would also like to thank Patrick Janot for the comments I have received from him in various e-mails.

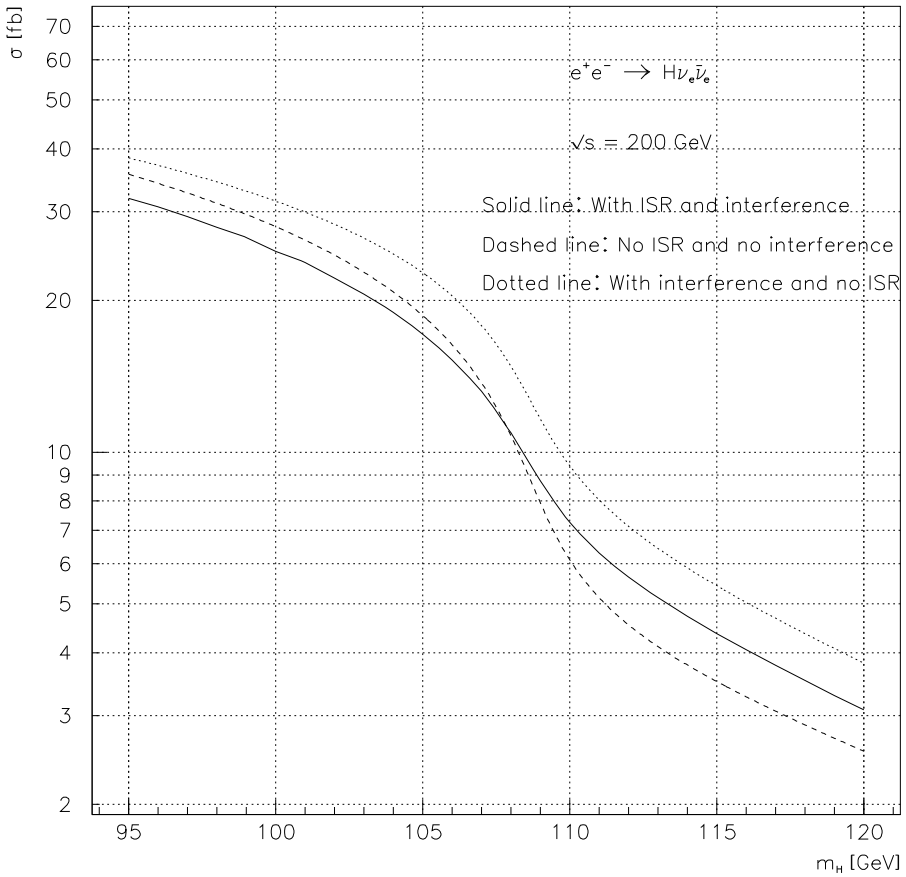

Figure 7: *Theoretical cross sections for $e^+e^- \to H\nu_e\bar{\nu}_e$ as functions of Higgs mass with and without ISR. The center of mass energy is 200 GeV. The solid line shows the cross section with ISR and interference, the dashed line shows the cross section with no ISR and no interference, and the dotted line shows the cross section with interference and no ISR.*

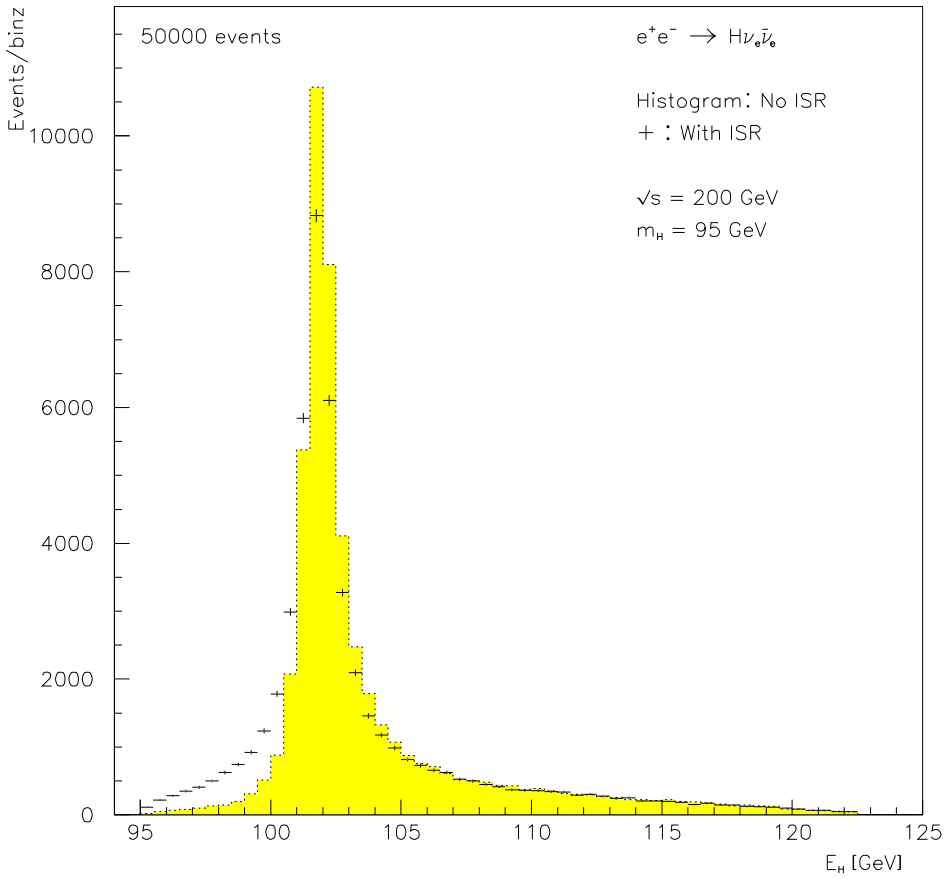

Figure 8: *The energy distribution for $e^+e^- \rightarrow H\nu_e\bar{\nu}_e$ including contributions from Higgs-strahlung, WW fusion and interference with and without ISR at $\sqrt{s}$ = 200 GeV and m_H = 95 GeV. The histogram is with no ISR and the crosses are with ISR.*

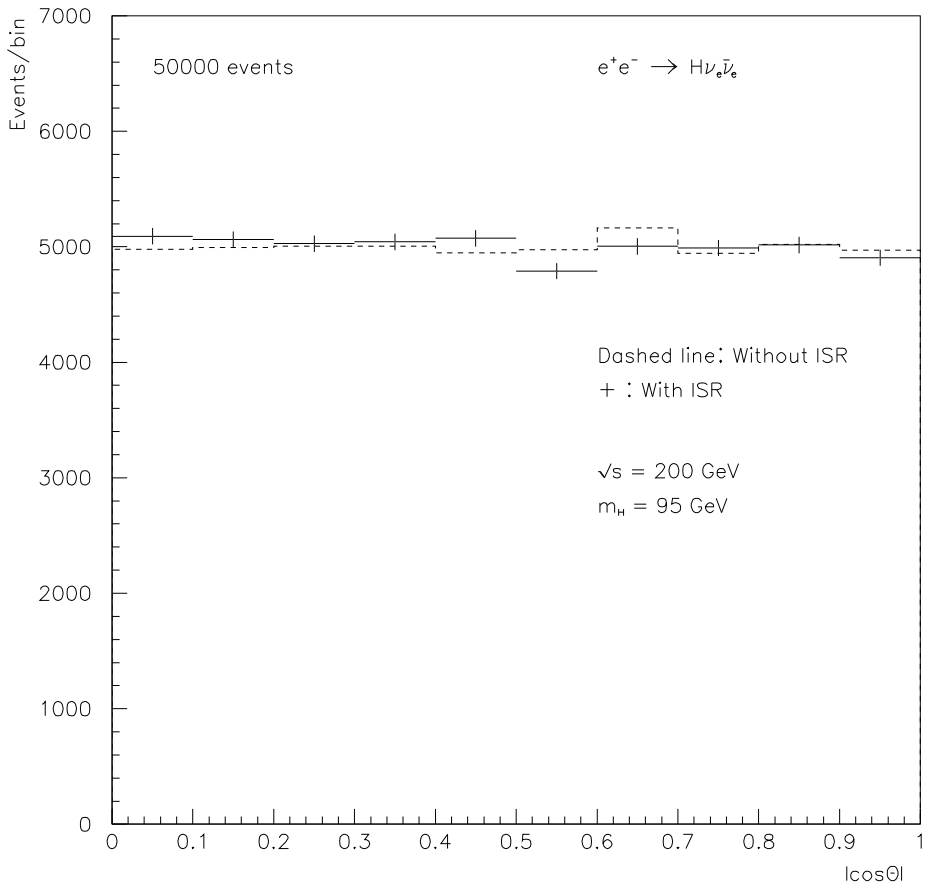

Figure 9: *The angular distribution for the Higgs-strahlung, WW fusion and interference term with and without ISR.* $\sqrt{s}$ *= 200 GeV and* m_H *= 95 GeV. The dashed line shows the distribution without ISR and the crosses are with ISR.*

A Appendix

The changes made to HZHA are listed below. Lines written in italic are the old code, while the lines written in typewriter style are new. What is written in bold is comments on what is done.

A.1 The cross section algorithm

This is the algorithm that computes the theoretical cross section for Higgs-strahlung, WW fusion and the interference term.

```
C
C -------------------------------------------------------------------
C! The cross section for the Higgs-strahlung (Z --> nue nuebar), WW-
C  fusion and interference term. Ref.: Kilian, Kramer and Zerwas, hep-
C  ph/9512355, 1995.
C
C  Thomas Fragat -- 26 march 1999.
C-------------------------------------------------------------------
      FUNCTION sinterference(sbeam)
C
      EXTERNAL HSUB2
      DIMENSION X(2)
C
      PARAMETER ( nchan=16, nhig=3 )
      COMMON / hmasss / amhig(nhig), amh, gmh, ama, amz, amw, gmz,
     .                  amtau, amb, amc, amt, ame, ammu, amu,
     .                  amd, ams, amhp, gmw, amst(2), amsb(2),
     .                  amsq, amneut(4),amchar(2), amarun
      COMMON / elweak / sw2,alpha(0:nhig),gweak2(0:nhig),
     .                  alphas(0:nhig),g_f,deltar,alpha2,sw,cw2,cw
C
      COMMON/ para/ pi,s,ve,ae,hma,rmz,rgz,cow2,wma
C
      COMMON/faster/wma2,rmz2,rgz2,rmgz2,cow4,cow8,ve2ae2,srs
C
      REAL*8 cow2,cow4,cow8,wma2,rmz2,rgz2,rmgz2,ve2ae2,
     .     s,pi,ve,ae,p1,p2,X,hma,rmz,rgz,wma,DGMLT2,srs,const1
C
C
      pi=3.1415926535897932364
C
C Some abbrevations for increasing the speed
C
      cow2 = cw2
      cow4 = cow2**2
      cow8 = cow4**2
```

```
      ve = -1. + 4.*sw2
      ae = -1.
      ve2ae2 = ve**2+ae**2
C
      hma = amh
      wma = amw
      rmz  = amz
      rgz  = gmz
      wma2 = wma**2
      rmz2 = rmz**2
      rgz2 = rgz**2
      rmgz2 = rmz2*rgz2
C
      s=sbeam
      srs = sqrt(s)
C
C
C Test to check if nothing unphysical happens
C
      IF (s .LT. hma**2)THEN
         sinterference = 0.
         GOTO 100
C
      ELSE
C
C Some integration limits
C
         p1 = -1.
         p2 = 1.
C
C Constant
C
         const1 = g_f**3 * rmz**8 *0.389D-3
     .        / (sqrt(2.)*pi**3*1.0D-15 )
C
         sinterference = const1* DGMLT2(HSUB2,p1,p2,9,6,X)
C
      ENDIF
C
 100  RETURN
      END
C
C Computation of the theoretical cross sections for Higgs-strahlung,
C WW-fusion and the interference term
C
      SUBROUTINE HSUB2(M,U2,F2,X)
      EXTERNAL HSUB1
```

```
      DIMENSION U2(*), F2(*), X(2)
      PARAMETER ( nchan=16, nhig=3 )
      COMMON / elweak / sw2,alpha(0:nhig),gweak2(0:nhig),
     .                  alphas(0:nhig),g_f,deltar,alpha2,sw,cw2,cw
      COMMON/ para/ pi,s,ve,ae,hma,rmz,rgz,cow2,wma
      COMMON/faster/wma2,rmz2,rgz2,rmgz2,cow4,cow8,ve2ae2,srs
C
      REAL*8 s,pi,ve,ae,y,z,X,hlo,hhi,
     .     F2,U2,DGMLT1,rmz,hma,Ehigh
C
      REAL*8 wma2,rmz2,rgz2,rmgz2,cow4,cow8,ve2ae2,srs
C
C Integration limits for the Higgs energy
C
      Ehigh = srs*(1.+hma**2/s)/2.
      hlo = hma
      hhi = Ehigh
C
      DO L = 1,M
C
         X(2) = U2(L)
C
         F2(L) = DGMLT1(HSUB1,hlo,hhi,9,6,X)
C
      ENDDO
      RETURN
      END
C
      SUBROUTINE HSUB1(M,U1,F1,X)
      DIMENSION U1(*), F1(*), X(2)
      COMMON/ para/ pi,s,ve,ae,hma,rmz,rgz,cow2,wma
      COMMON/faster/wma2,rmz2,rgz2,rmgz2,cow4,cow8,ve2ae2,srs
      REAL*8 cow4,cow8,wma2,rmz2,rgz2,rmgz2,ve2ae2
C
      REAL*8 s,pi,ve,ae,Gtot,X,hma,wma,rmz,rgz,cow2,hmom,
     .     F1,U1
      REAL*8 sw2,epsneu,sneu,
     .     s1,s2,s12,h1,h2,h12,ckhi,
     .     skhi2,t1,t2,r,rL,Gs,GI,Gw,
     .     srs,srr,sam1,sam2,sam3,sam4
C
C
      DO L = 1,M
C
         X(1) = U1(L)
C
C The Higgs momentum
```

```
C
         hmom = sqrt(X(1)**2 - hma**2)
C
         F1(L)= (hmom/s )*Gtot(X,hmom)
C
      ENDDO
      RETURN
      END
C
      FUNCTION Gtot(X,hmom)
      DIMENSION X(2)
      COMMON/ para/ pi,s,ve,ae,hma,rmz,rgz,cow2,wma
C
      COMMON/faster/wma2,rmz2,rgz2,rmgz2,cow4,cow8,ve2ae2,srs
      REAL*8 cow4,cow8,wma2,rmz2,rgz2,rmgz2,ve2ae2
C
      REAL*8 s,pi,ve,ae,sw2,cow2,hmom,
     .     epsneu,sneu,s1,s2,s12,h1,h2,h12,ckhi,
     .     skhi2,t1,t2,r,rL,Gs,GI,Gw,Gtot,X,
     .     hma,rmz,rgz,wma,srs,srr,sam1,sam2,sam3,sam4
C
C The neutrino pair energy
C
      epsneu = srs-X(1)
C
C The invariant mass squared of the neutrino pair
C
      sneu = epsneu**2-hmom**2
C
C Other expressions
C
      s1 = srs * (epsneu + hmom * X(2))
      s2 = srs * (epsneu - hmom * X(2))
      s12 = s1*s2
C
      h1 = 1. + 2.* wma2 / s1
C
      h2 = 1. + 2.* wma2 / s2
C
      h12 =h1*h2
C
      ckhi = 1. - 2.*s*sneu / (s12)
C
      skhi2 = 1. - ckhi**2
C
      t1 = h1 + ckhi*h2
C
```

```
      t2 = h2 + ckhi*h1
C
      r = h1**2 + h2**2 + 2.*ckhi*h12 - skhi2
      srr = sqrt(r)
C
      rL = log((h12 + ckhi + srr) /
     .     (h12 + ckhi - srr))
C
      sam1 = (sneu-rmz2)**2
      sam2 = rmz2*rgz2
      sam3 = rL/srr
      sam4 = (h1+1.)*(h2+1.)
C
C The WW-fusion
C
      Gw = (cow8/(s12*r))*(sam4*
     .     (2./(h1**2-1.)+ 2./(h2**2-1.)-
     .     6.*skhi2/r + (3.*t1*t2/r -ckhi)*
     .     sam3) - (2.*t1/(h2-1.) + 2.*t2/(h1-1.) +
     .     (t1+t2+skhi2)*sam3))
C
C The interference
C
      GI = (ve+ae)*cow4*(sneu- rmz2)/
     .     (8.*(s-rmz2)*(sam1+sam2))
     .     *(2.-(h1+1.)*log((h1+1.)/(h1-1.))-
     .     (h2+1.)*log((h2+1.)/(h2-1.))+sam4*sam3)
C
C The Higgs-strahlung
C
      Gs = (ve2ae2)*(s*sneu+s12)/(96.*
     .     (s-rmz2)**2*(sam1+sam2))
C
C Total cross-section
C
      Gtot = (Gs+GI+Gw)
C
      RETURN
      END
C
```

A.2 Event generation

In this section the algorithms for the generation of the Higgs energy and cosine θ is shown. To generate weights there is also a need for a maximum weight, which is here called `wmax`. The subroutine `wmax_init` computes the maximum weight for the process including Higgs-strahlung, WW fusion and

the interference term.

```
      SUBROUTINE dsigtot(ipro,ee,p1,p2,hh)
C ----------------------------------------------------------------------
C! Generate the total for Higgs-strahlung, WW-fusion and the
C  interference term.
C
C Input:    ee,   the effective centre-of-mass energy
C           ipro, = 10
C
C Output    p1,   the neutrino/e- momentum
C           p2,   the anti-neutrino/e+ momentum
C           hh,   the Higgs momentum
C
C Thomas Fragat -- 30 April 1999
C ----------------------------------------------------------------------
      PARAMETER ( nchan=16, nhig=3 )
      COMMON / hmasss / amhig(nhig), amh, gmh, ama, amz, amw, gmz,
     .                  amtau, amb, amc, amt, ame, ammu, amu,
     .                  amd, ams, amhp, gmw, amst(2), amsb(2),
     .                  amsq, amneut(4),amchar(2), amarun
      COMMON / lifeti / tauh(nhig)
      COMMON / conqcd / xlamda5
      COMMON / wwzzch / wwmax(2,nhig), jtyp(2,nhig), w1, w2
      COMMON / mixing / alfa, beta, topmix, botmix,
     .                  aa(nhig,4,4),bb(nhig,2,2),
     .                  fieldn(4,4), umat(2,2), vmat(2,2),
     .                  ssmat(4,4),qqmat(4,4)
      COMMON / coupls / sa, ca, sb, cb, ta, tb, sab2, cab2,
     .                  s2a, c2a, s2b, c2b, sb2, cb2, cab, sab
      COMMON / susyms / susM, susMU, susAt, susAb, susSMQ, susSMU,
     .                  susSMD, susSML, susSME, susM1, susM2
      COMMON / flags  / idbg
      DIMENSION suspar(11)
      EQUIVALENCE(susM,suspar(1))
C
      PARAMETER(nstep=20)
      COMMON / crocro / ecs(nstep),crs(nstep),wsup(nstep)
      COMMON / poidsm / wtot(5),wtot2(5),ntry(5),nacc(5)
C
      PARAMETER (L1MST=200, L1PAR=200)
      PARAMETER (L2PAR=500, L2PARF=2000 )
      PARAMETER (LJNPAR=4000)
      COMMON /LUDAT1/ MSTU(L1MST),PARU(L1PAR),MSTJ(L1MST),PARJ(L1PAR)
      COMMON /LUDAT2/ KCHG(L2PAR,3),PMAS(L2PAR,4),PARF(L2PARF),VCKM(4,4)
      COMMON /LUDAT3/ MDCY(L2PAR,3),MDME(L2PARF,2),BRAT(L2PARF),
     &                KFDP(L2PARF,5)
```

```
      COMMON /LUDAT4/ CHAF(L2PAR)
      CHARACTER*8 CHAF
      COMMON /LUJETS/ N7LU,K7LU(LJNPAR,5),P7LU(LJNPAR,5),V7LU(LJNPAR,5)
C
      PARAMETER (maxpro= 10)
      COMMON / cropro / cross(maxpro), sthr(maxpro), reduc(maxpro)
      CHARACTER*14 chapro(maxpro)
      DATA chapro /
     .             'e+e- --> h Z',
     .             'e+e- --> H Z',
     .             'e+e- --> h A',
     .             'e+e- --> H A',
     .             'W+W- --> h  ',
     .             'W+W- --> H  ',
     .             'Z Z  --> h  ',
     .             'Z Z  --> H  ',
     .             'e+e- --> H+H-',
     .             'e+e- -> h nu_e'
     .                                /
      COMMON / prosim / iproyn(maxpro),nevpro(maxpro)
      PARAMETER (PI=3.1415926535897932364,PI2=PI*PI,PI4=PI2*PI2)
      PARAMETER (TWOPI = 2.*PI , PIBY2 = PI/2., PIBY4 = PI/4.)
      PARAMETER (PIBY6 = PI/6. , PIBY8 = PI/8.)
      PARAMETER (PIBY12= PI/12., PIBY3 = PI/3.)
C
      COMMON / elweak / sw2,alpha(0:nhig),gweak2(0:nhig),
     .                  alphas(0:nhig),g_f,deltar,alpha2,sw,cw2,cw
C
      COMMON / miscl / loutbe,ecm,idb1,idb2,xrad,empir,empirm,ism,
     &                 iklei,icar,sdvrt(3),vrtx(4),tabl(26),
     &                 nevent(11)
      INTEGER loutbe,idb1,idb2,nevent,ism,iklei,icar
      REAL*4 ecm,sdvrt,vrtx,tabl,empir,empirm,xrad
C
      COMMON/ intwmax / wmaxx
      COMMON/ higgsm / hm1,stra
      REAL*8 wmaxx,wmax,weight
C
      DIMENSION p1(4), p2(4), pm(4), pp(4), hh(4), ptot(4)
      REAL*8 epsneu,sneu,s1,s2,t1,t2,h1,h2,h12,rL,ckhi,
     .     skhi2,r,GI,Gw,Gs,Gtot,ph,he,eb
      REAL*8 sam1,sam2,sam3,sam4,s12,rmz2,s,ehl,ehh
C
      ss   = ee**2
      eb   = ee/2.
      s    = ee
      wmax = wmaxx
```

```
C
C The incoming momenta
C
      pm(1) = 0.
      pm(2) = 0.
      pm(3) = eb
      pm(4) = eb
      pp(1) = 0.
      pp(2) = 0.
      pp(3) =-eb
      pp(4) = eb
C
C Some masses, widths and constants
C
      rmv  = amw
      rmz  = amz
      rgz  = gmz
      rmh  = pmas(25,1)
      rgh  = pmas(25,2)
      v1   = -1.+4.*sw**2
      v2   = -1.
C
      rmv2 = rmv**2
      rmh2 = rmh**2
      rmgh = rmh*rgh
      rmz2 = rmz**2
 10   CALL bwgene(0.,ee,rmh,rgh,rm1,djdum)
      rm2 = rm1**2
C
```

If ISR is included the center of mass energy put into this subroutine will vary because of the hard photons. Then the `wmax` value also have to change with the center of mass energy:

```
      IF(xrad .GT. 0.)THEN
         hm1 = rm1
         stra = xrad
         CALL wmax_init(ss)
         wmax = wmaxx
      ENDIF
C
C Integration limits
C
      ehl = rm1
      ehh = ee*(1.+rm2/ss)/2.
      csl = -1.
      csh =  1.
C
```

```
      deltaeh = ehh-ehl
      deltaco = 2.
C
C Constant in picobarns
C
      const1 = g_f**3*rmz**8/
     .     (sqrt(2.)*pi**3)*0.389D-3/1.0D-15
C
C Generation of the cosine tetha angle
C
 1    cste = -1. + 2.*RNDM(1)
C
C Generation of the Higgs energy
C
 2    he = ehl + RNDM(3)*(ehh-ehl)
```

With the new formulae it is not possible to generate a Higgs boson at rest. To prevent this we have to check if the Higgs energy, `he`, is greater than the Higgs mass, `rm1`. If not, a new Higgs energy should be generated. We also have to test if the Higgs mass is lower than the upper integration limit for the Higgs energy, `ehh`, if not, a new Higgs mass has to be generated. This is done in the next two lines of code.

```
C
C Tests to prevent the formulae to crash
C
      IF(rm1+1D-5 .GT. ehh)GOTO 10
      IF(he .LT. rm1+1D-5) GOTO 2
C
C The Higgs momentum
C
      hmom = sqrt(he**2 - rm2)
C
C Test for unphysical events
C
      IF(hmom**2+rm2 .GT. ss)THEN
         weight=0.
         GOTO 5
      ENDIF
C
C The energy of the neutrino pair
C
      epsneu = s-he
C
C The invariant mass squared of the neutrino pair
C
      sneu = epsneu**2-hmom**2
C
```

```
C Some other functions
C
      s1 = s * (epsneu + hmom * cste)
      s2 = s * (epsneu - hmom * cste)
      s12 = s1*s2
C
      h1 = 1. + 2.* rmv2 / s1
      h2 = 1. + 2.* rmv2 / s2
      h12 =h1*h2
C
      ckhi = 1. - 2.*ss*sneu / (s1 * s2)
      skhi2 = 1. - ckhi**2
C
      t1 = h1 + ckhi*h2
      t2 = h2 + ckhi*h1
C
      r = h1**2 + h2**2 + 2.*ckhi*h12 - skhi2
C
      rL = log((h12 + ckhi + sqrt(r)) /
     .     (h12 + ckhi - sqrt(r)))
C
C Increasing the effectivity
C
      sam1 = (sneu-rmz2)**2
      sam2 = rmz2*rgz**2
      sam3 = rL/sqrt(r)
      sam4 = (h1+1.)*(h2+1.)
C
C The WW-fusion
C
      Gw = (cw2**4/(s12*r))*(sam4*
     .     (2./(h1**2-1.)+ 2./(h2**2-1.)-
     .     6.*skhi2/r + (3.*t1*t2/r -ckhi)*
     .     sam3) - (2.*t1/(h2-1.) + 2.*t2/(h1-1.) +
     .     (t1+t2+skhi2)*sam3))
C
C The interference term
C
      GI = (v1+v2)*cw2**2*(sneu- rmz2)/
     .     (8.*(ss-rmz2)*(sam1+sam2)) * (2.-(h1+1.)*
     .     log((h1+1.)/(h1-1.))-(h2+1.)*log((h2+1.)/(h2-1.))+
     .     sam4*sam3)
C
C The Higgs-strahlung
C
      Gs = (v1**2+v2**2)*(ss*sneu+s12)/(96.*
     .     (ss-rmz2)**2*(sam1+sam2))
```

```
C
C The total
C
      Gtot = (Gs+GI+Gw)
C
      weight = const1*deltaeh*deltaco*(hmom/ss)*Gtot
C
C Generation of the phi angle
C
      phi = 2.*pi*RNDM(4)
C
C Apply the rejection algorithm
C
 5    IF ( weight .LE. 0. .AND. wmax .EQ. 0.) GOTO 1
      IF ( weight .GT. 1.05*wmax ) THEN
         WRITE(6,*) 'Warning at ECM = ',ee,' GeV'
         WRITE(6,*) 'Weight (',weight,') > Wmax (',wmax,')'
         wmax = 3.6*weight
         GOTO 1
      ELSEIF ( weight .GT. wmax ) THEN
         wmax = weight
      ENDIF
      ipr = ipro-5
      wtot (ipr) = wtot (ipr) + weight
      wtot2(ipr) = wtot2(ipr) + weight**2
      ntry (ipr) = ntry (ipr) + 1
C
      IF ( weight/wmax .LT. RNDM(weight) ) GOTO 1
C
C Construction of the Higgs and neutrino momenta vectors
C
      sinte=sqrt(1.-cste**2)
      hh(1) = hmom*sinte*cos(phi)
      hh(2) = hmom*sinte*sin(phi)
      hh(3) = hmom*cste
      hh(4) = rm1
C
      DO k=1,4
         p1(k) = -0.5*(pm(k)+pp(k)-hh(k))
         p2(k) = -0.5*(pm(k)+pp(k)-hh(k))
      ENDDO
C
      nacc(ipr) = nacc(ipr) + 1
C
      RETURN
      END
C
```

```
      SUBROUTINE wmax_init(sbeam)
C ----------------------------------------------------------------------
C! Computes wmax for the total of the WW-fusion, Higgs-strahlung
C  and the interference term.
C
C Input:    sbeam,   the centre-of-mass energy
C
C Thomas Fragat -- 30 April 1999
C ----------------------------------------------------------------------
      PARAMETER ( nchan=16, nhig=3 )
      COMMON / hmasss / amhig(nhig), amh, gmh, ama, amz, amw, gmz,
     .                  amtau, amb, amc, amt, ame, ammu, amu,
     .                  amd, ams, amhp, gmw, amst(2), amsb(2),
     .                  amsq, amneut(4),amchar(2), amarun
      PARAMETER (PI=3.1415926535897932364,PI2=PI*PI,PI4=PI2*PI2)
      PARAMETER (TWOPI = 2.*PI , PIBY2 = PI/2., PIBY4 = PI/4.)
      PARAMETER (PIBY6 = PI/6. , PIBY8 = PI/8.)
      PARAMETER (PIBY12= PI/12., PIBY3 = PI/3.)
C
      COMMON / elweak / sw2,alpha(0:nhig),gweak2(0:nhig),
     .                  alphas(0:nhig),g_f,deltar,alpha2,sw,cw2,cw
C
      PARAMETER (L1MST=200, L1PAR=200)
      PARAMETER (L2PAR=500, L2PARF=2000 )
      PARAMETER (LJNPAR=4000)
      COMMON /LUDAT1/ MSTU(L1MST),PARU(L1PAR),MSTJ(L1MST),PARJ(L1PAR)
      COMMON /LUDAT2/ KCHG(L2PAR,3),PMAS(L2PAR,4),PARF(L2PARF),VCKM(4,4)
      COMMON /LUDAT3/ MDCY(L2PAR,3),MDME(L2PARF,2),BRAT(L2PARF),
     &                KFDP(L2PARF,5)
      COMMON /LUDAT4/ CHAF(L2PAR)
      CHARACTER*8 CHAF
      COMMON /LUJETS/ N7LU,K7LU(LJNPAR,5),P7LU(LJNPAR,5),V7LU(LJNPAR,5)
C
      COMMON/ intwmax / wmaxx
      COMMON/ higgsm / hm1,stra
C
      REAL*8 epsneu,sneu,s1,s2,t1,t2,h1,h2,h12,rL,ckhi,
     .     skhi2,r,GI,Gw,Gs,Gtot,ph,he,ehh,ehl,eb,wmaxx,z
      REAL*8 sam1,sam2,sam3,sam4,s12,rmz2,s
C
      z     = 0.
      wmaxx = 0.
      ss    = sbeam
      s     = sqrt(ss)
      eb    = s/2.
C
C Some masses and widths and constants
```

```
C
      rmv  = amw
      rmz  = amz
      rgz  = gmz
      rmh  = pmas(25,1)
      v1   = -1.+4.*sw**2
      v2   = -1.
C
      IF(stra.GT.0.)rmh = hm1
C
      rmv2 = rmv**2
      rmh2 = rmh**2
      rmz2 = rmz**2
C
C Integration limits
C
      ehl = rmh + 5D-3
      ehh = s*(1.+rmh2/ss)/2.
      csl = -1.
      csh =  1.
      deltaeh = ehh-ehl
      deltaco = 2.
C
C Constant in picobarns
C
      const1 = g_f**3*rmz**8/
     .     (sqrt(2.)*pi**3)*0.389D-3/1.0D-15
```

The step length of the Higgs energy is 0.28 GeV. This value is the best that is found after a series of tests.

```
C
C Construction of wmax
C
      DO he = ehl,ehh, 0.28
         DO cste = csl,csh, 0.1
C
C The Higgs momentum
C
            hmom = sqrt(he**2 - rmh2)
C
C The energy of the neutrino pair
C
            epsneu = s-he
C
C The invariant mass squared of the neutrino pair
C
            sneu = epsneu**2-hmom**2
```

```
C
C Some other functions
C
            s1 = s * (epsneu + hmom * cste)
            s2 = s * (epsneu - hmom * cste)
            s12 = s1*s2
C
            h1 = 1. + 2.* rmv2 / s1
            h2 = 1. + 2.* rmv2 / s2
            h12 =h1*h2
C
            ckhi = 1. - 2.*ss*sneu / (s1 * s2)
            skhi2 = 1. - ckhi**2
C
            t1 = h1 + ckhi*h2
            t2 = h2 + ckhi*h1
C
            r = h1**2 + h2**2 + 2.*ckhi*h12 - skhi2
C
            rL = log((h12 + ckhi + sqrt(r)) /
     .           (h12 + ckhi - sqrt(r)))
C
            sam1 = (sneu-rmz2)**2
            sam2 = rmz2*rgz**2
            sam3 = rL/sqrt(r)
            sam4 = (h1+1.)*(h2+1.)
C
C The WW-fusion term
C
            Gw = (cw2**4/(s12*r))*(sam4*
     .           (2./(h1**2-1.)+ 2./(h2**2-1.)-
     .           6.*skhi2/r + (3.*t1*t2/r -ckhi)*
     .           sam3) - (2.*t1/(h2-1.) + 2.*t2/(h1-1.) +
     .           (t1+t2+skhi2)*sam3))
C
C The interference term
C
            GI = (v1+v2)*cw2**2*(sneu- rmz2)/
     .           (8.*(ss-rmz2)*(sam1+
     .           sam2)) * (2.-(h1+1.)*
     .           log((h1+1.)/(h1-1.))-(h2+1.)*log((h2+1.)/(h2-1.))+
     .           sam4*sam3)
C
C The Higgs-strahlung term
C
            Gs = (v1**2+v2**2)*(ss*sneu+s12)/(96.*
     .           (ss-rmz2)**2*(sam1+sam2))
```

```
C
C The total
C
            Gtot = (hmom/ss)*(Gs+GI+Gw)
C
 42         IF (Gtot .GT. z)THEN
               z = Gtot
            ENDIF
C
         ENDDO
      ENDDO
C
      wmaxx = const1*deltaeh*deltaco*z
C
      RETURN
      END
C
```

A.3 Changes in the original program code

To include the new process in **HZHA** some changes in the original code were made. In this section these changes are listed.

In subroutine `dsigma` the following was changed:

```
      CALL dsigwwh(ipro,ee,qh,qa,hh)

      IF (ipro .GE. 5 .AND. ipro .NE. 9 .AND. ipro .NE. 10) THEN
         CALL dsigwwh(ipro,ee,qh,qa,hh)
      ELSEIF (ipro .EQ. 10) THEN
         CALL dsigtot(ipro,ee,qh,qa,hh)
C
      ENDIF
```

In subroutine `hzha_init` the following was added:

```
      COMMON/ intwmax / wmaxx
      REAL*8 wmaxx
      COMMON / intf / inclu
```

and:

```
      inclu   = NINT(gene(8))
```

and:

```
C
C Initialize wmax for ipro = 10
C
```

```
      CALL wmax_init(sbeam)
C
```

and:

```
C
C To turn off the interference term if SM .NE. 1.
C
      IF (ism .NE. 1) inclu = 0
C
C To turn off the interference term if iklei = 0.
C
      IF (iklei .EQ. 0) inclu = 0
C
```

The following changes were made in subroutine `hzha_init`:

```
      DO ifs = 1, 11
        kselec(ifs) = gzdc(ifs)
      ENDDO
C
      braz(1) = brai(1) * kselec(1)
      DO ifs = 2, 11
        braz(ifs) = brai(ifs)*kselec(ifs)+braz(ifs-1)
      ENDDO
C
      fracz = braz(11)
      DO ifs = 1, 11
        braz(ifs) = braz(ifs)/braz(11)
      ENDDO
C
      pmas(23,1) = amz

      iproyn(maxpro) = 0
C
      IF (inclu .EQ. 1)THEN
         iproyn(5)  = 0
         iproyn(10) = 1
         DO ifs = 1, 11
            kselec(ifs) = gzdc(ifs)
         ENDDO
         IF (kselec(2) .EQ. 1)THEN
            write(*,*)'WARNING: You have asked for a decay channel,'
            write(*,*)'Z --> nu_e nu_e~bar, that is already included'
            write(*,*)'by process number 10, your choice to use'
            write(*,*)'Z --> nu_e nu_e~bar is automatically turned off!'
            print*
```

```
         ENDIF
         kselec(2) = 0
      ELSE
         DO ifs = 1, 11
            kselec(ifs) = gzdc(ifs)
         ENDDO
C
      fracz = braz(11)
C
      IF (braz(11) .EQ. 0) GOTO 42
C
      DO ifs = 1, 11
        braz(ifs) = braz(ifs)/braz(11)
      ENDDO

 42   pmas(23,1) = amz
```

and:

```
      CALL vzero(wtot (1),4)
      CALL vzero(wtot2(1),4)
      CALL vzero(ntry (1),4)
      CALL vzero(nacc (1),4)

      CALL vzero(wtot (1),5)
      CALL vzero(wtot2(1),5)
      CALL vzero(ntry (1),5)
      CALL vzero(nacc (1),5)

      reduc(1) = fracz * parwth(2) / width(2)
      reduc(5) = parwth(2) / width(2)
      reduc(7) = parwth(2) / width(2)

      reduc(1) = fracz * parwth(2) / width(2)
      reduc(5) = parwth(2) / width(2)
      reduc(7) = parwth(2) / width(2)
      reduc(10) = parwth(2) / width(2)
```

In subroutine hzha_event the following was changed:

```
      IF ( ipro .EQ. 5 .OR. ipro .EQ. 6 ) THEN
        kfn = 12
      ELSEIF ( ipro .EQ. 7 .OR. ipro .EQ. 8 ) THEN
        kfn = 11
      ENDIF

      IF ( ipro .EQ. 5 .OR. ipro .EQ. 6 .OR. ipro .EQ. 10) THEN
```

```
        kfn = 12
      ELSEIF ( ipro .EQ. 7 .OR. ipro .EQ. 8 ) THEN
        kfn = 11
      ENDIF
```

and:

```
      IF ( ipro .EQ. 5 .OR. ipro .EQ. 7 ) THEN
        kfh = 25
        jhig = 2
      ELSEIF ( ipro .EQ. 6 .OR. ipro .EQ. 8 ) THEN
        kfh = 35
        jhig = 1
      ENDIF

      IF ( ipro .EQ. 5 .OR. ipro .EQ. 7 .OR. ipro .EQ. 10 ) THEN
        kfh = 25
        jhig = 2
      ELSEIF ( ipro .EQ. 6 .OR. ipro .EQ. 8 ) THEN
        kfh = 35
        jhig = 1
      ENDIF
```

The following was added to subroutine `hzha`:

```
          sthr(10)= 0.1
```

and:

```
          IF (cross(10)*iproyn(10)*reduc(10) .GT. 0.)
     .      CALL remt1(e,sigma10,sthr(10),10,cross(10),xrad)
```

In subroutine `hzha_close` the following lines were changed:

```
      DO ipr = 1, 4
        ipro = ipr + 4
        IF ( ntry(ipr) .GT. 0 ) THEN
          sigto = wtot(ipr)/FLOAT(ntry(ipr))
          dsig  = SQRT((wtot2(ipr)/FLOAT(ntry(ipr)) - sigto**2)
     .           / FLOAT(ntry(ipr)))
C         WRITE(6,*) ' '
C         WRITE(6,*) '-------------------------------------------------'
C         WRITE(6,*) ' Generated cross section for ',chapro(ipro),' :'
C         WRITE(6,*) '    Sigma = ',sigto,' +/- ',dsig,' fb'
```

```
C         WRITE(6,*) '    # of trials          : ',ntry(ipr)
C         WRITE(6,*) '    # of accepted events : ',nacc(ipr)
C         WRITE(6,*) '-------------------------------------------------'
C         WRITE(6,*) ' '
          ENDIF
        ENDDO

        DO ipr = 1, 5
           IF (ipr .EQ. 5)THEN
              ipro=10
           ELSE
              ipro = ipr + 4
           ENDIF
           IF ( ntry(ipr) .GT. 0 ) THEN
              sigto = wtot(ipr)/FLOAT(ntry(ipr))
              dsig  = SQRT((wtot2(ipr)/FLOAT(ntry(ipr)) - sigto**2)
     .             / FLOAT(ntry(ipr)))
          WRITE(6,*) ' '
          WRITE(6,*) '-------------------------------------------------'
          WRITE(6,*) ' Generated cross section for ',chapro(ipro),' :'
          WRITE(6,*) '    Sigma = ',sigto,' +/- ',dsig,' fb'
          WRITE(6,*) '    # of trials          : ',ntry(ipr)
          WRITE(6,*) '    # of accepted events : ',nacc(ipr)
          WRITE(6,*) '-------------------------------------------------'
          WRITE(6,*) ' '
          ENDIF
        ENDDO
```

In function `crocom` **the following was added:**

```
        COMMON / intf / inclu
```

and:

```
        ELSEIF (ipro .EQ. 10) THEN
           crocom = sinterference(sbeam)
        ELSE
        ENDIF
```

and the following was changed:

```
          ELSE
            crocom = alpha2 * brwipj(sbeam,amh,width(2),amz)
C           IF ( ism .EQ. 0 ) THEN

          ELSE
            crocom = alpha2 * brwipj(sbeam,amh,width(2),amz)
```

```
          IF (inclu .EQ. 1 ) crocom = crocom*(1.-brai(2))
C          IF ( ism .EQ. 0 ) THEN
```

A.3.1 Changes in COMMON blocks, DATA etc.

These changes have to be made in the common blocks, data blocks, external declarations etc:

```
      EXTERNAL sigma5,sigma6,sigma7,sigma8,sigma9

      EXTERNAL sigma5,sigma6,sigma7,sigma8,sigma9,sigma10
```

and:

```
      COMMON / poidsm / wtot(4),wtot2(4),ntry(4),nacc(4)

      COMMON / poidsm / wtot(5),wtot2(5),ntry(5),nacc(5)
```

and:

```
      PARAMETER (maxpro= 9)

      PARAMETER (maxpro= 10)
```

and:

```
      COMMON /h_cards/ trig(2),debu(2),time(1),gene(7),gsmo(6),
     .                 gsus(11),pryn(9),gzdc(11),gch1(16),gch2(16),
     .                 gch3(16),ghhg(2),ghcc(8),gchc(19)

      COMMON /h_cards/ trig(2),debu(2),time(1),gene(8),gsmo(6),
     .                gsus(11),pryn(10),gzdc(11),gch1(16),gch2(16),
     .                gch3(16),ghhg(2),ghcc(8),gchc(19)
```

and:

```
      CALL vzero(pryn(1),9)

      CALL vzero(pryn(1),10)
```

and:

```
      DATA lenvar/2,2,1,7,6,11,9,11,16,16,16,2,8,19/

      DATA lenvar/2,2,1,8,6,11,10,11,16,16,16,2,8,19/
```

The following function was added to HZHA:

```
      FUNCTION sigma10(s)
      sigma10 = crocom(10,s)
      RETURN
      END
```

A.3.2 The data cards:

The data cards that control HZHA can be found in the file `runhzha.csh`. **The following should be added in** `runhzha.csh`:

```
*    INCL    : = 1 to compute e+e- --> h nu_e nu_e~bar with the inte-
*                 ference term (for both the Higgs-strahlung and the
*                 WW-fusion). The interference term is not included
*                 if iklei = 0 and/or SM = -1 or 0
*             = 0 the interference term is not included.
*
*
* ALL numbers MUST be REAL !
*
*    IKLEI IPROC XRAD  ECM  EMPIR  SM  ICAR  INCL
GENE   1.    5.   1.   200.  4.0   1.    1.   1.
*
```

References

[1] W. Kilian, M. Krämer, and P.M. Zerwas hep-ph/9512355.

[2] F.A. Berends and R. Kleiss, Nucl. Phys. **B260** (1985) 32.

[3] CERNLIB Short Writeups (May 1993) D110-1.

Appendix B

Second Delphi note

DELPHI Collaboration

DELPHI 2000-062 PHYS 863
27 April, 2000

Update of the HZHA02 generator with the interference term between Higgs-strahlung and WW fusion

T. Frågåt
Physics Department, University of Oslo, Blindern, 0316 Oslo, Norway

Abstract

The first modified version of HZHA02, including interference between Higgs-strahlung and WW fusion, suffered from some instabilities in the cross section for the $e^+e^- \to h\nu_e\bar{\nu}_e$ process (*Higgs-strahlung and WW fusion with interference between the two production amplitudes*) for small Higgs masses. The corrections are presented in this note together with the inclusion of Improved Born approximation and ZZH- and WWH-vertex corrections which were not present in the previous version of the modified HZHA02 for this process. Also some changes to the original formulae and some comparisons with the recently released HZHA03 (which is the official version of HZHA including interference in the $e^+e^- \to h\nu_e\bar{\nu}_e$ channel) are made. The new modified version of HZHA02, like HZHA03, also allows the CP even light scalar Higgs boson of the MSSM to be generated for the process $e^+e^- \to h\nu_e\bar{\nu}_e$ with interference.

1 Introduction

The first modified version of HZHA02[1] (called here HZHA02TF$_1$), including the interference term between Higgs-strahlung (where the Z boson decays into electron neutrinos) and WW fusion was released in September 1999 [1]. Since then a new modified version of HZHA02 (called here HZHA02TF$_2$) has been released with some new features and corrections in the $e^+e^- \to h\nu_e\bar{\nu}_e$ channel. In November 1999 a new official version of HZHA was released [2], namely HZHA03. This version also includes the interference term in the $e^+e^- \to h\nu_e\bar{\nu}_e$ channel, but the formulae and algorithms for this channel in HZHA03 are different from those in HZHA02TF. In this paper the new features of HZHA02TF are presented, and cross-checks of the official version HZHA03 for the $h\nu_e\bar{\nu}_e$ final state channel are made.

The changes from HZHA02TF$_1$ to HZHA02TF$_2$ are (all concerning the Higgs-strahlung with $h\nu_e\bar{\nu}_e$ in the final state, WW fusion and interference channel):

- Instabilities occuring in the cross section for low Higgs masses were corrected.
- Improved Born approximation and ZZH- and WWH-vertex corrections were included.
- Corrections to the original formulae were made, allowing generation of Higgs bosons almost at rest.
- Possibility to generate the CP even light scalar Higgs boson of the MSSM.

And the most important changes from HZHA02TF to HZHA03 are [2]:

- All routines were rewritten with double precision.
- A bug in the Higgs-strahlung production was corrected.
- A numerical singularity in the $h \to Z\gamma$ decay was corrected.
- Interference between the Higgs-strahlung and ZZ fusion with he^+e^- in the final state was included.
- Radiative corrections to Higgs boson masses in the MSSM were included.
- Top threshold two loop corrections to the Higgs boson masses and couplings were also implemented.
- Possibility to compute SUSY spectrum in the SUGRA framework.
- The linear combination of the gaugino mass terms M_1 and M_2 was replaced by M_2.
- Anomalous Higgs couplings were modified.

[1] The modified version of HZHA02 is *not* an official version of HZHA.

2 Cross section

In HZHA02TF$_2$ the theoretical cross section of Higgs-strahlung, WW fusion and interference are computed in a different way than in the previous version, although the formulae are the same [3]. Using the `CERNLIB` routine `DGMLT2` [4], which performs a Gaussian quadrature integration for double integrals, the number of integration intervals chosen was too small in the old version, so for low Higgs masses the cross section became unstable as shown in Fig. 1. The reason for this behavior can be found in the energy distributions of Higgs-strahlung and interference shown in Fig. 2. The peaks of the two distributions makes the integration harder to perform, and the number of integration intervals had to be increased. But to avoid the program from slowing down, especially when ISR, *Initial State Radiation*, is included [1, 5], the WW fusion cross section had to be calculated alone with a smaller number of integration intervals. This could be done since the energy distribution is almost flat. The same holds for the integration over $\cos\theta$, shown in Fig. 2, which also can be done with a small number of integration intervals. After these changes the cross section becomes stable, as shown in Fig. 1, without slowing down HZHA. But it is important to note that for Higgs masses below $\sim \sqrt{s} - 135$ GeV, the instabilities will occur again.

Improved Born approximation (IBA) and ZZH- and WWH-vertex corrections [6] are also accounted for in the new version. The new cross section as a function of the Higgs mass for $\sqrt{s} = 200$ GeV is shown in Fig. 1 together with

$$\frac{\delta\sigma}{\sigma} = \frac{\sigma_{HZHA03} - \sigma_{HZHA02TF_2}}{\sigma_{HZHA03}} \,. \tag{1}$$

One can see that the differences in the cross sections are below 1%, which is the claimed accuracy of HZHA.

3 Generation of Higgs bosons

As pointed out in [7] the differential cross section in [3] suffers from numerical instability when $p \to 0$ or $\cos\theta \to 0$. To remove the instability the following changes suggested in [7] are made. First define

$$\alpha \equiv 1 + c_\chi = \frac{2p^2(1-\cos^2\theta)}{(\epsilon_\nu^2 - p^2\cos^2\theta)} \tag{2}$$

$$\Delta_h \equiv h_2 - h_1 = \frac{2m_W^2}{\sqrt{s}} \frac{2p\cos\theta}{(\epsilon_\nu^2 - p^2\cos^2\theta)} \,. \tag{3}$$

The abbreviations are the same as in [3]. Then it follows that

$$c_\chi = \alpha - 1 \quad \text{and} \quad s_\chi^2 = 2\alpha - \alpha^2 \,. \tag{4}$$

The next step is to break up $\mathcal{G}_W$ into terms of nearly the same order to avoid numerical overflow,

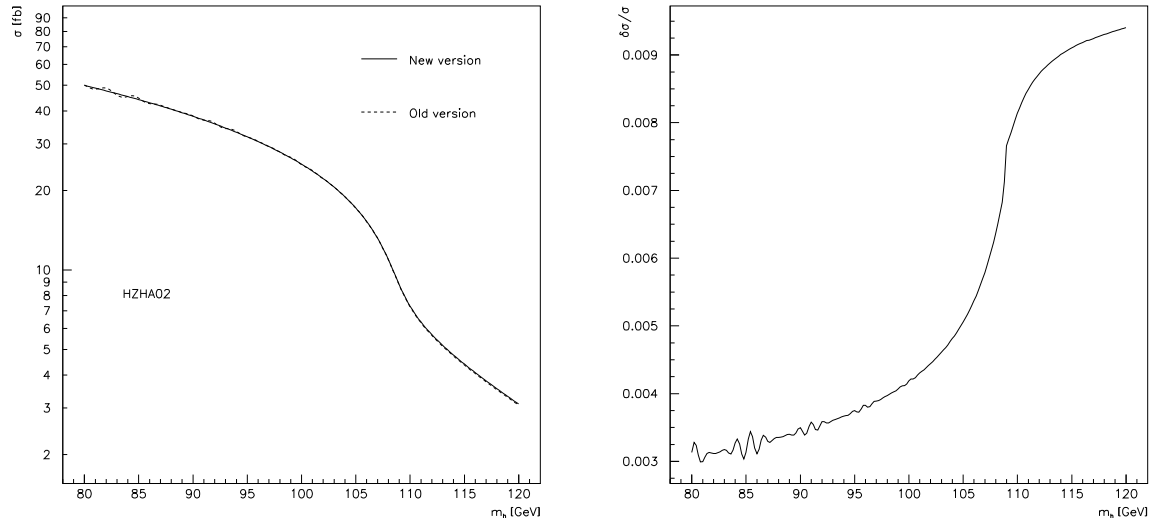

Figure 1: *The cross section with ISR for the process* $e^+e^- \to h\nu_e\bar{\nu}_e$ *with interference at* $\sqrt{s}$ *= 200 GeV (left). The dashed line shows the cross section for the HZHA02TF*$_1$*, while the solid line shows for the HZHA02TF*$_2$ *with IBA and ZZH- and WWH-vertex corrections. The plot to the right shows* $\delta\sigma/\sigma$ *(see the text) as a function of the Higgs mass.*

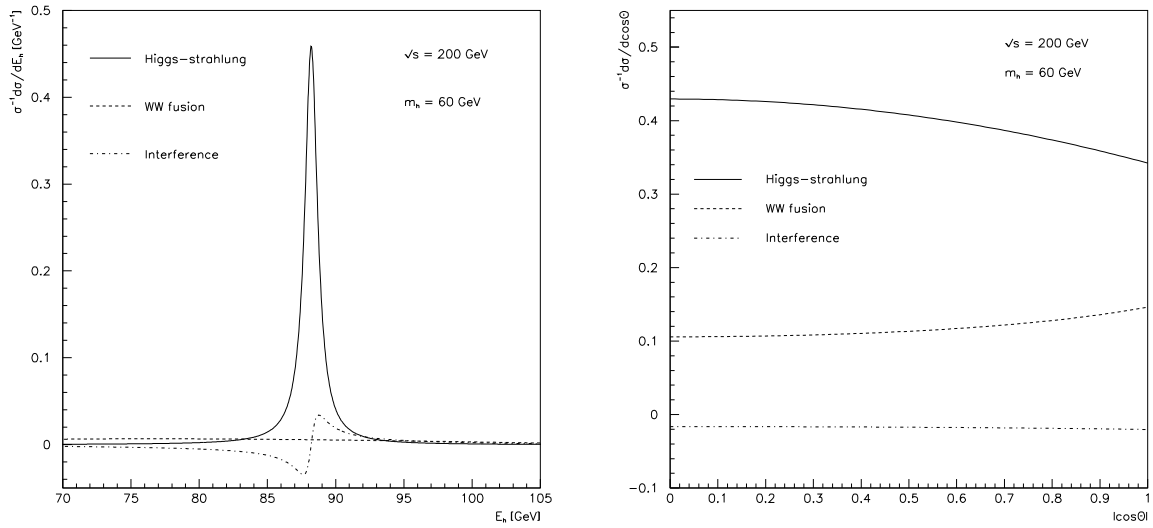

Figure 2: *The individual differential cross sections versus Higgs energy (left) and* $|\cos\theta|$ *(right) of the Higgs boson for the process* $e^+e^- \to h\nu_e\bar{\nu}_e$ *at* $\sqrt{s}$ *= 200 GeV and* m_h *= 60 GeV. The individual curves are normalized to the total cross section of 74.1 fb.*

$$\mathcal{G}_W = \frac{\cos^8\theta_W}{s_1 s_2 r}(\mathcal{A}+\mathcal{B}-\mathcal{C}-\mathcal{D}) \quad (5)$$

$$\mathcal{A} = (h_1+1)(h_2+1)\left[\frac{2}{h_1^2-1}+\frac{2}{h_2^2-1}-\frac{2\mathcal{L}}{\sqrt{r}}\right] \quad (6)$$

$$\mathcal{B} = (h_1+1)(h_2+1)\left[\left(2+\frac{3t_1t_2}{r}-c_\chi\right)\frac{\mathcal{L}}{\sqrt{r}}\right] \quad (7)$$

$$\mathcal{C} = (h_1+1)(h_2+1)\left[\frac{6s_\chi^2}{r}\right] \quad (8)$$

$$\mathcal{D} = \left[\frac{2t_1}{h_2-1}+\frac{2t_2}{h_1-1}+(t_1+t_2+s_\chi^2)\frac{\mathcal{L}}{\sqrt{r}}\right] . \quad (9)$$

Now $\mathcal{B}$ should be replaced by

$$\mathcal{B} = (h_1+1)(h_2+1) \times \left[(2\alpha\Delta_h^2+3\alpha^2(h_1h_2+1)-2\alpha^2(h_1h_2-1)+6\alpha(h_1h_2-1)-\alpha^3)\frac{\mathcal{L}}{r\sqrt{r}}\right] \quad (10)$$

to avoid the numerical problem. Although these changes have been made in HZHA02TF$_2$, the energy and angular distributions are not significantly affected. Anyway, this correction should be included because it allows the generation of Higgs bosons almost at rest.

4 MSSM

HZHA02TF$_2$ allows generation of the lightest CP even Higgs scalar in the Minimal Supersymmetric Standard Model, *MSSM*, for $e^+e^- \to h\nu_e\bar{\nu}_e$ with interference. This was not true in the previous version. The Standard Model formula is replaced by

$$\sigma(h)_{MSSM} = \sin^2(\beta-\alpha) \times \sigma(h)_{SM} . \quad (11)$$

The cross sections and energy and angular distributions were compared to those made with HZHA03. One comparison of the energy and angular distributions can be seen in Fig. 3. In Table 1 some cross sections are shown for $\sqrt{s} = 204$ GeV with various $\tan\beta$ and m_A for both HZHA02TF$_2$ and HZHA03 with and without ISR. The differences between m_h in HZHA02TF$_2$ and HZHA03 for fixed values of $\tan\beta$ and m_A are due to the implementation of radiative corrections to the Higgs boson masses and top threshold loop corrections in MSSM for HZHA03 [2]. Since m_h differs for the two versions of HZHA for fixed values of $\tan\beta$ and m_A, the cross sections also will be slightly different. In Table 2 the HZHA03 cross sections are the same as in Table 1, while the MSSM cross sections for the HZHA02TF$_2$ are first calculated for the SM with the same Higgs masses as for HZHA03 and then multipied by $\sin^2(\beta-\alpha)$ (Eq. 11) which was calculated by HZHA03 for each Higgs mass. As can be seen the resulting cross sections are within the claimed accuracy of HZHA.

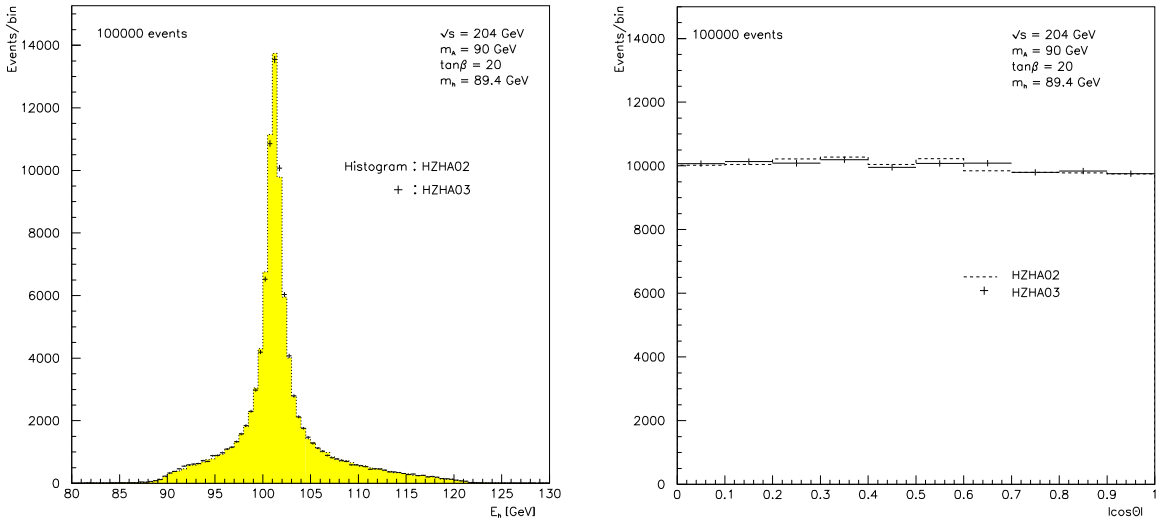

Figure 3: *The generated energy distribution (left) and angular distribution (right) for the process* $e^+e^- \to h\nu_e\bar{\nu}_e$ *with interference and ISR in MSSM at* $\sqrt{s} = 204$ *GeV,* $m_A = 90$ *GeV and* $\tan\beta = 20$.

		HZHA02TF$_2$			**HZHA03**		
m_A [GeV]	$\tan\beta$	m_h [GeV]	σ [fb]	σ_{ISR} [fb]	m_h [GeV]	σ [fb]	σ_{ISR} [fb]
75	2	60.08	46.42	46.03	60.84	45.61	45.13
75	20	74.67	1.096	1.035	74.69	1.045	0.9866
90	2	66.18	48.28	46.92	67.07	47.32	45.87
90	20	89.35	1.805	1.602	89.40	1.654	1.470

Table 1: *Cross sections for Higgs-strahlung, WW fusion and interference in MSSM for the lightest neutral Higgs at* $\sqrt{s} = 204$ *GeV (*σ *is the cross section without ISR, while* σ_{ISR} *is with ISR).*

		HZHA02TF$_2$			**HZHA03**		
m_A [GeV]	$\tan\beta$	m_h [GeV]	σ [fb]	σ_{ISR} [fb]	m_h [GeV]	σ [fb]	σ_{ISR} [fb]
75	2	60.84	45.19	44.70	60.84	45.61	45.13
75	20	74.69	1.036	0.9784	74.69	1.045	0.9866
90	2	67.07	46.92	45.47	67.07	47.32	45.87
90	20	89.40	1.647	1.461	89.40	1.654	1.470

Table 2: *Cross sections for Higgs-strahlung, WW fusion and interference in MSSM for the lightest neutral Higgs at* $\sqrt{s} = 204$ *GeV (*σ *is the cross section without ISR, while* σ_{ISR} *is with ISR). In this table the cross sections of HZHA03 are computed in the usual way, while the cross sections of HZHA02TF*$_2$ *are first computed in the SM with the same* m_h *as for the HZHA03 cross sections and then multipied by* $\sin^2(\beta-\alpha)$ *(which was calculated for each Higgs mass by HZHA03) to obtain the MSSM cross section (Eq. 11).*

5 Conclusion

The part of HZHA02TF that deals with the Higgs-strahlung, WW fusion and interference for the $H\bar{\nu}_e\nu_e$ final state has been improved and tested and it has also been compared to HZHA03 both for the SM and MSSM. The cross sections of HZHA02TF$_2$ and HZHA03 are now within 1% of each other and the energy and angular distributions are in very good agreement. HZHA03 (the updated public version of HZHA) should therefore be used for generating such events.

6 Acknowledgement

I would like to thank my supervisors Lars Bugge and Alex Read for their support and comments.

References

[1] T. Frågåt, DELPHI 99-161 PHYS 836.

[2] P. Janot, http://alephwww.cern.ch/~janot/Generators.html.

[3] W. Kilian, M. Krämer, and P.M. Zerwas, hep-ph/9512355.

[4] CERNLIB Short Writeups (May 1993) D110-1.

[5] F.A. Berends and R. Kleiss, Nucl. Phys. **B260** (1985) 32.

[6] E. Gross, A. Kniehl, and G. Wolf, hep-ph/9404220.

[7] K. Cranmer, http://www-wisconsin.cern.ch/~cranmer/fusefix.ps, private communication.

Bibliography

[1] T. Frågåt, DELPHI 99-161 PHYS 836.

[2] T. Frågåt, DELPHI 2000-062 PHYS 863.

[3] Lloyd Motz, and Jefferson Hane Weaver, *The Story of Physics*, Avon Books (1989).

[4] Pedro Waloschek, http://www-library.desy.de/elbooks/wideroe/WiE-CONT.htm.

[5] Zbigniew Zwolinski, http://hum.amu.edu.pl/ zbzw/ph/sci/gc.htm.

[6] *Spinoffs in our daily life*, http://www.cern.ch/Public/TECHNOLOGY/dailylife.html

[7] http://delphi.web.cern.ch/Delphi/Welcome.html.

[8] http://delphiwww.cern.ch/ offline/physics/delphi-detector.html.

[9] http://delonline.cern.ch/delphi$specific/cp/monitor/presenter/help_files/mub_descrip.html.

[10] M. Kaku, *A Modern Introduction to Quantum Field Theory*, Oxford University Press, Inc. (1993).

[11] F. Halzen, and D. Martin, *Quarks & Leptons, An Introductory Course in Modern Particle Physics*, John Wiley & Sons, Inc. (1984).

[12] The LEP working group for Higgs boson searches, CERN-EP-2000-055.

[13] G. G. Ross, Contemporary Physics **34** (1993) 79-88.

[14] ATLAS TDR 15, CERN/LHCC 99-15.

[15] John F. Gunion, Howard E. Haber, Gordon Kane, and Sally Dawson, *The Higgs Hunters Guide*, Addison-Wesley Publishing Company, Inc. (1990).

[16] F. A. Berends and R. Kleiss Nucl. Phys. **B260** (1985) 32-60.

[17] G. Altarelli, B. Mele, and F. Pitolli, Nucl. Phys. **B287** (1987) 205.

[18] W. Kilian, M. Krämer, and P.M. Zerwas, hep-ph/9512355.

[19] W. Kilian, M. Krämer, and P.M. Zerwas, hep-ph/9605437.

[20] K. Cranmer, http://www-wisconsin.cern.ch/~cranmer/fusefix.ps, private communication.

[21] P. Janot, http://alephwww.cern.ch/~janot/Generators.html.

[22] M.L. Mangano, *et al.*, *Event Generators for Discovery Physics*, in *Physics at LEP2*, edited by G. Altarelli, T. Sjöstrand, and F. Zwirner, CERN 96-01.

[23] J. Hilgart, R. Kleiss, and F. Le Diberder, CERN-PPE/92-115.

[24] CERNLIB Short Writeups (May 1993) D110-1.

[25] E. Gross, A. Kniehl, and G. Wolf, hep-ph/9404220.

[26] P. Janot, private communication.

[27] A. Djouadi, J. Kalinowski, P.M. Zerwas, DESY 92-168.